Application of hydrochemistry and residence time constraints to distinguish groundwater systems in the Karoo Basin prior to shale-gas exploration

Kelley Swana 16174305

Submitted in Full Fulfillment of MSc Geology Department

of Earth Science, Stellenbosch University

March 2016

Supervisor: Dr Jodie Miller

DECLARATION

I declare that *Application of hydrochemistry and residence time constraints to distinguish groundwater systems in the Karoo Basin prior to shale-gas exploration* is my own work, that it has not been submitted for any degree or examination in any other university, and that all the sources I have used or quoted have been indicated and acknowledged by complete references.

Full name: Kelley Swana

Date: March 2016

ACKNOWLEDGEMENTS

I would like to express my deepest gratitude to the following people for their contribution to this project. Firstly to my supervisor, Jodie Miller, for her continuous patience, guidance and encouragement throughout my MSc. I would like to extend my thanks to Ricky Murray from Groundwater Africa for initiating the project and for personal funding. Thanks also to the National Research Foundation (NRF) for personal funding. Thank you to the Water Research Commission (WRC) of South Africa, in particular, Shafick Adams for funding the project. To the Honours students and sampling team - Anya Eilers, Kay-Lee Kaywits, Tyron Hartle, Kes Murray, Andrew Watson, Billy Eymold and Ryno Botha – thank you for your assistance in the field as well as with data compilation. Thank you to the farm owners and municipal and spa managers, without whom this project would not have been possible. Your kind hospitality is so appreciated. Thank you to Mike Butler from iThemba LABS in Johannesburg for the analyses of stable isotopes, radiocarbon and tritium, Keith Fifield at the Australian National University for the chlorine-36 data, as well as Petrus Le Roux from the University of Cape Town, for strontium isotope analysis. Thank you to Avner Vengosh and Thomas Darrah for co-authoring the WRC report, for various data analyses as well as for your expert advice in the field and over skype! To Siep Talma and Gideon Tredoux, I am especially grateful for the invaluable advice and wisdom you have shared with me over the past two years, as well as for co-authoring the WRC report. Special thanks to my fellow MSc student, Alexander Dunford for his continuous assistance throughout this project, as well as the other MSc students for their endless support. Finally, I would like to thank my parents for giving me the opportunity to persevere in my studies, and for their perpetual support throughout my entire university career.

ABSTRACT

The possibility of shale-gas development in the semi-arid Karoo Basin, South Africa has created the need to develop a hydrochemical baseline for deep Karoo groundwater. However, it is uncertain how the process of hydraulic fracturing (fracking) will affect the surrounding groundwater and environments, particularly shallow groundwater sources. Therefore, it is important to have a good understanding of the characteristics of the deep groundwater and its connectivity to the shallower groundwater systems which are of utmost importance to the farmers and local communities in the region. As a result of the requirement for information regarding the deeper groundwater in the Karoo Basin, this project was initiated in order to create a baseline of the deeper groundwater and assess how it differentiates from the shallow groundwater. Nineteen groundwater samples were collected from 8 locations throughout the Karoo Basin. At each site a deep sample was collected from a warm spring or borehole, and a corresponding shallow site was collected from a nearby shallow borehole. Following an initial assessment of the groundwater samples, three groups were identified; deep, shallow and mixed. The shallow samples could be identified by temperatures less than 25°C, high alkalinities, the presence of Mg^{2+}, NO_3^- and U, as well as higher δ^2H and $\delta^{18}O$ values. Warmer temperatures usually above 25°C, low alkalinities less than 80 $mg.L^{-1}$ HCO_3^-, elevated Na^+ and F^- as well as lower δ^2H and $\delta^{18}O$ values were characteristic of the deep samples. The results of the mixed samples consistently feel between those of the deep and shallow samples, indicates that natural mixing occurs between the deep and shallow aquifer systems. This has important implications as upward migration of poor quality deep groundwater and contaminants resulting from fracking activities have been known to occur in the USA. Significant differences are observed between the deep and shallow samples, resulting from different controls on the groundwater chemistry. For example, the process of nitrification occurs in the shallow groundwater resulting in elevated NO_3^- concentrations, whereas the dissolution of fluorite results in elevated F^- concentrations in the deep groundwater. Furthermore, increased contact time with the host lithologies results in increased Na concentrations in the deep groundwater. Residence times of the groundwater samples were calculated using four isotopic tracers, namely, tritiogenic helium, radiocarbon, helium-4 and chrlorine-36. Overall, the deep groundwater samples showed much longer residence times than shallow groundwater, with radiocarbon producing the most probable residence times. Pollution and contamination of shallow aquifers as a result of fracking is possible. Therefore, continuous baseline monitoring is essential before, during and after fracking activities in order to identify abnormalities that could be associated with fracking.

Keywords: Hydraulic fracturing; baseline; groundwater chemistry; residence times; Karoo Basin.

TABLE OF CONTENTS

LIST OF FIGURES

LIST OF TABLES

LIST OF EQUATIONS

CHAPTER 1 – Literature review and WRC report summary

1.1 Introduction

The population is increasing worldwide and as a result so is the demand for natural resources, triggering the development of a serious energy security crisis. It is predicted that by 2040 there will be a 37% increase from the current global energy demand (IEA, 2014). Projected energy consumption and production forecasts predict that by the year 2040 unconventional gas production from shale formations will produce 25% of the world's total energy supply (IEA, 2014). The other 75% is equally divided between oil, coal and low-carbon/renewable energy sources (IEA, 2014). The energy security problem is particularly prominent in Sub-Saharan Africa where it is estimated that 620 million people do not have access to electricity (IEA, 2014). Where electricity is available the supply is often unpredictable due to lack of maintenance of both power stations and lines. It is estimated that by 2040 the population of Sub-Saharan Africa will double, and as a result the energy demand will increase by 80% (IEA, 2014).

One of the current solutions of the energy security problem is to make use of unconventional or shale-gas trapped within shale rock layers deep within the earth as conventional oil reserves decline (IEA, 2014). The extraction of shale-gas involves the process of hydraulic fracturing also known as "fracking". Global shale-gas reserves are estimated to be 25300 trillion cubic feet (TCF) (Boyer, et al., 2011), of which the largest portion of that (28%) is in North America (Boyer, et al., 2011). As a result of this large natural resource, shale-gas supports approximately one quarter of the energy consumption in the USA (IEA, 2014). Like all fossil fuels, shale-gas reserves are not sustainable, therefore it is only a temporary solution as opposed to renewable energy sources such as solar, wind and hydro. Therefore, research on renewable and environmentally cleaner energy sources should continue whilst shale-gas extraction and production processes develop.

The method of fracking has been in practice for almost 200 years (Boyer, et al., 2011), with the first shale-gas well drilled in New York, USA in 1821 (Boyer, et al., 2011). Since then the technology involved in fracking has significantly changed and evolved. Originally the practice made use of vertical drilling until horizontal drilling was introduced. Horizontal drilling allows for extended contact with considerably larger portions of the shale-gas bearing layers ultimately allowing for an increase in the total amount of extractable gas (Boyer, et al., 2011; Weber, 2014; Vengosh, et al., 2013; Jackson, et al., 2014). Horizontally drilled wells also allow for the use of smaller well pads and require less space above ground, thus allowing for smaller

areas to be taken over by fracking activities. However, there are concerns about the potential effects fracking has and will have on the surrounding environments.

The environmental concerns regarding fracking include surface water contamination, air pollution, noise pollution, greenhouse gas emissions and radiation (Vengosh, et al., 2014; Zhao & Yang, 2015; Engelder, et al., 2014; Theodori, et al., 2014; Stringfellow, et al., 2014; Jackson, et al., 2013). Of these, the possibility of contamination and pollution of shallow groundwater resources close to the fracking sites has elicited the most concern from the public. Extensive research is being conducted regarding the establishment of baseline and monitoring systems in order to observe changes of the natural environment, specifically in groundwater (Mayer, et al., 2015; Jackson, et al., 2013; Vengosh, et al., 2014; Vidic, et al., 2013). Much of this research is occurring in areas with large shale-gas resources, such as in North America. Four potential risks to water resources in areas surrounding fracking were identified by Vengosh et al., (2014): 1) stray gas leaks causing contamination of shallow aquifers; 2) insufficient disposal and treatment of wastewater that may leak/spill, polluting surface water and shallow aquifers; 3) the build-up of toxic and radioactive compounds in spills or near disposal sites; and 4) the occurrence of water shortages, especially in water stressed regions, due to the use of large volumes of water during the fracking process. Although these problems were identified in the North American context, they are likely to be applicable to any region that is subject to fracking and therefore have implications for the fledging shale-gas industry in South Africa.

The Karoo Basin has been identified as a potential region for shale-gas exploration in South Africa. The target is the Whitehill Formation, which forms part of the Permian Ecca Group in the Karoo Supergroup, with an estimated shale-gas reserve of between 30-500 TCF (Dept Mineral Resources, 2012). In spite of the known risks of fracking, shale-gas is an attractive option for South Africa to help alleviate the pressure on electricity supply generated by aging infrastructure and a growing and upwardly mobile population. However, the Karoo is a water stressed region with an arid to semi-arid climate and it is also an important agricultural region. Agriculture in the Karoo is a multibillion dollar industry, which is spread across thousands of smaller farms (McCreadie, 2015). The Karoo region is the country's main supplier of red meat (specifically lamb), wool and mohair, as well as other export products such as ostrich feathers and venison (McCreadie, 2015). As such, contamination of the limited water resources would have significant implications for food security and on the economy of South Africa.

Research has been conducted on the Karoo shallow groundwater aquifers (<300m) as this is the dominant source of water to various farmers and local, rural communities (Woodford & Chevallier, 2002). However, there is a lack of knowledge about Karoo deep groundwater (>1500m) which may be affected by the fracking process. With the exception of borehole

SA1/66 drilled by Soekor, now PetroSA, in the 1960s (discussed in further detail in Section 1.4.2 Deep groundwater in the Karoo) as well as three current deep borehole drilling projects conducted by the Council for Geoscience, there is no access to the deep groundwater. The deep and shallow aquifers could be connected by natural conduits created by the intrusion of Jurassic dolerite dykes and sills. Evidence of connectivity between poor quality, deep formation water and fresh, shallow aquifer systems has been shown in the Marcellus Shale play in Pennsylvania, USA, in the form of distinctive geochemical and isotopic ratios (Sharma, et al., 2014; Warner, et al., 2014; Warner, et al., 2012). These geochemical signatures indicate that upward migration of deep groundwater has occurred and therefore this must be considered a possibility in the Karoo Basin. It is therefore essential to have an understanding of the deep and shallow groundwater reserves, as well as the natural and potentially induced connectivity between the aquifers in the form of a deep and shallow groundwater baseline (Humez, et al., 2015). However, access to the deep groundwater sources is required in order to create such a baseline.

The existence of thermal springs boreholes in the Karoo Basin are the closest approximation through which one can obtain an idea of the nature of deep groundwater. This is assumed due to the lack of other sources of heat in the Karoo, such as granites or other hot intrusive rocks, which would raise the groundwater temperature. These thermal springs and boreholes have been monitored and temperatures recorded over the past century (Rindl, 1916; Kent, 1949; Heaton, et al., 1986; Olivier, et al., 2012). Groundwater in southern Africa with temperatures between 25 and 37°C were classified as warm while those with temperatures between 37 and 50°C wrere classified as thermal (Kent, 1949). Therefore, the deeper groundwater sampled in this study is catagorised as warm. The minimum depths of the thermal springs that are known in the Karoo are in the order of 500 -1500 m (Kent, 1949; Kent, et al., 1966). If there is vertical flow of groundwater from greater depths, then analysing the water emanating from thermal or warm springs is likely to be the most accurate method of observing the characteristics of this deeper groundwater. An investigation of the detailed composition of such warm spring water is therefore likely to give the best estimate of the type of water to be found at greater depths.

Between 2013 and 2015, the Water Research Commission (WRC) of South Africa funded a research project to determine the geochemical parameters that would be indicative of deep groundwater in the Karoo as a precursor to fracking. The aim of the WRC project was to create a baseline of the deep groundwater in the Karoo and to investigate potential connectivity to the shallow groundwater resources that are used for domestic and agricultural purposes. Deep groundwater could potentially migrate upwards, either through natural or manmade conduits as a result of the fracking process. Should this groundwater be of poor quality, the migration could allow for the contamination of shallow groundwater aquifers, some of which are good

quality and used daily by farmers and local communities. Deep groundwater could also potentially be polluted by the chemicals used in fracking fluids or stray gas leaks. Detailed knowledge about the deeper groundwater and how it could possibly affect the shallow groundwater, will allow the government to make an informed decision about the environmental impacts of fracking in the Karoo Basin. The WRC project resulted in a list of parameters (geochemical tracers) considered to be indicative of deep and shallow groundwater in the Karoo Basin and laid out recommendations for groundwater monitoring.

The aim of this study is to expand on the ideas produced in the WRC project in order to further understand the deeper groundwater and its connectivity to the shallow aquifers. This will be done in two parts; firstly by investigating the natural geochemical processes occurring, including the precipitation/dissolution reactions as well as the redox conditions of the deeper and shallow groundwater. Secondly, estimate the residence times of the deeper groundwater in comparison to the shallow groundwater in order to assess the robustness of the residence times. This study, in conjunction with the WRC project, will aid in the decision making process regarding fracking in the Karoo Basin.

1.2. Aims and objectives

The aim of this study is to further examine the geochemical tracers identified as being indicative of deep and shallow groundwater in the WRC project, in order to determine the mechanisms that are responsible for the geochemical trends observed. The residence times of the groundwater samples collected will also be estimated in order to assess the robustness of the residence times, as well as recharge implications of the deeper groundwater in the Karoo Basin.

Key objective one: To explain the differences observed between the deeper and shallow groundwater in the Karoo Basin

1. What are the hydrochemical characteristics of the deep, shallow and mixed groundwater samples?

2. What redox conditions, precipitation/dissolution reactions and/or water-rock interactions are controlling the chemistry of the deep, shallow and mixed groundwaters?

3. Are the processes occurring in the deep groundwater affected by geographical variation?

Key objective two: To calculate and compare the residence times of the deeper and shallow groundwater in the Karoo Basin

1. What are the residence times of the deep and shallow groundwater samples when using $^{3}H/^{3}He$, ^{14}C, ^{36}Cl and ^{4}He?

2. How do the residence times of the deep groundwater samples compare to those of the shallow and mixed groundwater samples?

3. What are the implications of the residence times in terms of recharge in the Karoo Basin?

Key objective three: To create a conceptual model of the deeper groundwater in the Karoo Basin and how this ties in with the monitoring guidelines produced in the WRC project

1. Is there a natural connection between the deeper and shallow aquifers in the Karoo Basin?

2. Is there a potential mixing zone between the deeper and shallow aquifers?

3. Are the shallow groundwater aquifers at risk of contamination should fracking commence in the Karoo Basin?

1.3 Unconventional shale-gas

It was originally thought that shale could only function as a source rock of free gas, or conventional gas, which is stored in adjacent porous layers such as sandstones and limestones. However, it was then discovered that unconventional or “tight” gas trapped within impermeable shale layers can escape either naturally over millions of years or when artificially stimulated through fracking. Unconventional gas is typically composed of methane (CH_4) (Boyer, et al., 2011) and its extraction typically involves fracking from low permeability, tight shale layers (Jackson, et al., 2014). In the past decade there has been a significant increase in the exploration for shale-gas and the extraction of shale-gas by fracking throughout the world. The largest estimated resources are in the USA, however, Canada, South America, China, Southern Africa and Australia also have large potential shale-gas basins (Boyer, et al., 2011; Zhao & Yang, 2015). The current global estimate of natural gas reserves are approximately 25300 TCF (Boyer, et al., 2011).

1.3.1 The host rocks

Shale is a sedimentary rock, which typically consists of quartz and clay minerals, as well as organic matter (Boggs, 2009; Merriman, et al., 2003). Dissolved gases such as methane, carbon dioxide, hydrogen sulphide, nitrogen and helium are also commonly present together with numerous trace elements (Boggs, 2009). These rocks are typically deposited as mud in a low energy environment, such as a tidal flat or deep water basin. Over extended periods of time the muds and organic matter in the form of decomposed animal and plant remains accumulate and consolidate into thick sequences (Merriman, et al., 2003). In reducing environments, such as an anoxic lake, under elevated pressures and temperatures e.g. through the deep burial of the sediments, the decaying organic matter eventually evolves into organic oil and thermogenic gas (Boyer, et al., 2011).

Not all shale formations contain economically viable natural gas as there are various specific conditions and components that must exist. For example, the shale must be organically rich and comprise of a high total organic content (TOC) greater than 2% (EIA/ARI, 2013). A high quartz content is favourable as this allows the shale to be more brittle, and therefore the rock layers react more favourably to hydraulic simulation (EIA/ARI, 2013; Nunn, 2012). This is opposed to shale layers with a low quartz content which tend to behave in a more ductile manner and are more resistant to fracking. It is important for the shale to be thermally mature which is measured by the degree to which the shale has been exposed to high temperatures in order for the decomposition of organic matter into hydrocarbons to occur (EIA/ARI, 2013). Thermal maturity is measured in R_0 as a percentage. For example, areas that are inclined to contain viable oil should have a R_0 value of between 0.7 and 1% (EIA/ARI, 2013). Potential areas of wet gas and condensate should have an R_0 value between 1 and 1.3% (EIA/ARI, 2013), whereas areas likely to contain dry gas typically have an R_0 values greater than 1.3% (EIA/ARI, 2013). A burial depth of between 1000 and 5000m is ideal for the production of shale-gas (EIA/ARI, 2013; Nunn, 2012). Formations shallower than 1000m will not have experienced the pressures and temperatures at which hydrocarbons are produced. Formations at depths greater than 5000m will have permeabilities too low for fracking, not to mention the extra incurred cost of deeper drilling (EIA/ARI, 2013).

1.3.2 Fracking as a means of shale gas extraction

The technologies in practise today have significantly improved from the original fracking methods. Instead of vertically drilled wells producing low flow rates of natural gas, horizontal drilling and high volume hydraulic fracturing techniques are used to produce high flow rates of natural gas (Vengosh, et al., 2014; Boyer, et al., 2011; Jackson, et al., 2014; Jackson, et al., 2013). Deep wells are drilled (the depth of the borehole is dependent on the depth of the shale formation) vertically and then extended horizontally into the shale formations (Figure 1). The boreholes are cased using a cement casing. In order to create the fractures in the shale layers millions of litres of water, fracking fluid and a proppant (usually sand) are pumped down the borehole at extremely high pressures. This allows the trapped, natural gas to escape from the rocks and enter into the well where it is collected at the surface (Jackson, et al., 2014).

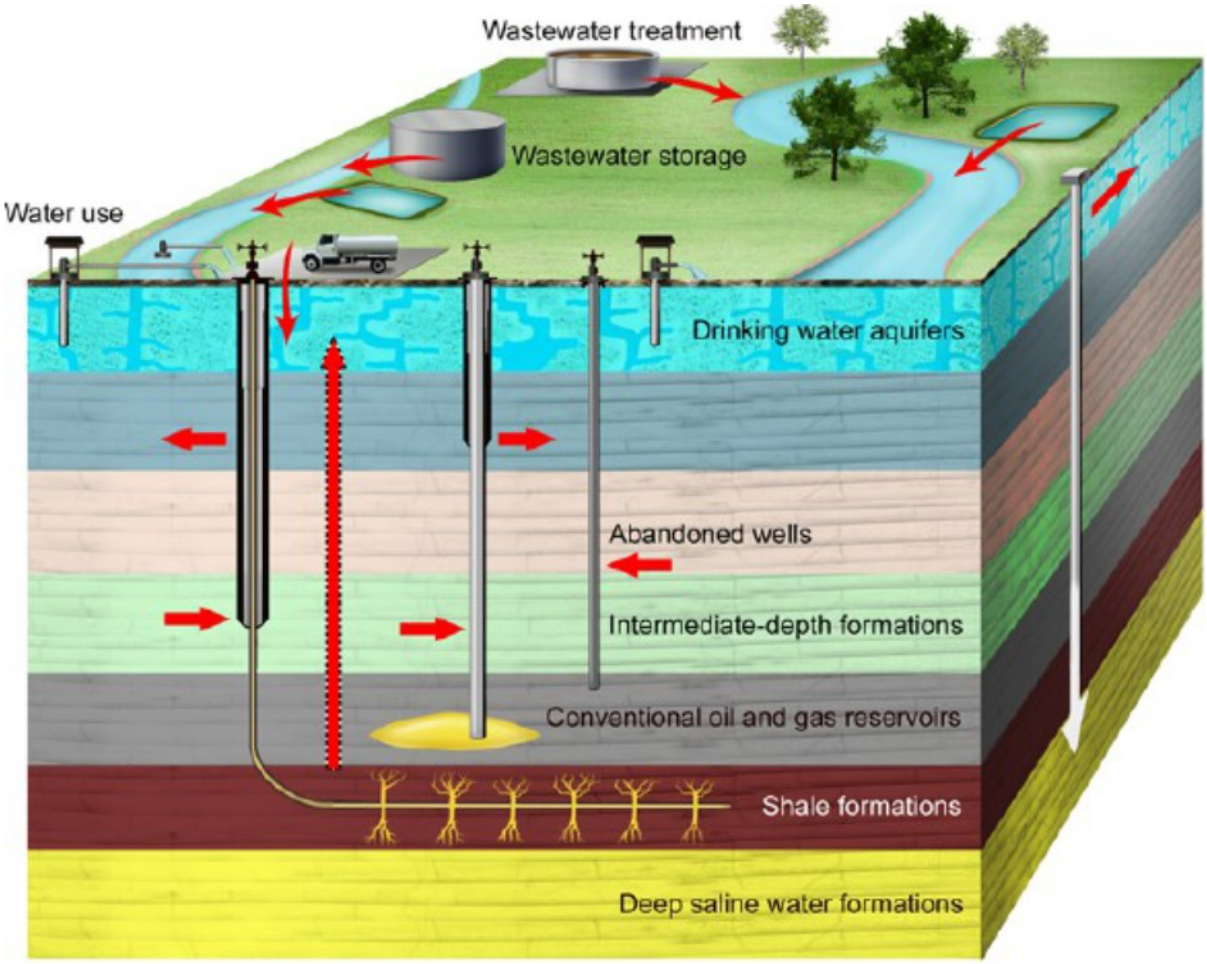

Figure 1: *Schematic representation (not drawn to scale) of hydraulic fracturing showing potential modes of groundwater contamination associated with shale-gas activities (Vengosh, et al., 2014).*

1.3.3 Environmental considerations

There is significant public concern regarding fracking, specifically the potential environmental impacts on the surrounding environment. This section discusses potential environmental problems including water usage, well integrity, and contamination of shallow groundwater with poor quality deep groundwater, fracking fluids and/or stray gas, the disposal of wastewater, potentially induced microseismicity as well as air, noise and visual pollution.

1.3.3.1 Water requirement versus water availability

Much of the fracking activity occurs in water stressed regions with scarce water resources available to even the local communities. As previously mentioned, millions of litres of water are used in the fracking process. The amount of water used per well is dependent on a number of aspects and varies with the specific shale play, associated rock formations, the drill operator and the depth of the well (Nicot & Scanlon, 2012). On average, up to 20 million litres of water are required per well in order to achieve the high volume hydraulic fracturing needed to create fissures and fractures within the shale layers (Vengosh, et al., 2014). Currently, fresh water

(TDS < 1000 mg.L^{-1}) is used in the fracking process to create the high pressures needed. This fresh water is sourced from nearby surface or groundwater resources depending on availability in the area. However, there is the possibility of using brackish water instead of fresh water for future fracking projects as this will greatly reduce the need for scarce, fresh water resources (Nicot & Scanlon, 2012). Research is still being conducted on this because the friction reducers included in the chemical additives of the fracking fluid function best in fresh water (Paktinat, et al., 2011).

1.3.3.2 Fracking fluid

A mixture of chemicals, referred to as fracking fluid, is added to the fresh water that is pumped into the well during the first stages of the fracking process. Figure 2 depicts a typical fracking fluid composition which includes 99.2% water and 0.79% chemicals displayed as a pie chart (FracFocus, 2015). The main component of the fracking fluid is a gellant, making up 0.5% of the total fracking fluid. Other components include acid (0.07%), corrosion inhibitor (0.05%), friction reducer (0.05%) and clay control (0.034%) (Figure 2). The remaining 0.01% consists of a proppant, usually sand, that is used to keep the fractures open in the shale layer (FracFocus, 2015; Jackson, et al., 2014). The exact ingredients of the fracking fluid differs from well to well, depending on the geological formations as well as the drilling company. Some companies prefer to not disclose the chemicals used in their fracking fluid, resulting in public concern and anxiety (Howarth, et al. 2011). However, FracFocus, an online national hydraulic fracturing chemical registry in the USA, was created in order to provide the public with general information regarding fracking. This includes specific information about the wells in close proximity to their homes, including the chemicals used in the fracking fluids. Currently the site has 106132 registered wells (FracFocus, 2015). Several studies have undergone the task of fingerprinting flowback water, which is inclusive of formation water and fracking fluids (Warner, et al., 2014). This aids in identifying potential contamination sources of shallow groundwater as the fracking fluid and formation waters have their own isotopic signatures which can be traced (Sharma, et al., 2014; Warner, et al., 2014).

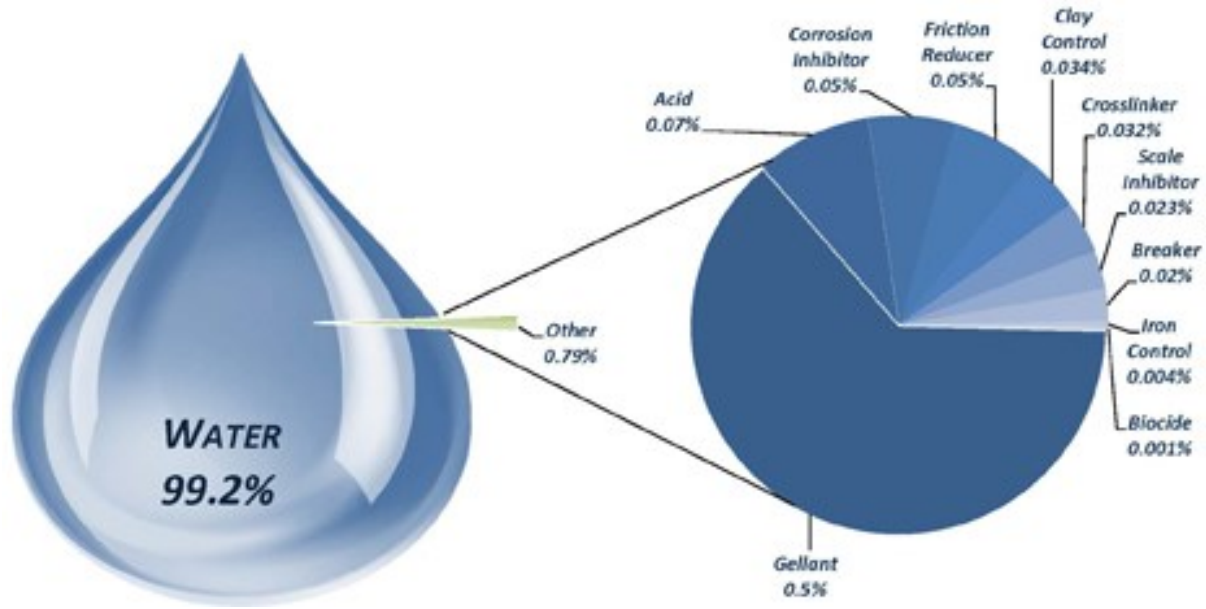

Figure 2: *Average hydraulic fracturing fluid composition for shale plays in the USA (FracFocus, 2015).*

1.3.3.3 Stray gas and well integrity

Leaking of stray gas is a result of either poorly constructed and maintained wells/casings, or the result of gas escaping through faults or fissures created in the shale layers through high volume fracking (Jackson, et al., 2014). The integrity of deep boreholes may also be compromised decades or centuries after abandonment through the slow degradation of the sealing cements used in borehole grouting and plugging (Vengosh, et al., 2014; Flewelling, et al., 2013). Likewise, the high pressure fracking process may marginally open existing fractures that were previously impermeable and thus allow for the very slow upward migration of deep-seated groundwaters (Sharma, et al., 2014). It is also possible that it is only in years to come that the impact of fracking on upward movement of water through old or new faults and fractures will be felt (Flewelling, et al., 2013). The most important step in addressing the issue of stray gas it to record natural gas emissions before fracking occurs and monitor these levels during and after fracking occurs. This can be done by doing baseline studies of drinking water wells in close proximity to the potential fracking areas before fracking commences and isotopically identifying the signatures of the natural gas that is present. Studies show that by using isotopic signatures and hydrocarbon ratios it is possible to trace the dissolved gases in order to determine the source of the stray gas (Osborn, et al., 2011). For example, studies conducted on the Marcellus Shale Formation concluded that the source of stray gas was indeed from the Marcellus shale production gases as they had matching isotopic signatures and hydrocarbon ratios (Osborn, et al., 2011; Warner, et al., 2014). In contrast, other studies suggested that the stray gas was linked to topographic factors, meaning that the stray gas

was of natural origin and not as a result of fracking activities (Molofsky, et al., 2011). Levels of gas concentrations should be monitored during the fracking process and once the drilling wells have been abandoned (Osborn, et al., 2011).

1.3.3.4 Contamination of shallow groundwater and surface water

As previously mentioned, one of the primary concerns of fracking is the potential contamination and pollution of groundwater. Four potential risks to water resources were outlined by (Vengosh, et al., 2014; Jackson, et al., 2014; Vengosh, et al., 2013; Warner, et al., 2012; Jackson, et al., 2013) and mentioned in Section 1.1. In summary, the possible sources of contaminants are stray gas, chemical additives in fracking fluid, waste material containing radioactive components as well as poor quality, deep groundwater. Contamination from stray gas and waste material could occur through leakages in the wells or from accidnetal spills on the surface. Elevated levels of methane and other hydrocarbons in shallow groundwater may cause flammability risks to homes and private boreholes (Vengosh, et al., 2014). The contamination of shallow groundwater aquifers with poor quality deep groundwater has occurred in Pennsylvania, USA, particularly in the Marcellus Shale play. Contamination occurred as a result of upward migration of brine formation water into the fresh, shallow aquifers (Warner, et al., 2012). In some instances the TDS of this brine water has been measured as high as 200000 $mg.L^{-1}$ (Haluszczak, et al., 2013). It is therefore crucial to have an understanding of the chemical characteristics of the deep groundwater in order to determine how it could potentially affect good quality, shallow groundwater (Warner, et al., 2012; Sharma, et al., 2014).

1.3.3.5 Wastewater disposal

Wastewater produced as a result of fracking activities includes flowback water which is defined as the fluids that return to the surface after they are injected into deep wells (Vengosh, et al., 2014). Within the flowback water is between 10 and 40% of the fracking fluid as well as produced water which is defined as the water that flows to the surface during the production of the gas (Vengosh, et al., 2014). The outstanding 60 to 90% of the fracking fluid remains underground. In some cases the produced water is saline to hypersaline (TDS of between 35000 and 200000 $mg.L^{-1}$) and contains naturally occurring yet harmful elements such as barium, arsenic and mercury (Jackson, et al., 2014; Engelder, et al., 2014; Theodori, et al., 2014). More than 7.5 trillion litres of wastewater are produced daily in the United States from oil and gas production (Jackson, et al., 2014). Currently there are several methods of disposing of the wastewater, including deep underground injection. However, it is unclear how this may affect seismic activity (see Section 1.3.3.6) (Vengosh, et al., 2014). Another method of disposal is sending the wastewater to advanced treatment facilities where it is treated by

methods such as desalinisation (Engelder, et al., 2014). However, potential leaks and spills during either the transporting of the wastewater or while it is being stored in ponds near the drill site, as well as illegal disposal of untreated or inadequately treated wastewater, poses a threat on the surface water and soil of the surrounding environments (Vengosh, et al., 2014; Engelder, et al., 2014).

1.3.3.6 Microseismicity and earthquake risk assessment

Induced microseismicity either from the fracturing of the shale layers or from the deep injection of wastewater is another concern regarding the process of fracking. As mentioned in Section 1.3.3.3 Stray gas and well integrity, further fracturing may open up the possibility of leaking of stray gas and/or upward migration of poor quality deep-seated groundwater (Flewelling, et al., 2013). A study conducted throughout North America by Flewelling, et al., (2013) measured the height of fractures and recorded seismic activity during fracking with magnitudes in the range of -4.4 to 0.86, although seismic events with negative magnitudes are not felt by humans (USGS, 2015). However, based on the magnitude of the seismic activity, Flewelling et al., (2013) concluded that connectivity between the deep shale formations and shallow, potable aquifers is unlikely to occur. On the other hand, Ellsworth, (2013), concluded that deep injection of wastewater and material were a more likely cause of earth quakes and microseismic activity.

1.3.3.7 Air, noise and visual pollution

The production of shale-gas results in atmospheric emissions from various sources. This is inclusive of large amounts of dust from the drilling of the wells, the noise of the drilling and production activities, leaking of stray gas from the wells and the visual pollution caused by the drill sites (Figure 3) (Pacsi, et al., 2015). A large number of vehicles transporting water, gas and waste materials to and from the drill sites will increase carbon monoxide (CO) emissions in the atmosphere (Adgate, et al., 2014). The CO_2 emissions produced during the fracking process are less than that of oil and coal production (Jackson, et al., 2014). However, it is unclear how stray natural gas emissions will impact ozone concentrations (Pacsi, et al., 2015).

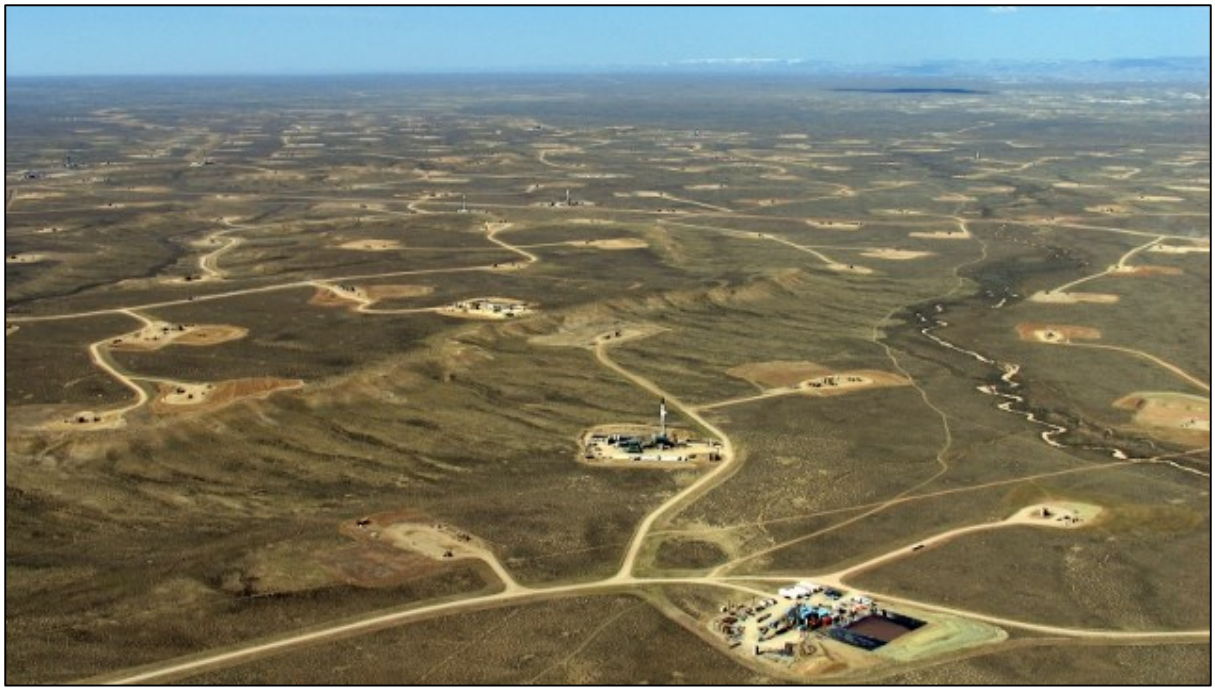

Figure 3: *An example of the visual pollution caused by fracking in agricultural areas on the USA (Fox, 2012).*

1.3.4 The economics of shale gas

From a South African economic perspective, fracking would result in an influx of money as well as an increase in job opportunities (Dept of Mineral Resources, 2012; Weber, 2014). However, it is important that the government receives a large proportion of the income generated in order to return it to the population in the form of upgraded infrastructure. The potential allowance for the country's energy independence is also an appealing factor (Weber, 2014). For example, studies in China show that the natural gas industry has made an important contribution to the development of society and economy in Sichuan, China (Zhao & Yang, 2015). The GDP growth rate increased proportionally with an increase in the production of shale gas (Zhao & Yang, 2015). It is estimated that for every billion cubic feet of natural gas produced in the USA, 18.5 jobs are created (Weber, 2014). Therefore, approximately 18500 jobs are created for every TCF of natural gas produced.

1.3.5 Shale-gas potential of the Karoo Basin

The Karoo Basin is a potential shale-gas region. Approximately 275 Ma ago the Karoo Basin was a large anoxic lake. At the base of the lake, dead organic matter accumulated and was buried. After having been under high pressures and temperatures the formation of oil and gas occurred. 'Free' or conventional gas and oil has since naturally leaked away through conduits in the rocks (Roswell & De Swart, 1976), but 'tight' or unconventional gas may remain preserved in shale formations. However, it is unclear what impact the intrusion of dolerite dykes during Karoo volcanism at 170 Ma ago has had on the shale layers as heat from

intrusive rocks is known to have driven degassing processes in other areas (Boyer, et al., 2011).

A typical shale within the Ecca Group of the Karoo Supergroup consists of quartz, muscovite, clay (illite), chlorite, plagioclase and pyrite as an accessory mineral (Geel, et al., 2013). More specifically the Whitehill Formation (of the Ecca Group), is considered the prime target for shale-gas development. The Whitehill Formation is a shale that contains fine grained and finely layered black shale that consists mostly of clay (illite) (Geel, et l., 2013). The shale contains a high quartz content of approximately 50%, a thermal maturity of between 1 and 4% is prevalent and the formation has a high TOC averaging at 4.5% (Geel, et al., 2013). The Whitehill Formation is between 2000 and 4000 m deep, and has a thickness of between 10 and 80m (Roswell & De Swart, 1976). The Karoo Basin covers a vast area and has a regional continuity of approximately 200000km^2. These factors contribute to making the Karoo Basin a potentially economically viable shale-gas region.

1.4 Deep groundwater

One of the main driving factors for this project was the potential contamination of the shallow groundwater aquifers in the Karoo Basin. The region is already water stressed (annual precipitation typically less than 400mm/year) and an important agricultural region, therefore any contamination to the scarce groundwater resources would be detrimental. Therefore, it is essential to have an in depth understanding of the deep groundwater in the Karoo Basin.

1.4.1 Characteristics of deep groundwater

Of the wide variety of chemical and isotopic geochemical tracers available, many can be used to fingerprint generic deep groundwater or specifically groundwater in the Karoo Basin. Groundwater found at depth typically has a higher temperature than groundwater found in shallower aquifers. In the Karoo Basin, this is the result of the geothermal gradient since there are no other significant heat sources in the area, such as granites or other hot intrusive rocks. However, some groundwater may migrate slowly from depth, allowing the temperature to cool and obscuring the deep source. Therefore, other geochemical parameters also need to be assessed.

Major ion concentrations are important as they give an indication of the geochemical processes and water-rock interactions occurring in the aquifers. For example, ion exchange within clay rocks leads to replacement of calcium (Ca^{2+}) and magnesium (Mg^{2+}) with sodium (Na). Therefore, groundwater with longer residence times should have a higher Na concentration and higher (Na+K)/(Ca+Mg) ratio than shallow groundwater. This has been established in Karoo aquifers (Vogel, et al., 1980; Tredoux & Kirchner, 1981; Talma, 1981). In

contrast, the behaviour of Mg^{2+} is opposite to that of Na^{+}. The divalent bonds of Mg^{2+} atoms are bound more tightly during ion exchange within clays, resulting in low concentrations of Mg^{2+} in deeper groundwater (Vogel, et al., 1980). Elevated nitrate (NO_3^-) concentrations in groundwater generally result from agricultural or human activities. In semi-arid regions shallow groundwater also contains nitrate produced by nitrogen fixing bacteria in soils (Tredoux & Talma, 2006; Tredoux, 2009). Nitrate levels can be reduced in older water as a result of the reducing conditions that develop over the course of time (Heaton, et al., 1983). Kent (1949) noticed that higher fluoride (F^-) concentrations occur in warmer groundwater than in nearby cool water in the Karoo Basin. Woodford and Chevallier (2002) found evidence to suggest a relationship between F^- concentrations and age, origin and temperature of groundwater throughout the Karoo Basin. Ryan & Langmuir, (1993) stated that boron has great potential as a tracer of deep earth fluids and in the recycling of crustal materials in the solid earth geochemical cycle. Previous research in the Karoo also indicated higher lithium (Li^+) concentrations in deep groundwater compared to shallow groundwater (Kent, 1949).

It is a worldwide phenomenon that palaeowaters have more negative oxygen-18 ($\delta^{18}O$) values than recent groundwater because of differences in climatic conditions in comparison to those of the present (Mook, 2006). This is especially so when comparing recharge from the Pleistocene with that of the Holocene and has been observed in southern Africa (Heaton, et al., 1986; Kulongoski, et al., 2004). However, lower $\delta^{18}O$ values in groundwater can also be the result of changes of the recharge pattern in a specific location: stormy and aridity changes (Mook, 2006).

Radioactive isotopes are also important tools for differentiating deep from shallow groundwater as deeper groundwater will have lower activities as a result of decay over time. Deep groundwater is not in contact with the atmosphere from where carbon-14 (^{14}C) is derived. The original ^{14}C present in the groundwater then decays over time, resulting in decreased ^{14}C activities with longer residence times. Dissolution of carbonate rocks, which contain only ^{12}C and ^{13}C, and not ^{14}C, results in dilution of the $^{14}C/^{12}C$ ratio, thereby further decreasing the ^{14}C activities in groundwater. Similarly tritium (^3H) is transported to shallow groundwater through recharge, but decays to ^3He over time, resulting in low to negligible tritium concentrations in deeper, older groundwater (Aggarwal, et al., 2005). Typically ^3H is used as an indicator of the presence of recent (post-1960) recharge (Mook, 2006; Aggarwal, et al., 2005). Large amounts of atmospheric tritium were added by hydrogen bomb testing in the 1950s. However, ^3H values in southern African rainfall recorded as high as 100 TU in the 1960s have steadily decreased to the present 2-3 TU (Talma & Van Wyk, 2013). Chlorine-36 (^{36}Cl) is a useful tracer of old groundwater and the ratio of $^3Cl/Cl$ is commonly used in dating old groundwaters. The initial ^{36}Cl content of groundwater is determined by the levels present

in rainwater. During underground flow, the total chloride in groundwaters typically increases through leaching of some sort. The complexity of the evolution of the Cl content and its isotope ratio reflects the complexity of its geochemistry over time. Nevertheless, many aquifers show decreasing $^{36}Cl/Cl$ ratio with time/downflow, making it a useful tracer for water age (Phillips, 2013).

1.4.2 Deep groundwater in the Karoo Basin

Little research has been conducted on the deep groundwater sources in the Karoo Basin, resulting in a lack of understanding of the deeper groundwater. In the 1960's Southern Oil Exploration Corporation (SOEKOR), now known as PetroSA, drilled 24 deep boreholes (greater than 2000m) throughout South Africa as part of a project to assess the existence of economic resources of oil (Roswell & De Swart, 1976). The project was deemed unsuccessful and the boreholes were sealed. However, one of the seals has since failed on the borehole named SA1/66 in the small town of Merweville in the Western Cape. This borehole is discussed in further detail in Chapter 2. The Council for Geoscience is currently conducting a project in which three deep boreholes are being drilled in the Karoo Basin. With the exception of these boreholes and potentially a few deep mining exploration boreholes, there are no other boreholes that tap the depth at which fracking would take place, which is between 2000 and 4000m. The only two open boreholes that could be located during the sampling season for this project that access the required depths, are the originally 4169 m deep, Soekor borehole SA1/66 near Merweville, and the 1425 m deep borehole VFB1 near Trompsburg, neither of which are ideally suited to represent the geochemistry of the Ecca Group shale. However, many thermal/sub-thermal springs are scattered throughout the country and throughout the Karoo Basin, therefore these springs were selected as proxies for deeper circulating groundwater in the Karoo Basin for this project.

A temperature of 25 °C is used in general to distinguish cold from warm groundwater in South Africa (Kent, 1949). This is consistent with a global idea that groundwater is characterised as thermal when it has a temperature significantly higher than the mean annual temperature of the specific site (La Moreaux & Tanner, 2001). An average geothermal gradient of 25°C/km is assumed, therefore the depth of the origin/source of the groundwater is reflected by the temperature of the thermal spring (La Moreaux & Tanner, 2001).

1.5 The Karoo Basin

The Karoo Supergroup covers an extensive area of southern Africa (Johnson, et al., 2006). The Karoo Supergroup consists of sedimentary rocks with strata of 12km thick in the west, thinning towards the east as seen in the cross section shown in Figure 5. These sediments

were deposited into two major basins (Figure 4A). The first being the Kalahari Basin which stretches across Botswana, Namibia and central-north South Africa (Figure 4A). Secondly the Main Karoo Basin which stretches across most of central South Africa (Oesterlen, 1991) (Figures 4A and B). In this study, the Main Karoo Basin will be referred to as the Karoo Basin in South Africa. The Supergroup is of significant economic importance to South Africa, being host to all coal deposits (Johnson, et al., 1996) as well as to any potential shale-gas plays (Boyer,et al., 2011). A large uranium deposit is also situated in the western and central parts of the basin, specifically within the Adelaide Formation in the Beaufort Group (Johnson, et al., 2006).

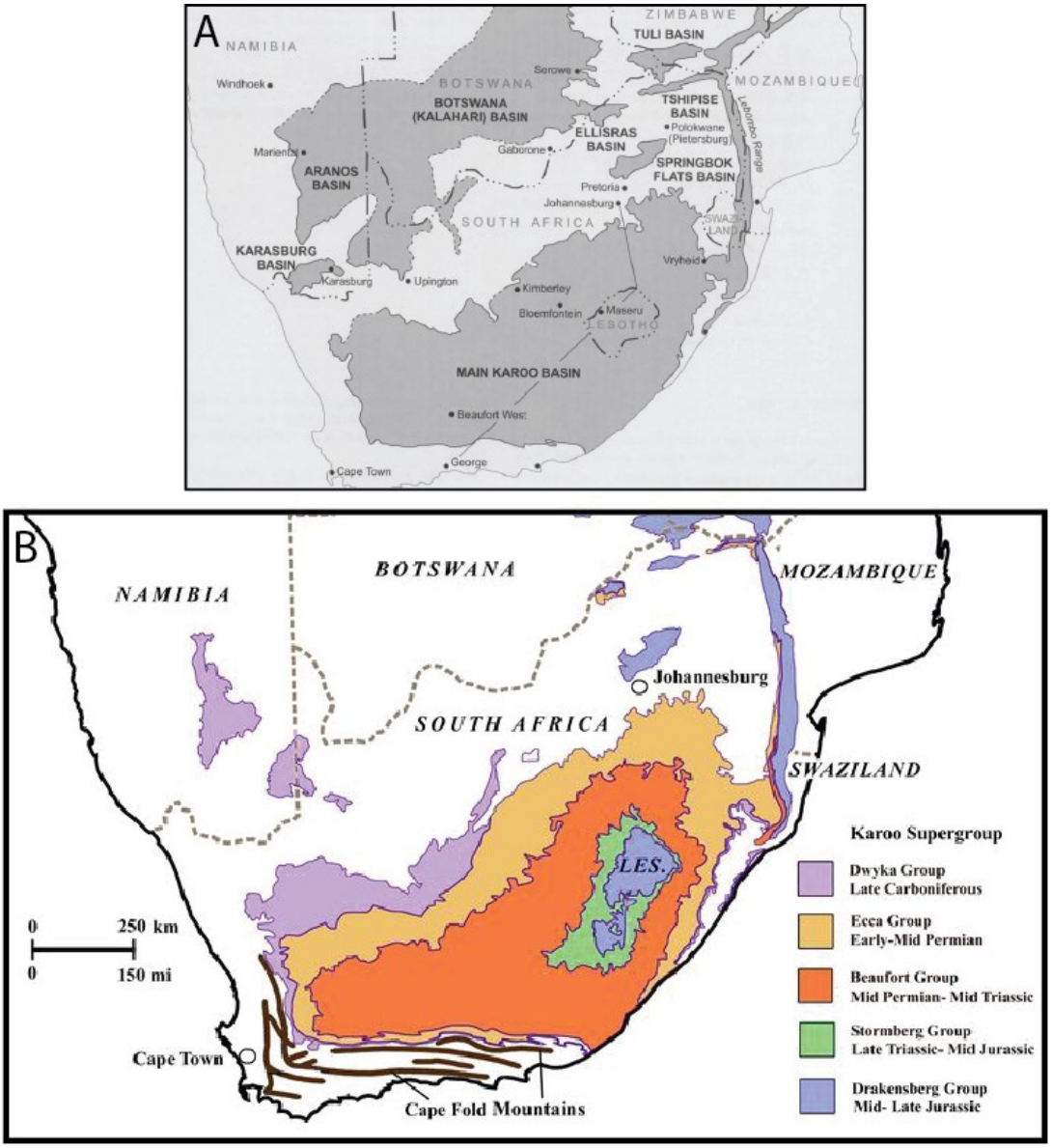

Figure 4: *A) Map of southern Africa showing the Kalahari and Main Karoo Basins; B) Simplified geology of the Karoo Basin in South Africa.*

1.5.1 Tectonic setting

The Karoo Basin developed as a retro-arc foreland basin situated behind a fold-thrust belt, known as the Cape Fold Belt (Johnson, et al., 1996) which formed during the late Palaeozoic to the mid Mesozoic (Johnson, et al., 2006; Catuneanu, et al., 2005; Cadle, et al., 1993). The majority of the Ecca and Beaufort Group Formations were derived from the arc during the Permian while the Stormberg Group was derived from the rapidly rising Cape Fold Belt during the Triassic (Oesterlen, 1991). The source of the north-eastern part of the basin was from cratonic highlands located to the north-west, north, north-east and east (Oesterlen, 1991). The remaining part of the southern basin represents intracratonic thermal sag, although evidence

of marine influence in the early stages of its development is observed in the south-western part of the basin (Johnson, et al., 2006). Faults, which most likely developed during the deposition process, occur along the northern and north-western parts of the margins of the basin (Johnson, et al., 1996). Thick sequences of course, clastic sediments occur in the Cabora Bassa and Mid-Zambezi basins in Zimbabwe and in the Waterberg basin in Namibia are associated with the faults (Oesterlen, 1991). A cross section of the Karoo Basin is shown in Figure 5.

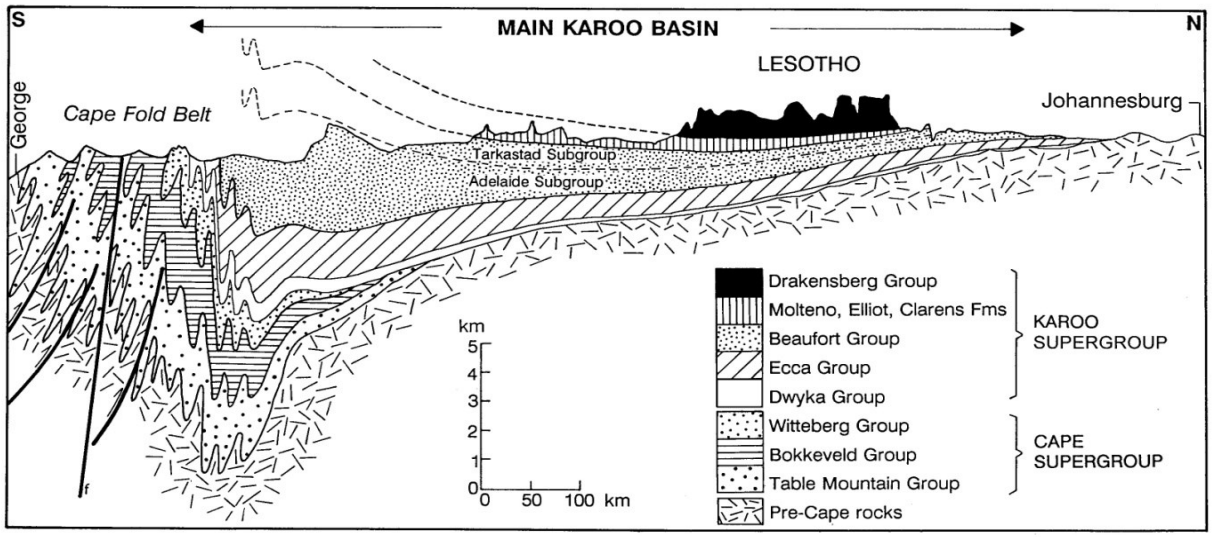

Figure 5: *Cross section of the Karoo Basin (Woodford & Chevallier, 2002).*

1.5.2 Lithostratigraphy

A general overview of the lithostratigraphy of the Karoo Basin is shown in Figure 6. The Karoo Supergroup was deposited during the late Carboniferous to the Middle Jurassic period and consists mostly of marine glacial to terrestrial deposits of sandstone and shale (Johnson, et al., 2006). The Permian Ecca group hosts the target formation for shale-gas development, the Whitehill Formation. This is underlain by the Prince Albert Formation and overlain by the Collingham Formation (Johnson, et al., 2006). The Prince Albert Formation (Lower Ecca) extends across the south-western part of the Karoo Basin and accumulated in a deep marine environment. The thickness of the formation ranges from 40 to 150m, but has been known to reach a maximum thickness of 300m in some areas (Veevers, et al., 1994). The formation can be divided into a northern facies and a southern facies based on rock composition. The northern facies consists of grey to green micaceous and silty shale, black carbonaceous shale (with a C_{org} value reaching 5.1%), fine to medium grained feldspathic arenite and wacke (Johnson, et al., 2006). The southern facies consists of grey pyrite-bearing shale, siltstone, chert and phosphatic nodules and lenses (Woodford & Chevallier, 2002)

The Whitehill Formation (Lower Ecca) ranges in thickness from 10 to 80 m and consists of black carbonaceous pyrite-bearing shale (up to 14% carbonaceous material) (Johnson, et al., 2006). The carbonaceous shale formed by suspension settling in an under-filled foreland basin in a highly anoxic environment (Veevers, et al., 1994). Within the shale cleavages, gypsum ($CaSO_4.2H_2O$) is present, which typically forms in highly evaporative conditions through reactions between sulphides (pyrite), water and dolomite (Johnson, et al., 2006). The lithology becomes less distinct towards the north-east where the lower section consists of siltstone and fine grained sandstone (Woodford and Chevallier, 2002; Geel, 2012). The Collingham Formation (Upper Ecca) ranges in thickness from 30 to 70m (Johnson, et al., 2006). It consists of alternating hard, grey, siliceous mudrock and soft, yellowish tuff (K-bentonite) (Johnson, et al., 2006). The western part of the formation consists of the Matjiesfontein Chert Bed (0.2 to 0.6 m thick), located towards the base of the formation, as well as an upper sandstone and siltstone unit (Woodford & Chevallier, 2002). The Jurassic Karoo volcanics intruded into the Karoo sediments approximately 180 Ma ago and comprise dolerite dykes, sills and ring complexes (Johnson, et al., 1996; Catuneanu, et al., 2005; Cadle, et al., 1993).

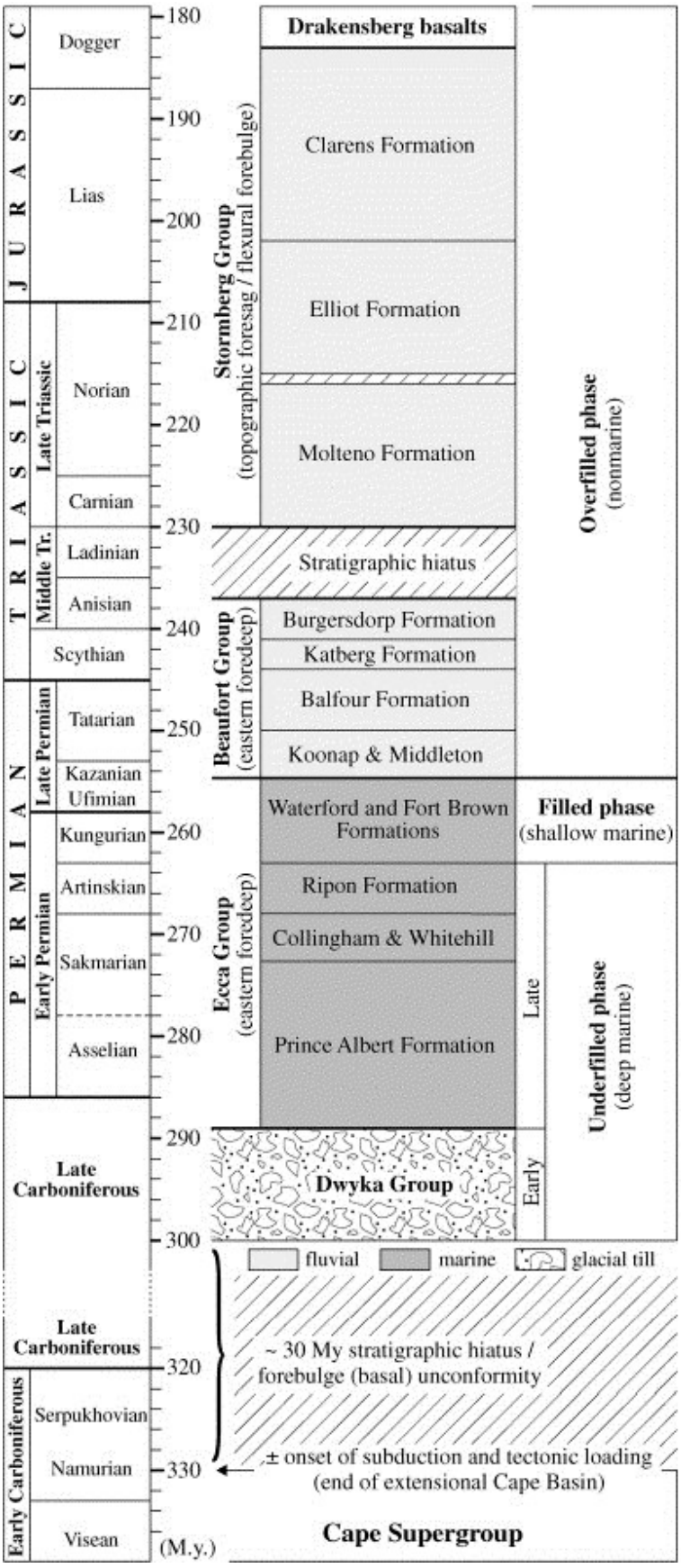

Figure 6: *Stratigraphic column with the major lithostratigraphic subdivisions of the Karoo Supergroup in the Karoo Basin of South Africa (Catuneanu, et al., 2005).*

1.5.3 Water in the Karoo Basin

The Karoo is an arid to semi-arid region with temperatures reaching above 30°C in the height of summer and below 0°C in the winter months. The main source of water in this semi-arid region is groundwater.

1.5.3.1 Groundwater

The majority of the groundwater in the Karoo is stored in shallow aquifers, which typically occur within 200m of the surface (Rosewarne, et al., 2013). Groundwater levels are commonly measured between 5 and 15m deep (Rosewarne, et al., 2013). The aquifers in the Karoo Basin are mostly hard-rock, fractured aquifers with preferential flow paths determined by secondary permeability (Rosewarne, et al., 2013; Le Maitrea, et al., 2009). These aquifers typically occur in areas receiving low precipitation and are then recharged during flood events (Le Maltre, et al., 2009). Natural and induced flow through Karoo aquifers can be thought of as being slower through the unfractured matrix and faster through fractured zones. Moreover, the quality of groundwater from these aquifers differ significantly. The quality of the groundwater changes from the local to the regional scale and is a function of the soil type, host rock lithologies, rainfall and climate. In general, groundwater sourced from fractured rock aquifers is less saline and younger than from the unfractured zones and while precipitation increases towards the east, salinity shows the opposite of this trend (Woodford & Chevallier, 2002). The permeable areas are primarily associated with dolerite dyke, rings and sills, thick alluvial deposits as well as folded and faulted formations. The deeper aquifer systems in the Karoo (deeper than 1000m), are not well understood and require more in depth research.

1.5.3.2 Precipitation

The Karoo Basin covers almost two thirds of South Africa, and hence precipitation patterns differ significantly across the country and therefore within the Karoo Basin itself. Figure 7 displays the annual precipitation throughout South Africa (Lynch, 2003) and indicates that precipitation increases from west to east across the country. On average the Karoo receives precipitation of approximately 300-400mm/year (Milton & Dean, 1999; Midgley, et al., 1994), and because of the vast size of the area, it experiences both winter and summer rainfall in different parts of the basin (Van Wyk, et al., 2011).

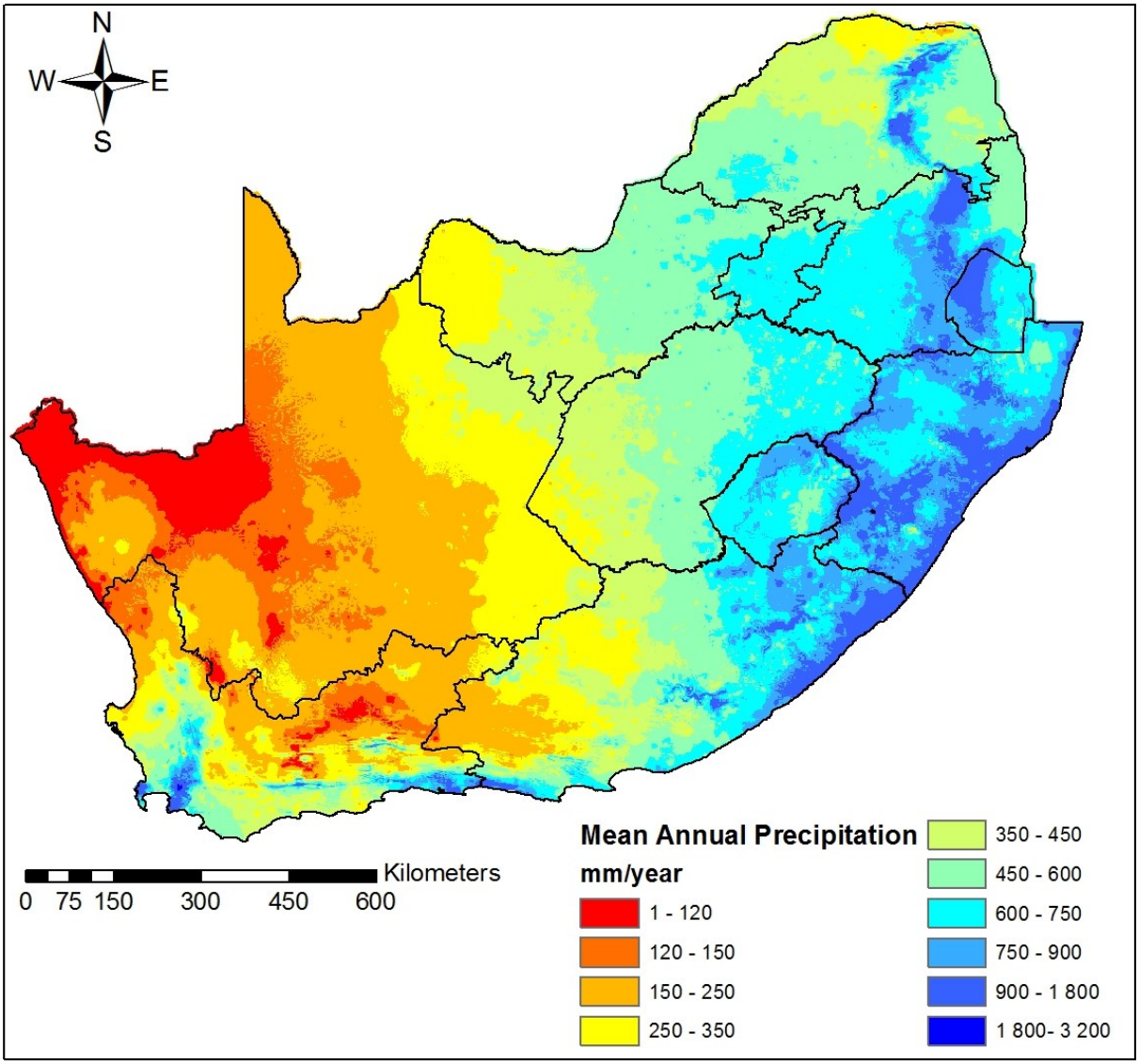

Figure 7: *Map of South Africa with the average annual precipitation in mm/year (Lynch, 2003).*

1.5.3.3 River systems

Figure 8 shows the dry, non-perennial and perennial rivers of South Africa. The Karoo Basin primarily consists of non-perennial rivers, with the exception one major perennial river, the Orange River (Le Maltre, et al., 2009). The trend of increasing precipitiation from west to east (Figure 7) is mirrored in the river systems of the country (Figure 8). Combined, Figures 7 and 8 display the severity of the dryness in the Karoo Basin, whereby reiterating the crucial need for the protection of groundwater aquifers in the region.

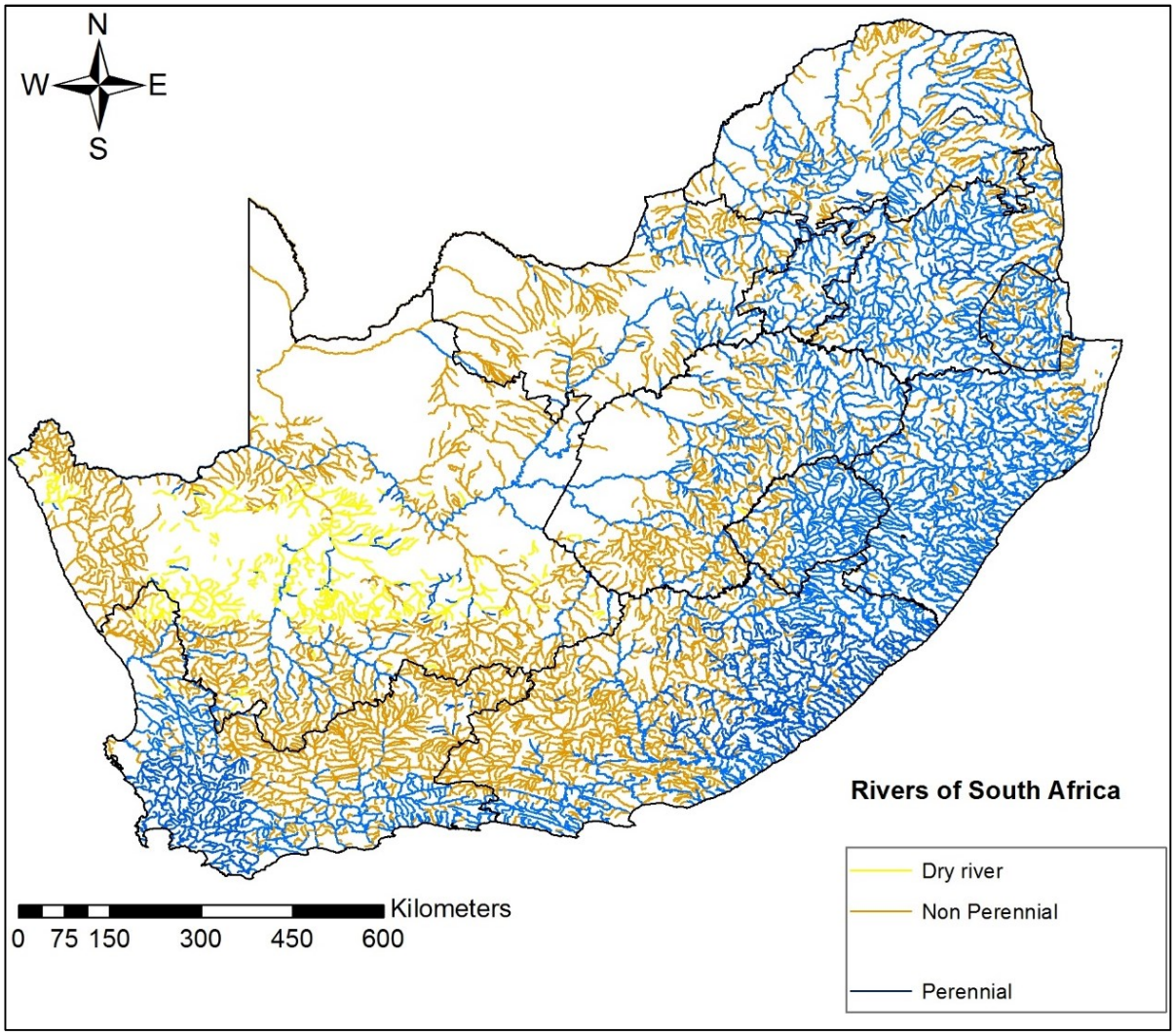

Figure 8: *Map of South Africa showing the dry, non-perennial and perennial rivers of South Africa. The shapefiles were provided by the Council for Geoscience of South Africa.*

1.6 Water Research Commission Report 2254/1/15

As mentioned in Section 1.1 above, the purpose of the WRC project was to create a baseline of the deep and shallow groundwater in the Karoo Basin for future monitoring purposes as a result of the potential shale-gas exploration in the region. The following sections outline the aims and objectives, theoretical methodology and a summary of the project findings as detailed in Murray et al., (2015).

1.6.1 Project objectives

The overall aims and objectives of the WRC project were to firstly characterise deep (warm) and shallow (cold) groundwater in the Karoo Basin. This was conducted by analysing the samples collected from boreholes and springs for major ions, trace elements, heavy metals, rare earth elements, stable and radiogenic isotopes and noble gases. Secondly, to identify specific parameters, from the above mentioned, that distinguish deep from shallow

groundwater and whether specific areas associated with shallow groundwater samples contain traces of deeper groundwater. Finally, for regulatory purposes, a list of parameters was compiled in order of monitoring importance for both shallow and deep boreholes in future shale-gas exploration and development areas.

1.6.2 Project methodology

Potential sampling locations were selected based on (1) their host lithologies being within the Karoo Formations, (2) historical information indicating the presence of warm water and/or unusual groundwater chemistry and (3) suitability for sample collection. Eight final locations were selected throughout the Karoo Basin (see Chapter 2 for full descriptions of each location). Sampling took place in June/July of 2014. One deeper site and one shallow site in close proximity to the deeper site was required at each location in order to compare and contrast groundwaters from the deeper and shallow groundwater systems within the same area. At some locations, more than one shallow sample was collected.

1.6.3 Characterisation of groundwater types

The 19 groundwater samples collected were initially grouped into provisional deep and shallow categories based on measured temperature or in a couple of cases historical temperature. However, it became clear that some ‘shallow’ samples were more distinctive of deep groundwater based on other geochemical parameters. Therefore, the data was put through a second assessment using major ion chemistry in the form of standard Stiff diagrams. From these two assessments, the groundwater samples were classified into three groups: deep, shallow and mixed. The assessment using temperature and the shape of the stiff diagram was then validated by the radiocarbon content of the samples (Figures 9, 10 and 11). In summary, the shallow groundwater was characterised by a hexagonal shaped Stiff diagram, high radiocarbon content of above 60 pmC and a temperature below 25°C. In contrast the deeper groundwater was characterised by a ‘Y’ shaped Stiff diagram, low radiocarbon content and a temperature above 25°C. The mixed group has ambiguous shaped stiff diagrams and intermediate radiocarbon contents and temperatures. The major ion chemistry and remaining geochemical parameters are discussed in further detail in Chapter 2, and the radiocarbon data and remaining radiogenic isotopes are discussed further in Chapter 3.

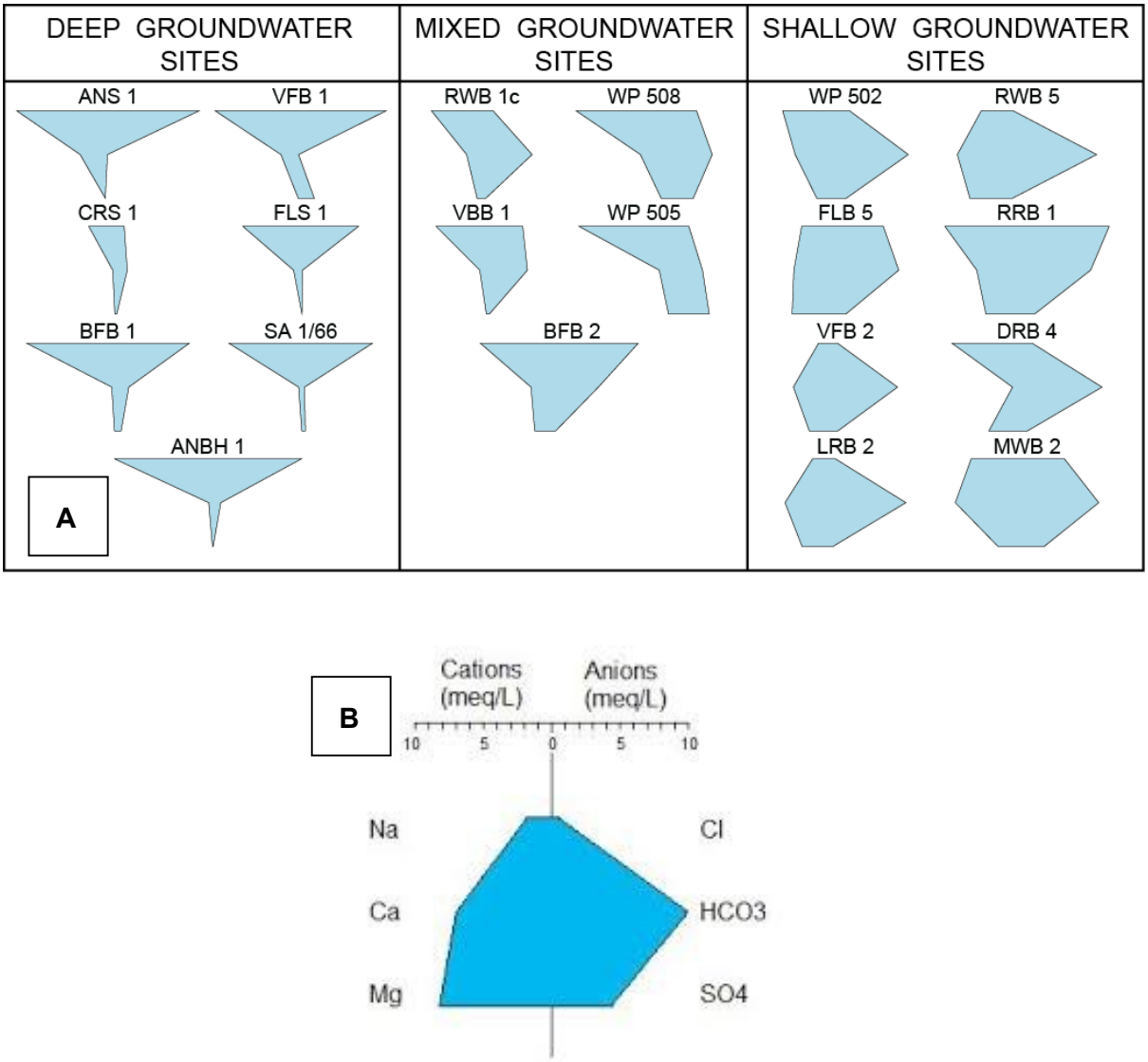

Figure 9: *A) Presentation of all Stiff diagrams of samples separated into the three groundwater depth groups; B) key for a Stiff diagram.*

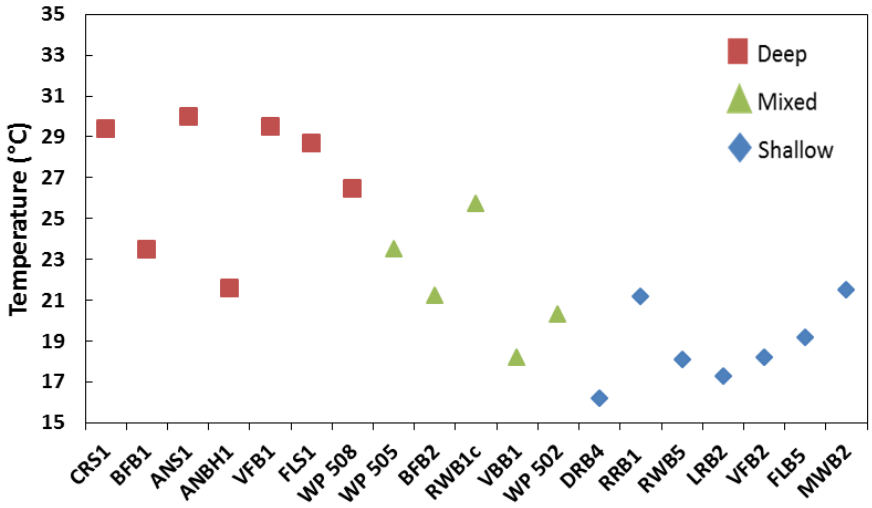

Figure 10: *Groundwater temperatures versus the site names of the samples collected in the Karoo Basin. Red squares = deep sites, blue diamonds = shallow sites, green triangles = mixed sites.*

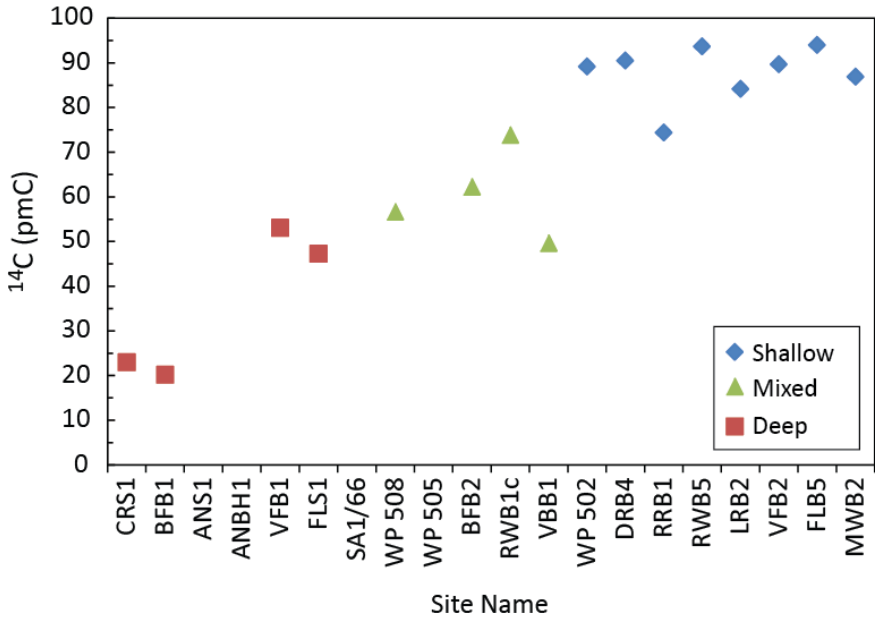

Figure 11: *^{14}C values versus the site names of the samples collected in the Karoo Basin separated into the three groundwater depth groups. Red squares = deep sites, blue diamonds = shallow sites, green triangles = mixed sites.*

1.6.4 Assessment of potential deep groundwater indicators

All of the geochemical parameters analysed during the project were divided into four groups, based on how successfully they were able to differentiate between deep, shallow and mixed groundwater samples (Table 1). Group 1, consisting of ^{14}C, δ^{18}O, δ^{2}H, fluoride, % sodium, magnesium, uranium and alkalinity, would be the first choice in any groundwater monitoring program in the Karoo Basin where shale-gas exploration is being considered. Group 4, whilst not being particularly useful in this study may provide further information on contamination processes after shale-gas development and hence should also have their place in any monitoring program. Of the original parameters described as being indicative of deeper

circulating groundwater identified in Section 1.4.1 Characteristics of deep groundwater, ^{14}C, $\delta^{18}O$, fluoride, percentage Na (but not Na concentration in $mg.L^{-1}$) and Mg were very successful at differentiating deep from shallow groundwater. However, uranium (U) concentrations and alkalinity ($mg.L^{-1}$ of HCO_3^-), which were not identified in the original list of parameters, had the same success rate. The remaining parameters that were analysed had variable success rates.

Table 1: *Ranking of all determinands in classification matrix for prioritisation in long term monitoring of deep groundwater in the Karoo*.

Group	Success Rate	Specific Determinands
Group 1	100%	**^{14}C, $\delta^{18}O$, $\delta^{2}H$, fluoride, %sodium, magnesium, uranium, alkalinity**
Group 2	>75%	**Boron, vanadium, lithium, $\delta^{11}B$, $^{36}Cl/Cl$, $^{222}Radon$, H_2S**
Group 3	50-75%	**Sodium, pH, tritium, nitrate, temperature, ^{4}He, $^{3}He/^{4}He$, CH_4**
Group 4	< 50%	**$^{87}Sr/^{86}Sr$ ratios, $\delta^{13}C$, rare earth elements, other trace elements**

Figure 12 shows the range and median for the deep, shallow and mixed groundwater samples for each of the seven parameters (with the exception of δ^2H) that 100% successfully classified the samples into the three groundwater depth groups (Group 1 in Table 1). It is clear from this that whilst the median is distinct for the deep, shallow and mixed samples, the total range in values for each parameter in many cases overlaps and somewhat reduces the potential effectiveness of the classification scheme. However, much of the overlap lies within the mixed samples and the deep and shallow samples are quite distinct from one another.

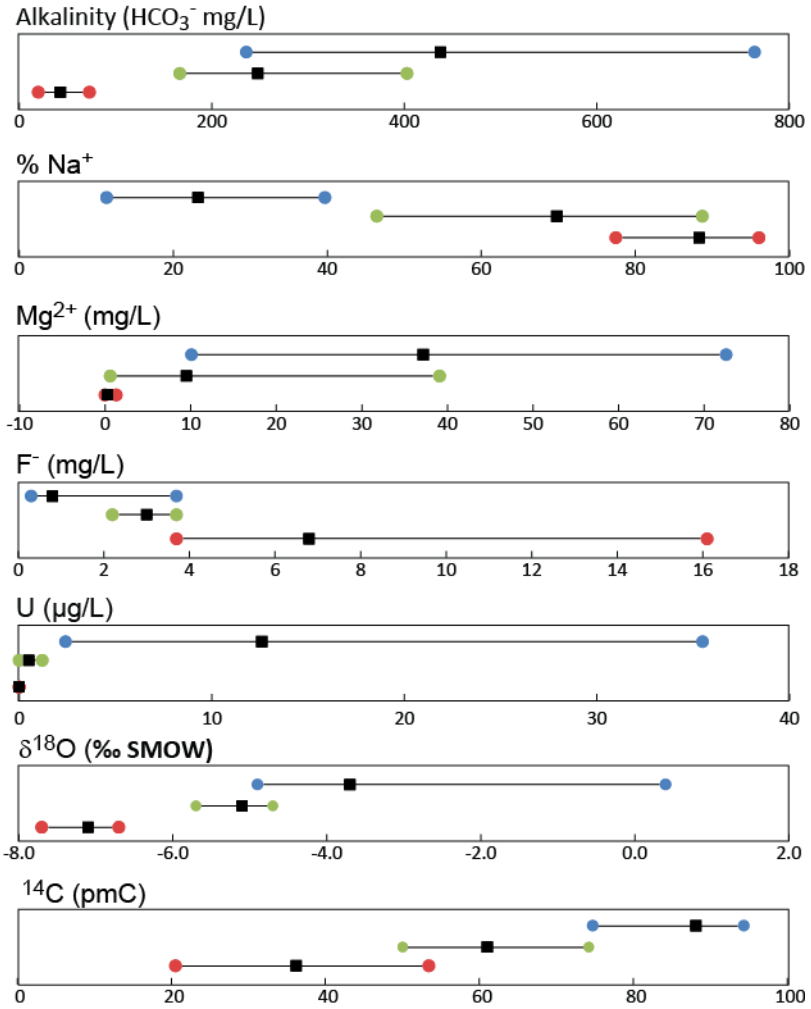

Figure 12: *Diagrams indicating the ranges and medians of the seven parameters that are most successful to identify deep as well as shallow water. Red = deep sites, blue = shallow sites, green = mixed sites.*

1.6.5 Monitoring recommendations

For operational and exploratory purposes, there are a number of other factors besides scientific strength that must be considered when determining which parameters are the most useful and practical indicators of deep groundwater. The most important of these are: (1) cost per analysis; (2) sampling difficulty; (3) the time needed for analysis; and (4) the availability of suitable analytical laboratories in South Africa. Table 2 is an attempt to produce a score card weighting these different factors. It provides an evaluation of these individual factors by giving them a (subjective) weight, based on the experience of the authors of the WRC report.

Table 2: *Ranking of all determinands based on reasons other than success rates for operational and exploratory purposes in the Karoo Basin.*

Group	Reasoning	Specific Determinands

Priority 1	Easy to obtain, cost effective and available in South Africa	**$\delta^{18}O$, $\delta^{2}H$, uranium, alkalinity, pH, temperature**
Priority 2	Relatively easy to obtain and available in South Africa but less useful than P1 determinands	**Vanadium, lithium, ^{222}Radon, H_2S**
Priority 3	More difficult to analyse, time consuming and higher cost	**^{14}C, ^{3}H, $^{87}Sr/^{86}Sr$, rare earth elements**
Priority 4	Not currently available in South Africa	**$\delta^{11}B$, $^{36}Cl/Cl$, ^{4}He, $^{3}He/^{4}He$, CH_4**

1.6.6 Deep groundwater indicators versus tracers of shale gas development

The WRC project focussed on identifying natural constituents of groundwater which can successfully differentiate deep from shallow groundwater and includes most of the determinands listed in Table 1. However, it is important to note that some geochemical parameters that were not important for differentiating deep from shallow groundwater within the scope of the WRC project, such as $^{87}Sr/^{86}Sr$ ratio, Br/Cl ratio, $\delta^{13}C$ and $\delta^{11}B$, might become relevant once the properties of deep groundwater from the shale bearing formations become known. These have been shown to be of importance in other shale-gas plays, in particular for isotopically fingerprinting fracking fluids.

1.7 Scope of thesis

This thesis is divided into four parts. Part one of this thesis identified the potential problems associated with fracking, summarized the results obtained in the WRC project (Murray, et al., 2015) and also outlines the aims and objectives of this project. Part two of this thesis will further assess the remaining geochemical parameters analysed in this project and investigate the differences observed between the three groundwater depth groups. In part three of this thesis I will estimate residence times of the groundwater samples collected using four different isotopes. I will then compare the residence times calculated with the various isotopic tracers in order to assess the robustness of the residence times. Part four of the thesis is the general conclusion chapter. This will amalgamate the results of Chapters 2 and 3, and evaluate their findings in terms of potential future fracking activities in South Africa. Chapters 2 and 3 form the basis of two publications that intend to be published.

CHAPTER 2 – Distinguishing groundwater systems using hydrochemical characteristics

2.1 Introduction

In semi-arid to arid regions of southern Africa, groundwater is a critical resource. Low precipitation coupled with high evaporation rates means that local communities, consisting of both subsistence and commercial farming practices, are dependent on the groundwater resources. The Karoo Basin in South Africa is regarded as a water stressed region receiving on average between 300 and 400mm/year of rainfall coupled with a semi-arid climate (Milton & Dean, 1999). With shallow groundwater aquifers being the primary source of water in the Karoo, considerable effort has been put into understanding the shallow groundwater system (e.g. Heaton & Vogel, 1979; Woodford & Chevallier, 2002; Vermeulen, 2013; Talma & Esterhuyse, 2015). In contrast, significantly less effort has gone into understanding the deeper groundwater system, largely because of difficulties in accessing this system. Thermal springs in existence throughout South Africa have been the focus of various projects monitoring and recording their temperatures and chemical compositions over at the last century (Shabalala, et al., 2015; Kent, 1949; Kent, et al., 1966; Mazor & Verhagen, 1983; Olivier, et al., 2012; Olivier, et al., 2008; Rindl, 1916). As discussed in Chapter 1, it is thought that the thermal springs represent the closest approximation to deep groundwater in the Karoo Basin.

The region has been identified as a potential source of unconventional shale-gas to be extracted using hydraulic fracturing (fracking). This has caused considerable concern amongst various stakeholders regarding the potential impact on the surrounding environment. In particular, there is much concern on how fracking could potentially contaminate the already scarce groundwater resources in the Karoo through pollution with fracking fluids, poor quality deeper groundwaters and flow back fluids from the fracking process. Therefore, it is essential to have an understanding of the shallow aquifers and their natural connectivity to deeper aquifers. Should the shallow groundwater aquifers be contaminated as result of the fracking processes it would detrimental to the farmers and local communities in the Karoo Basin. Particular interest in the oil and gas resources of the Karoo Basin began in the 1960s when SOEKOR, now PetroSA, drilled 24 deep boreholes in order to evaluate potential oil resources in the region (Roswell & De Swart, 1976). When this exploration project was deemed unsuccessful the boreholes were filled in with cement and abandoned. However, the seal failed on one borehole, namely SA1/66, which is discussed in detail in Section

2.3.1.8 Merweville. More recently, the potential unconventional shale-gas resources in the Karoo Basin have given rise to baseline monitoring projects such as Murray, et al., (2015) (see Chapter 1) This study focussed on characterising different groundwater depth groups (deep, mixed and shallow groundwaters) in the Karoo Basin using a wide variety of environmental and geochemical tracers and isotopes (summary given in Chapter 1). However, explanations for the geochemical differences observed between the three groundwater depth groups were not fully discussed.

It is uncertain what main factors and processes are responsible for the significant distinctions observed between the deep, shallow and mixed groundwater samples mentioned in Chapter 1. In this chapter multiple geochemical parameters are used to recognise redox conditions, geochemical processes such as the precipitation or dissolution of minerals and also to identify depositional environments and the potential sources/origins of the parameter (Edmunds & Smedley, 2000; Phillips, 2013; Kim, et al., 2003; Elliot, et al., 1999; Adams, et al., 2001). The objective of this chapter is to evaluate the geochemical differences observed between the three groundwater depth groups of the samples collected throughout the Karoo Basin and assess the potential explanations for the differences. It is debated whether increased residence time, redox reactions or interactions with host rock lithologies dictates the geochemistry of the groundwater.

The future of fracking in the Karoo Basin is currently unclear. However, we should proceed as if it will become a reality at some point in the future. Therefore, it is essential to have an in depth understanding of the geochemical processes occurring in the groundwater before any exploration or fracking takes place. Assuming the natural gas reserves are proven to be economical, this knowledge about the groundwater will aid in making an informed decision about the environmental impacts associated with fracking. By understanding the current connectivity and mixing processes occurring in the groundwater, it will enable us to create a monitoring baseline applicable specifically to the groundwater of the Karoo Basin. This will result in being able to quickly identify any contamination issues which would be detrimental to the groundwater resources as well as the communities and agricultural activities dependent on them. Therefore, by understanding the natural hydrogeochemical processes and quantifying water-rock interaction occurring between the different aquifer systems, it will allow for the effective management of the groundwater for future monitoring schemes to occur. Proper management of the scarce groundwater resources is also crucial for future economic development of the Karoo Basin.

2.2 Geological overview

The Karoo Basin developed as a retro-arc foreland basin situated behind the fold thrust belt known as the Cape Fold Belt located in south-west Gondwana (Johnson, et al., 2006; Johnson, et al., 1996; Catuneanu, et al., 2005; Cadle, et al., 1993). It covers an area of over 200 000 km^2 representing approximately two thirds of South Africa (Johnson M. R., et al., 2006). The basin is comprised of a succession of sedimentary strata (shale, sandstone and mudstone) of the Karoo Supergroup, overlain by basaltic lavas belonging to the Jurassic Karoo Volcanic Province. The intracratonic basin was active for approximately 100 Ma from the Permo-Carboniferous (280-310Ma) until early Jurassic, when the Karoo sedimentation finished with the breakup of Gondwana supercontinent (Catuneanu, et al., 2005; Cadle, et al., 1993; Johnson, et al., 1996).

The Karoo Basin trends east-west and thins to the north with the thickest sedimentary packages, up to 12km thick, found in the central part of the basin. The Karoo Supergroup includes several groups, in stratigraphic order from bottom to top: Dwyka, Ecca, Beaufort, Stormberg and Drakensberg (Johnson, et al., 2006). Sedimentation of the Dwyka group began when Gondwana was located over the South Pole which resulted in an ice sheet covering the basin and depositing glacial sediments, mainly tillite, at the base of the basin (Cadle, et al., 1993; Johnson, et al., 2006). The lower Ecca Group formed in a shallow marine environment resulting in the deposition of marine clays and muds, while the upper Ecca Group was deposited in a deltaic environment from where it then shifted into the Ecca Sea (Cadle, et al., 1993; Johnson, et al., 1996). The Whitehill Formation of the Ecca Group consists of black carbonaceous shale that weathers white allowing it to be differentiated from other shale units in the basin (Johnson, et al., 1996). The Beaufort Group was formed during the deposition of fluvial sediments on the alluvial plain. The Elliot Formation of the Stormberg Group consists of redbeds which formed due to the aridification and tectonic deformation of the basin (Johnson, et al., 2006). The Clarens Formation of the Stromberg Group was formed as a result of wind-dominated deposition (Catuneanu, et al., 2005). The Drakensberg Group intruded into the Karoo Supergroup approximately 180 Ma ago in the form of dolerite dykes and sills (Johnson, et al., 2006).

2.3 Sampling procedures and analytical techniques

Following an initial assessment of various databases and literature, several suitable deep groundwater sampling sites were selected based on their agreement with the following criteria: 1) the sites are situated within the Karoo Supergroup and located throughout the Karoo Basin; 2) the presence or historical evidence of warm/thermal water; 3) evidence of unusual groundwater chemistry with similarities to other known warm/thermal spring/borehole water

(Kent, 1949; Kent, 1969; Heaton & Vogel, 1979; Mazor & Verhagen, 1983; Vogel, et al., 1980). Sites considered to be suitable were visited in January of 2014 to assess their access and sampling suitability. The final sampling locations are shown with the simplified geology of the Karoo Basin in Figure 13.

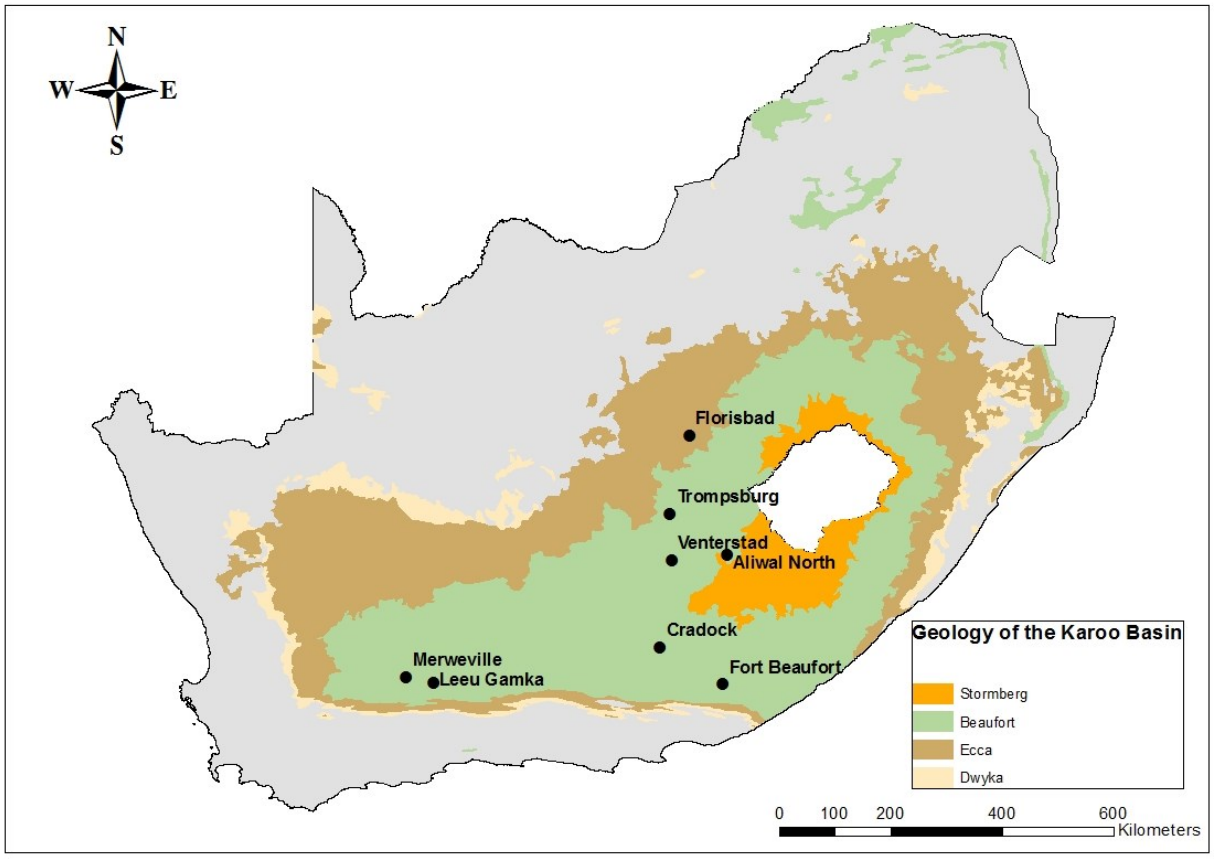

Figure 13: *Map of South Africa including simplified geology of the Karoo Basin with the 8 sampling locations (Shapefiles provided by Council for Geoscience of South Africa). The Stormberg, Beaufort, Ecca and Dwyka Groups are shown.*

2.3.1 Study locations

Sampling was carried out in June-July of 2014 for two weeks. Eight locations throughout the Karoo Basin (Figure 13) were selected for the sampling of deeper groundwater and within a few kilometres of these sites, one or two shallow boreholes were selected to represent shallow groundwater. Descriptions of the sampling locations and specific sites within the locations are given in the sections below. Where available, specific information regarding the boreholes is given, such as total depth of the borehole and depth to water. Table 3 gives a summary of the town name, location/farm name, and what depth/type of groundwater was sampled.

Table 3: *Summary of the Town, sampling locations, farm names and site names.*

Town	Location	Deep	Shallow	Mixed
Florisbad	Florisbad Spa	FLS1		
Florisbad	Private farm		FLB5	
Trompsburg	Vlakfontein	VFB1	VFB2	
Venterstad	Vaalbank/La Rochelle		LFB2	VBB1
Venterstad	Rooiwal		RWB5	RWB1c
Aliwal North	Aliwal North Spa	ANS1		
Aliwal North	Private farm	ANBH1		
Cradock	Cradock Spa	CRS1		
Cradock	Private farm		DRB4	
Fort Beaufort	Bath Farm	BFB1	RRB1	BFB2
Leeu Gamka	Kruidfontein			WP 508
Leeu Gamka	Groot Kruidfontein		WP 502	WP 505
Merweville	Private farm		MWB2	

2.3.1.1 Florisbad

Florisbad is situated approximately 50km north-west of Bloemfontein in the Free State Province. The area consists of surficial Quaternary aeolian sand deposits and calcretes which are underlain by Ecca and Beaufort Group sediments (predominantly shales, siltstones and sandstones) which in turn rest on lavas of the Ventersdorp Supergroup. These basement lavas overlie Archean granites and gneisses (Grobler & Loock, 1988; Loock & Grobler, 1988). There are numerous dolerite sills and dykes in this area. The warm site, FLS1 (Figure 14A), was collected from a spring that sits in a topographically low-lying area at the edge of a salt pan and has a fairly constant temperature of 29°C since first measured in the early 1900s (Rindl, 1916). The spring now discharges into an enclosed pool from which the sample for this project was collected. The shallow site is a borehole, FLB5 (Figure 14B), and is located approximately 2km away from FLS1 on a private farm, also in a topographically low-lying area. The borehole is approximately 36m deep and the water emanated with a high pressure flow. The main use of the groundwater is for domestic and agricultural purposes.

Figure 14: *The two deep sites in Florisbad, A) FLS1 collected at the Florisbad spa resort; B) FLB5 collected on a private farm approximately 2km away from FLS1.*

2.3.1.2 Trompsburg

A deep, warm, artesian borehole, VFB1 (Figure 15A), lies approximately 15km north-west of the small agricultural town of Trompsburg between Colesberg and Bloemfontein in the Free State Province. The borehole was drilled in the late 1940s and water was struck in the mafic basement rocks at a depth of approximately 1425m, therefore the artesian flow is sourced from these basement rocks (Anhaeusser, 2006). This is supported by the highly radiogenic Sr isotope ratio which is discussed in the sections below. It is unclear whether there is any contribution from deep circulating groundwater within the Karoo Supergroup lithologies (Kent, 1949). Drilling records show that the area is underlain by the Adelaide Formation of the Beaufort Group, consisting of sandstones interbedded with mudstones to a depth of approximately 150m (Anhaeusser, 2006). Thereafter, lie Ecca Group shales to approximately 700m, and then a thin lens of Dwyka Formation tillites (less than 25m thick). These Karoo-age rocks lie unconformably on intrusive gabbro-anorthosite basement rocks (Archean granites and gneisses) which in places have a layer of marble in between. The area has also been intruded by Karoo dolerite dykes, sills and ring structures which are all visible at the surface (Anhaeusser, 2006). The shallow site for this location is a borehole, VFB2 (Figure 15B), located on the same farm as VFB1. The depth of this borehole is 30m. The groundwater is used for agricultural and livestock farming.

Figure 15: *The two sampling sites in Trompsburg are both situated on a private farm, A) the deep site VFB1; B) the shallow site VFB2.*

2.3.1.3 Venterstad

The small agricultural town of Venterstad is situated approximately 10 km south of the Gariep Dam in the Eastern Cape Province. The area is underlain by the Tarkastad Formation of the Beaufort Group, which consists of interbedded mudstones and sandstones. Karoo dolerites in the form of dykes, sills and ring structures are abundant in the area and contribute to deformation of the Tarkastad Formation. (Woodford & Chevallier, 2002). Three private farms, namely Vaalbank, La Rochelle and Rooiwal, were targeted during this study due to their association with thermal springs mentioned in the Annals of the Geological Survey (Kent, et al., 1966). The Vaalbank/La Rochelle area lies on the inside margin of a 20 km wide dolerite ring structure which is transected by numerous major dykes (Kent, 1949). The location of the mixed borehole, VBB1 (Figure 16A), lies 130m away from a large, NE-SW trending dyke. The total depth of the borehole is approximately 17m and the depth to water was 1m at the time of

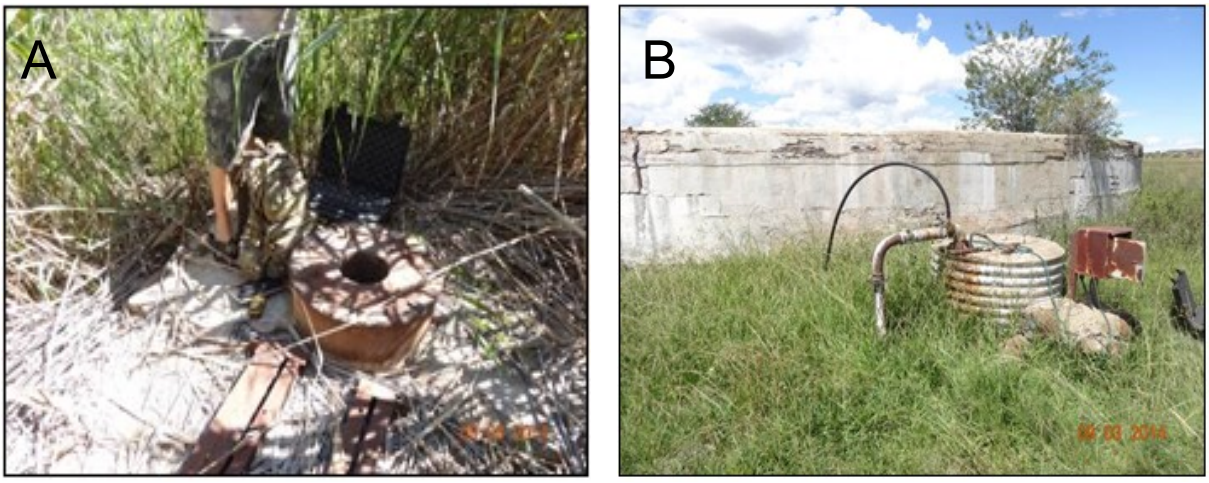

Figure 16*: Two sites at Vaalbank/La Rochelle farm in Venterstad, A) the mixed site VBB1; B) the shallow site LRB2.*

sampling. This borehole is located approximately 10m from what is thought to be the original spring. The shallow site, borehole LRB2 (Figure 16B), is located approximately 4km away from VBB1. The total depth of the borehole is 36m. The main usage for the groundwater is agricultural.

The Rooiwal thermal spring is also located adjacent to a major NE-SW trending dyke which crosses and merges with other dykes (Heaton & Vogel, 1979). The area surrounding this has also been intruded by sills and ring structures. The thermal spring could not be directly sampled. Therefore a nearby open borehole, RWB1c, containing warm water was the sampling site (Figure 17A). The depth of the borehole was not determinable, however the depth to water was 8.25m at the time of sampling. The shallow site, borehole RWB5 (Figure 17B), is located approximately 1.5km away from the deep site and is connected to the main farming house for domestic uses.

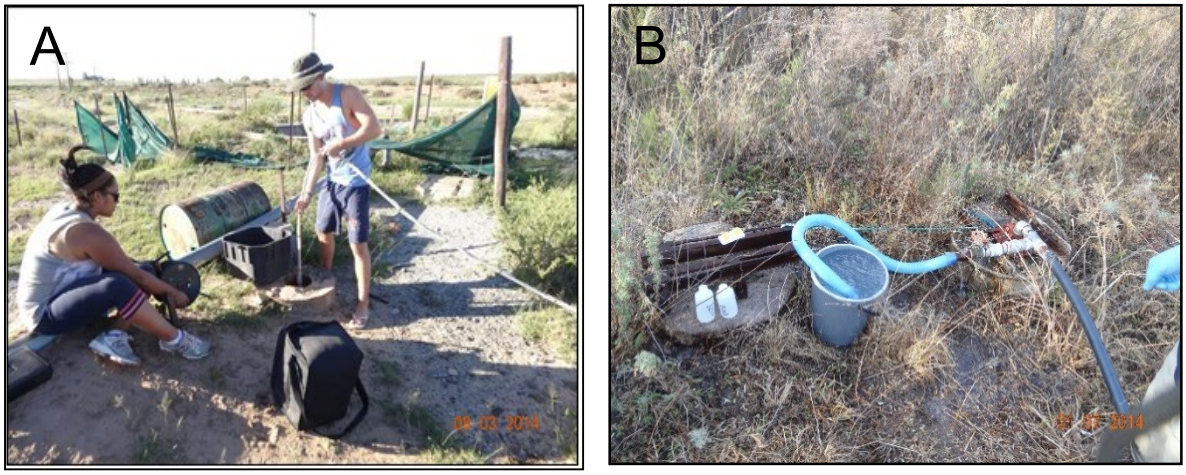

Figure 17: *Two sampling sites at Rooiwal farm in Venterstad, A) the deep site RWB1c; B) the shallow site RWB5.*

2.3.1.4 Aliwal North

Aliwal North is a small town located in the Eastern Cape Province and is situated in close proximity to the Orange River. The warm spring was once a popular tourist attraction, however, due to lack of funding the resort has not been maintained. The spring is located on the south-western side of a large dolerite ring structure (Mazor & Verhagen, 1983). This structure is cut by a major north-south trending dyke which at surface appears to have “cut-off” the south-western part of the ring structure. The sub-surface geology of this area is complicated, and like other dyke, sill and ring complexes, it is not possible to identify particular structures that may impede flow at depth and provide conduits for upward flow. The Aliwal North spring, together with the Cradock spring (discussed in the next section), recorded the highest temperatures when measured by Kent, (1949) of 36.9°. The main spring discharges into the

base of an indoor pool (Figure 18A) from where the deep site, ANS1, was collected. The shallow site, borehole ANBH1 (Figure 18B) is situated on a private farm approximately 4km away from Aliwal North Spa.

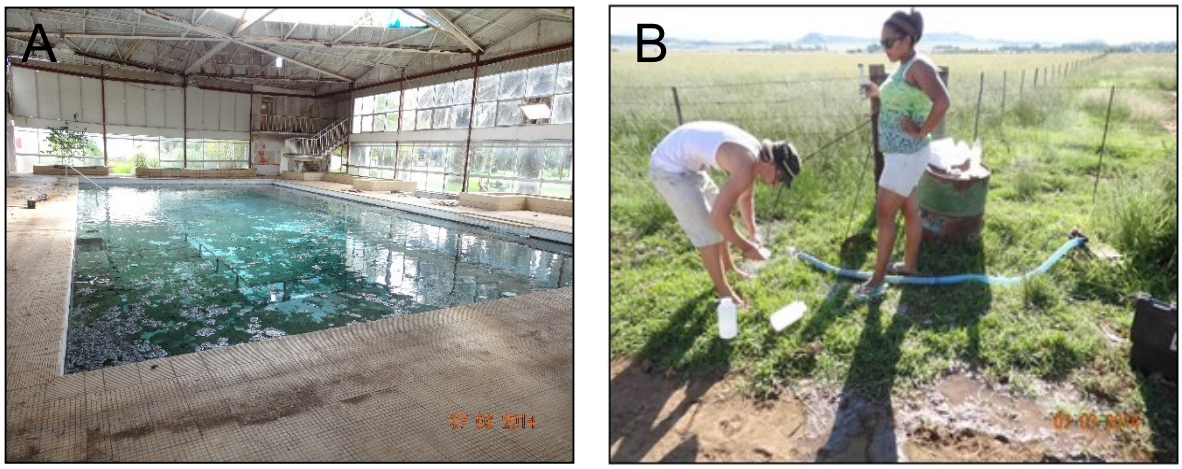

Figure 18: *Two sampling sites in Aliwal North, A) the deep site ANS1 collected from the indoor pool at the old warm spring resort; B) ANBH1 was collected on a private farm approximately 4km away from ANS1.*

2.3.1.5 Cradock

Cradock is also a small town in the Eastern Cape Province in close proximity to the Groot Visrivier. Like Aliwal North, the warm spring used to be a popular tourist atraction. The Cradock thermal spring emanates from the Balfour Formation of the Beaufort Group, which consists mostly of mudstone with intercalated fine-grained sandstone (Kent, 1949). A dense distribution of dolerite sills and dykes can be seen at the surface, with one fairly major north-west trending dyke cropping out 1km west of the spring (Kent, 1949). The spring itself appears to be located outside the western edge of a complex ring structure. The highest measured temperature of this warm spring was 31°C (Kent, 1949). Similar to Aliwal North, the main spring and deep site, CRS1, discharges into a swimming pool with a sump at its base where the bubbling spring water rises (Figure 19A). The shallow site for this location, DRB4, is an enclosed borehole and is located approximately 9km away from CRS1 on a private farm and is used for livestock farming and domestic use (Figure 19B). The total depth of the borehole is 60m and the depth to water was 10m at the time of sampling.

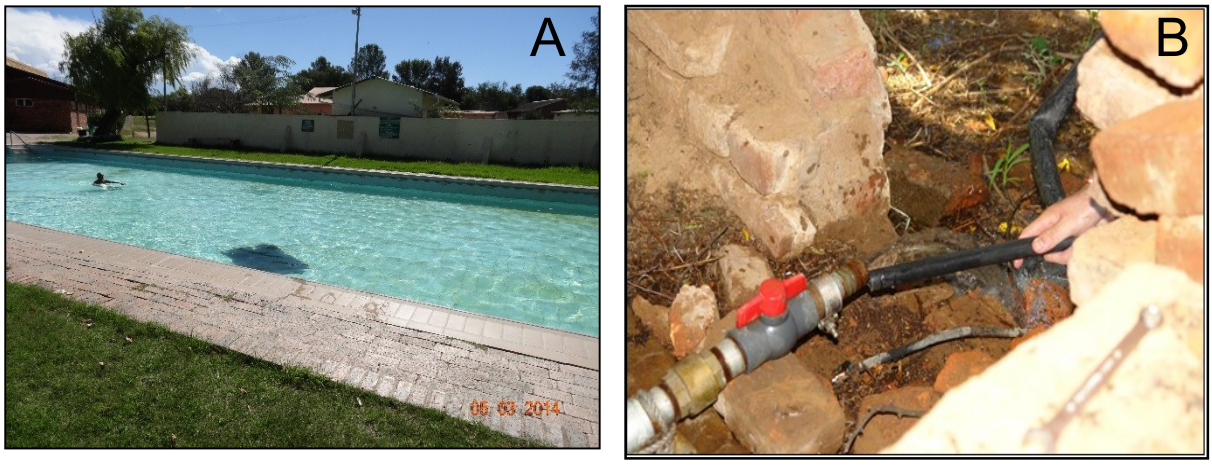

Figure 19: *The two sampling sites in Cradock, A) the deep site CRS1 collected from the outdoor pool at the warm spring resort; B) the shallow site DRB4 collected on a private farm situated approximately 9km away from CRS1.*

2.3.1.6 Fort Beaufort

The small town of Fort Beaufort in the Eastern Cape lies just south of the great escarpment and thus outside the central Karoo Basin. However, the dolerites are still present in this area, and the spring site sits approximately 3km north of a 100km long dolerite sheet that runs into the Indian Ocean. The area is characterised by folded sediments of the Middleton Formation of the Beaufort Group, which consists mostly of mudstone with interbedded sandstone, and the spring emanates from a point between anticline and syncline axes (Johnson, et al., 2006). The source of the spring flow is not known, but is postulated that recharge takes place above the escarpment some 20km north of the spring. The artesian, warm spring is situated on a private citrus farm, Bath Farm. Its temperature was reported to be 27-29˚C in 1947 (Kent, 1949). An artesian borehole, approximately 30m away from the inaccessible eye of the spring was sampled as the deep site, BFB1 (Figure 20A). Two suspected shallow sites were sampled in Fort Beaufort (BFB2 and RRB1). However, BFB2 (Figure 20B) was classified as a mixed site once the initial classification of the samples was conducted (explained in Chapter 1). This borehole is approximately 100m deep and approximately 3km away from site BFB1. RRB1 (Figure 20C) is therefore the only remaining shallow site in Fort Beaufort. RRB1 is an enclosed borehole that is controlled by a solar panel situated approximately 10km away from site BFB1. The total depth of the borehole is approximately 65m and the depth to water at the time of sampling was approximately 50m. Both BFB2 and RRB1 are used for agricultural purposes.

2.3.1.7 Leeu Gamka

Figure 20: *Three sampling sites in Fort Beaufort. All three sites were collected on private farms within 10km of each other. A) The deep site BFB1; B) the mixed site BFB2; C) the shallow site RRB1.*

Leeu Gamka is a small town in the Western Cape situated south-west of the town of Beaufort West along the N1 highway. Leeu Gamka and Merweville (Section

2.3.1.8 Merweville) are located on arenaceous and argillaceous sediments of the Abrahamskraal Formation which overlie the Cape Supergroup sediments (Johnson, et al., 2006). The impact of the Cape Fold Belt is evident in the east-west trending shallow folds throughout this area. The source of the deep water is thought to be from recharge in the Cape Mountains to the south, and then via faults or fracture zones associated with the Cape Fold Belt. Boreholes on two farms, Kruidfontein and Groot Kruidfontein, located south of Leeu Gamka were sampled for this project. The potentially deep site at this location was unable to be sampled, therefore only one shallow and two mixed sites were sampled at this location. The shallow site, WP 502 (Figure 21A) was sampled on Groot Kruidfontein farm. The mixed boreholes, WP 505 and WP 508 (Figure 21B and C) were sampled on Kruidfontein and Groot Kruidfontein farms respectively. All of the groundwater sampled at this location is used for domestic and agricultural purposes.

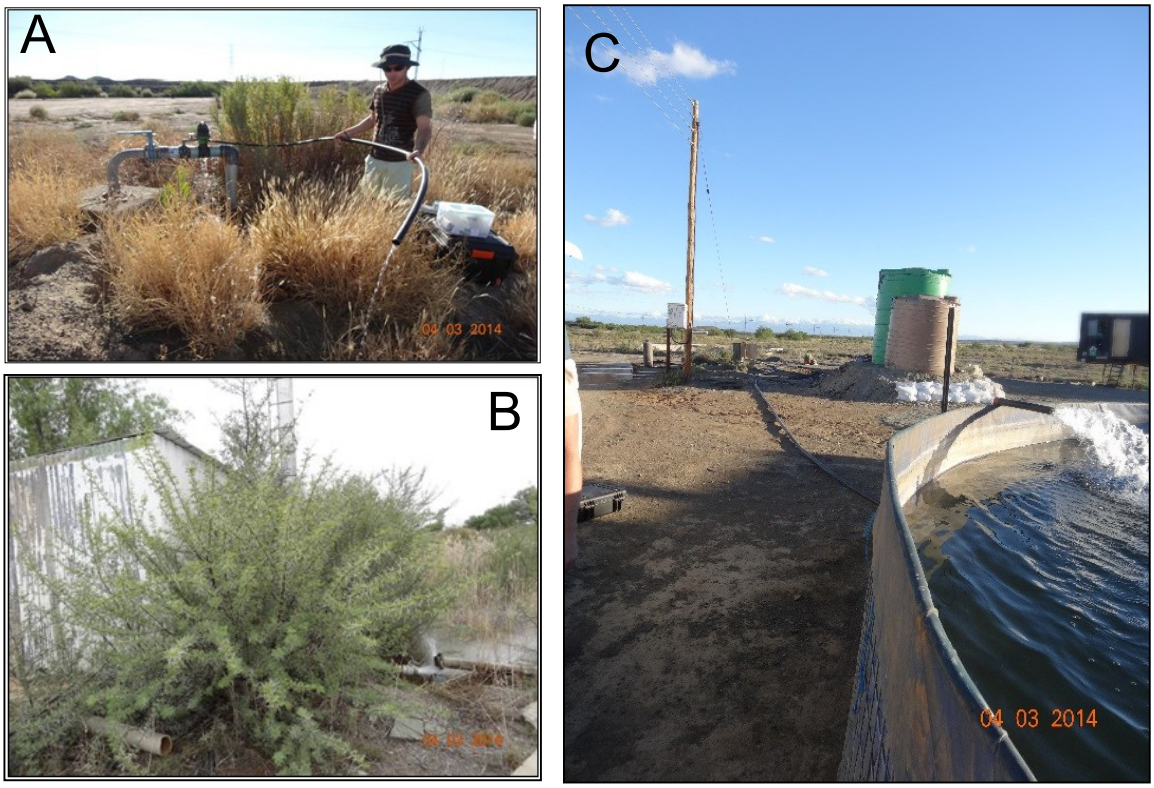

Figure 21: *Three sites in Leeu Gamka, collected on two private farms. A) Shallow site WP 502 collected on the Groot Kruidfontein farm; B) Mixed site WP 508 collected on the Kruidfontein farm; C) mixed site WP 505 collected on the Groot Kruidfontein farm.*

2.3.1.8 Merweville

As mentioned above, the Merweville and Leeu Gamka sites lie in similar geological settings. The Cape Supergroup forms the basement of the Karoo Supergroup in this area. The area is relatively low-lying when compared to the great escarpment to the north and the Cape Fold Belt to the south. Like other areas sandwiched between these two prominent geologic features, is a setting conducive to artesian pressures at depth.

In 1965 Soekor, now PetroSA, along with the Geological Survey of South Africa drilled 24 deep exploration wells throughout South Africa. The aim of this project was to investigate the existence of economic accumulations of oil in South Africa (Roswell & De Swart, 1976). No oil was found at the time and hence the boreholes were sealed with cement as part of the conditions of the exploration license that was granted. However, the seal on borehole SA1/66 in Merweville (Figure 22A) failed and the groundwater was successfully sampled in 2012 as a result of artesian flow that was present at the time. The total depth of the borehole is 4169m and water was struck within the Dwyka Group at 3206m (Roswell & De Swart, 1976). The

original drilling/geological log describes the water as artesian with a temperature of 46°C, a TDS of 8745 ppm and “a very high gas content” (Roswell & De Swart, 1976). Since 2012, the artesian character of the borehole has diminished and the borehole could not be sampled during this project. Therefore only a shallow site was collected at the Merweville location. The shallow borehole, MWB2 (Figure 22B) is situated on the same farm as SA1/66 approximately 10km away. This groundwater is used for domestic purposes.

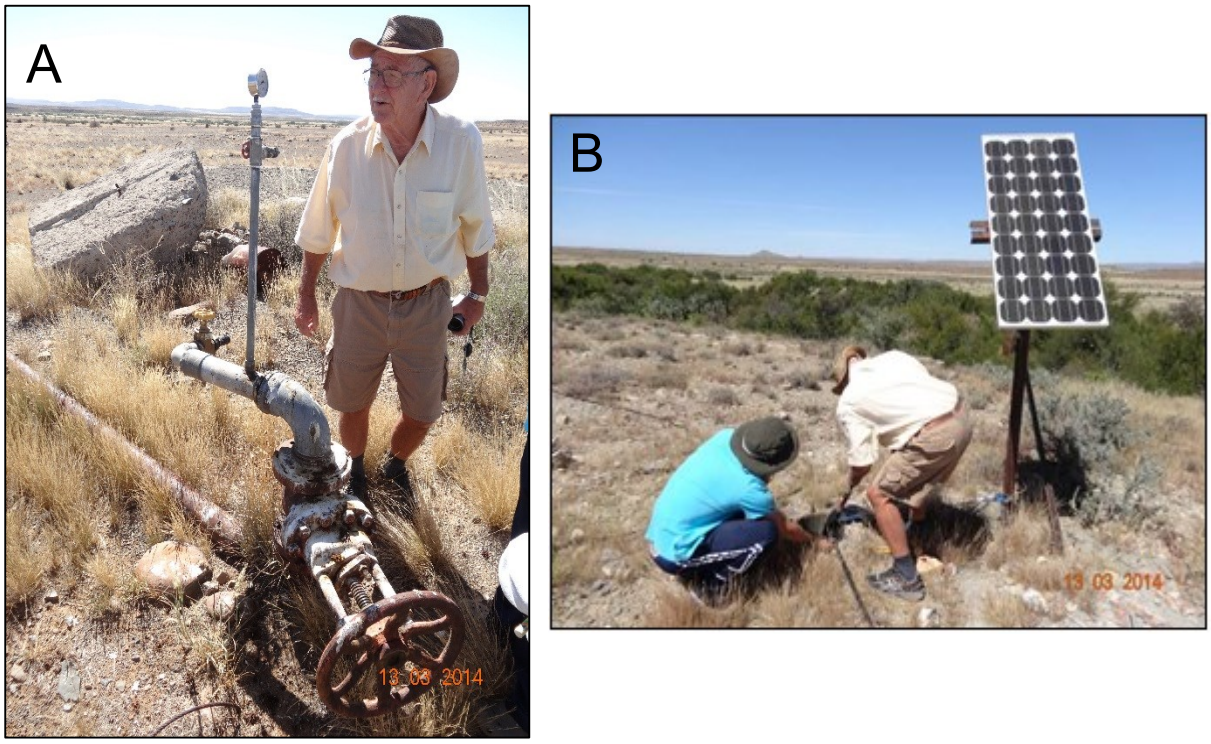

Figure 22: *Two samples sites in Merweville collected on a private farm. A) One of the deep SOEKOR exploration boreholes, SA1/66; B) the shallow borehole MWB2 approximately 10km away from SA1/66.*

2.3.2 Sampling procedure

All boreholes were pumped for at least 30 minutes prior to sampling in order to remove any stagnant water and to ensure that “fresh” groundwater was sampled. The electrical conductivity (EC) was monitored whilst pumping took place and the sample was collected once the EC had stabilized. pH and temperature were then measured using an Extech EC500 combined pH, EC and temperature probe. All the probes were calibrated on a daily basis. Field alkalinity was determined using a Hach digital titrator, and titrated to a pH of 4.5 using 1.5M or 0.15M sulphuric acid and Green-Methyl Red and Phenolphthalein indicators. In all samples the total alkalinity was equal to the bicarbonate alkalinity ($mg.L^{-1}$ HCO_3^-). Alkalinity was also measured in the Department of Soil Science at Stellenbosch University using a Metrohm 905 Titrano Autotitrator as well as at Duke University, USA. Samples for cations and anions, trace elements as well as boron, strontium, oxygen and hydrogen isotopes were collected in PP acid washed conical tubes. All water samples were filtered on site with 0.45µm

cellulose acetate filters. Cation samples were acidified to a pH less than 2 using ultrapure concentrated nitric acid. All samples were kept at less than 4°C in the field and transferred to fridges in the laboratory.

2.3.3 Analytical techniques

Major cations and trace elements were analysed on field acidified samples by ICP-MS/AES Laboratory in the Central Analytical Facility at Stellenbosch University using an Agilent 7700 ICP-AES and 7700 ICP-MS respectively. Anion analysis was performed using a Waters IC-Pak 717 Autosample- conductivity detector-Agillent 1120 pump in the Mass Spectrometry laboratory also in the Central Analytical Facility at Stellenbosch University. A charge balance was calculated using Cl^-, Br^-, NO_3^-, SO_4^{2-}, Ca^{2+}, K^+, Mg^{2+} and Na^+ all of which were analysed at Stellenbosch University, as well as laboratory alkalinity (mg.L^{-1} HCO_3^-) analysed at Duke University. With the exception of four samples, namely FLB5, CRS1, ANS1 and FLS1, the samples produced good charge balances within 5% difference.

δ^2H and $\delta^{18}O$ isotopes were analysed relative to the SMOW, using a Finnigan GasBench II in the laboratories of the Environmental Isotope Group (EIG) at iThemba LABS in Johannesburg. Samples were calibrated to the SMOW standard and analytical precision is 0.2‰ for O and 0.8‰ for H. $\delta^{11}B$ ratios were analysed by thermal ionization mass spectrometry (TIMS) on a Thermo Fisher Triton at the Duke University TIMS Laboratory, USA. $^{11}B/^{10}B$ ratios were measured as BO_2^- ions in negative mode and normalized to a NIST standard NBS SRM-95124. Oxygen, hydrogen and boron isotopes were reported in the usual δ notation:

$$\delta\ (‰) = \left(\frac{R_{sample} - R_{standard}}{R_{standard}}\right) \times 1000$$

where R represents the $^{18}O/^{16}O$, D/H or $^{11}B/^{10}B$ ratio isotope.

$\delta^{13}C$ ratios of the dissolved inorganic carbon ($\delta^{13}C_{DIC}$) were measured with the radiocarbon samples at either iThemba LABS in Johannesburg or at Beta Analytic in Florida, USA. Two 10ml ampoules were collected for the ^{13}C sample. This occurred while the samples were being pumped under backing vacuum. The $\delta^{13}C$ ratio is then measured using an isotope ratio mass spectrometer (IRMS). Two in house standards were used at iThemba LABS, namely CSS and MHS1 with $\delta^{13}C$ values of -6.8 and -2.82‰ respectively relative to PDB. The standard deviation for analyses was 0.05‰. At Beta Analytic the $\delta^{13}C$ is analysed relative to VPDB. The standard deviation for analyses was 0.3‰. $^{87}Sr/^{86}Sr$ isotope ratios were measured on a NuPlasma HR MC-ICP-MS in the Department of Geological Sciences at the University of Cape

Town, South Africa and calibrated to the standard reference NIST987 standard using a value of 0.710255.

2.4 Results

As discussed in Chapter 1, the samples collected for this study have been divided into three groups; deep, shallow and mixed. In total, 19 samples were collected which include 8 shallow samples, 5 mixed samples and 6 deep samples. In all of the graphs the deep samples are represented by red squares, the shallow samples by blue diamonds and the mixed samples by green triangles. Many of the graphs show the parameter as a function of temperature of the samples. As mentioned in Chapter 1, temperature was one of the original proxies used for depth during this project. All of the results discussed in this chapter are presented in Table 4.

2.4.1 Field parameters

EC, pH, Oxidation-Reduction potential (ORP), temperature and the presence of H_2S were measured in the field. Of these pH, ORP, temperature and H_2S showed clear differences between the deep groundwater samples and the shallow groundwater samples. The deep samples had pH values between 9.1 and 10 (A and B), negative ORP values between -165 and -53 mV (D) and temperatures generally above 25°C (). An exception to these values was ANBH1 where the pH was 7.5 and the temperature was relatively cold at 18°C (A). The shallow samples had lower pH levels of between 7.1 and 7.9 (A and B), positive ORP values between 80 and 130mV (D) and cooler temperatures lower than 25°C (). The mixed samples slightly overlapped with the shallow and deep samples with pH values between 7.4 and 8.4 (A and B), negative ORP values between -106 and -169mV (D) and temperatures ranging from 18 to 27°C (). In comparison EC values did not show a clear differentiation between shallow and deep groundwater samples (C). The total range of EC values was between 21 and 1019 mS/m with a mean value of 174 mS/m. The shallow samples have values between 50 and 249 mS/m, the mixed samples between 49 and 200 mS/m and the deep samples between 21 and 1019 mS/m. The presence of H_2S indicated by the smell of rotten eggs/sulphur is a common feature of thermal springs and has been observed by Kent (1949) and Vogel, et al. (1980). The smell of rotten eggs as was observed in the field at specific sites (E) and was confirmed by the presence of H_2S through noble gas analysis (F). H_2S is observed in all of the deep and mixed samples, with the exception of site ANBH1, with values ranging between 5 and 47 μcm^3 STP/kg for the deep samples and between 3 and 23 μcm^3 STP/kg for the mixed samples (E and F). Site ANBH1 contained negligible concentrations, as did all of the shallow samples.

Table 4 continued...

Table 4: *Results of fie... e shown.*

	Town	Sample No.	Li	Sr	B	V	U	δ^2H	$\delta^{18}O$	$\delta^{13}C_{DIC}$	$\delta^{11}B$	$^{87/86}Sr$	H_2S	K/Na	Na/Ca	Mg/Ca	Cl/Br	Na/Cl
			1	1	1	1	1	3		3	2	4	5					
	Town		µg/L	µg/L	µg/L	µg/L	µg/L	‰ SMOW		‰ PDB	‰		µcm³ STP/kg	molar ratio				
SHALLOW GROUP	Leeu Gamka	WP 502	99.053	1689.35	110.585	1.491	4.118	3	0.4	-10.3		0.71158	0.09					
SHALLOW GROUP	Cradock	DRB4	14.523	646.53	753.402	93.181	26.558	-13	-2.4	-13.6	32.9	0.71233	0.03	0.027	2.584	0.427	654	3.014
SHALLOW GROUP	Fort Beaufort	RRB1	43.703		295.139	1.240	11.784	-24	-4.8	-11.6	35.1	0.70962	0.19	0.009	16.13	3.786	711	6.063
SHALLOW GROUP	Venterstad	RWB5	41.897	878.33	98.093	8.426	40.851	-26	-4.9	-11.7		0.71043	0.78	0.011	3.307	0.811	520	0.932
SHALLOW GROUP	Venterstad	LRB2	34.334		42.577	9.929	3.141	-26	-4.8	-9.2		0.71003	0.08	0.022	0.956	0.729	324	2.549
SHALLOW GROUP	Trompsburg	VFB2	39.083	602.61	55.222	12.499	3.594	-28	-4.8	-8.6		0.71066	0.06	0.020	0.726	0.608		2.408
SHALLOW GROUP	Florisbad	FLB5	18.047		72.264	7.837	2.536	-21	-3.4	-4.6	32.9	0.71840	0.07	0.038	0.711	0.598	295	3.074
SHALLOW GROUP	Merweville	MWB2	264.791	7110.35	223.956	0.610	15.070	-28	-5.2	-13.3	26.9	0.71031	0.07	0.135	1.421	1.048	576	0.588
														0.016	1.486	0.336	563	1.069
MIXED GROUP	Leeu Gamka	WP 508	540.376	2721.11	333.373	< 0.017	0.664	-29	-5.0	-14.8	8.9	0.71157	3.03	0.012	7.373	0.115	575	2.657
MIXED GROUP	Leeu Gamka	WP 505	945.822	3195.11	664.527	< 0.017	0.544	-26	-4.7	-17.6	9.3	0.71119	5.23	0.006	18.47	0.042	420	4.503
MIXED GROUP	Fort Beaufort	BFB2	170.430	3212.47	760.912	0.049	1.310	-24	-4.9	-12.9	19.9	0.70887	4.22	0.003	6.094	0.847	674	0.907
MIXED GROUP	Venterstad	RWB1c	164.969	1057.23	389.946	< 0.017	0.023	-32	-5.4	-11.3	6.5	0.71016	23.58	0.003	7.034	0.236	425	3.926
MIXED GROUP	Venterstad	VBB1	49.734	299.55	406.398	< 0.017	0.040	-29	-5.7	-11.5	5.9	0.71054	18.22	0.004	10.75	0.308	595	1.584
DEEP GROUP	Cradock	CRS1	166.896	76.41	473.452	0.506	0.048	-39	-7.7	-7.2		0.71006	5.23	0.004	29.54	0.007	663	2.740
DEEP GROUP	Fort Beaufort	BFB1	650.003	376.90	1909.278	< 0.017	0.001	-36	-7.2	4.7	5.4	0.71004	7.77	0.008	61.57	0.004	673	1.161
DEEP GROUP	Aliwal North	ANS1	539.581	1408.14	924.623	< 0.017	0.004	-36	-6.8	-11.6	9.5	0.71206	47.34	0.003	6.983	0.001	803	0.939
DEEP GROUP	Aliwal North	ANBH1	540.465	664.25	670.059	0.030	0.003	-36	-6.7	-19.8	15.2	0.71206	0.16	0.002	42.4	0.143	877	1.116
DEEP GROUP	Trompsburg	VFB1	6813.931	17782.23	3065.510	0.031	0.002	-39	-7.5	-25.5	29.9	0.77719	15.92	0.004	9.536	0.001	373	0.942
DEEP GROUP	Florisbad	FLS1	842.807	4276.44	2030.805	0.047	0.004	-37	-6.9	-26.0	23.2	0.75392	28.36	0.006	14.08	0.001	581	1.038

Notes: *(1) Stellenbosc... n, South Africa; (5) Ohio State University.*

Notes: *(1) Stellenbosch University Central Analytical Facility, South Africa; (2) Duke University, USA; (3) iThemba LABS, South Africa; (4) University of Cape Town, South Africa; (5) Ohio State University.*

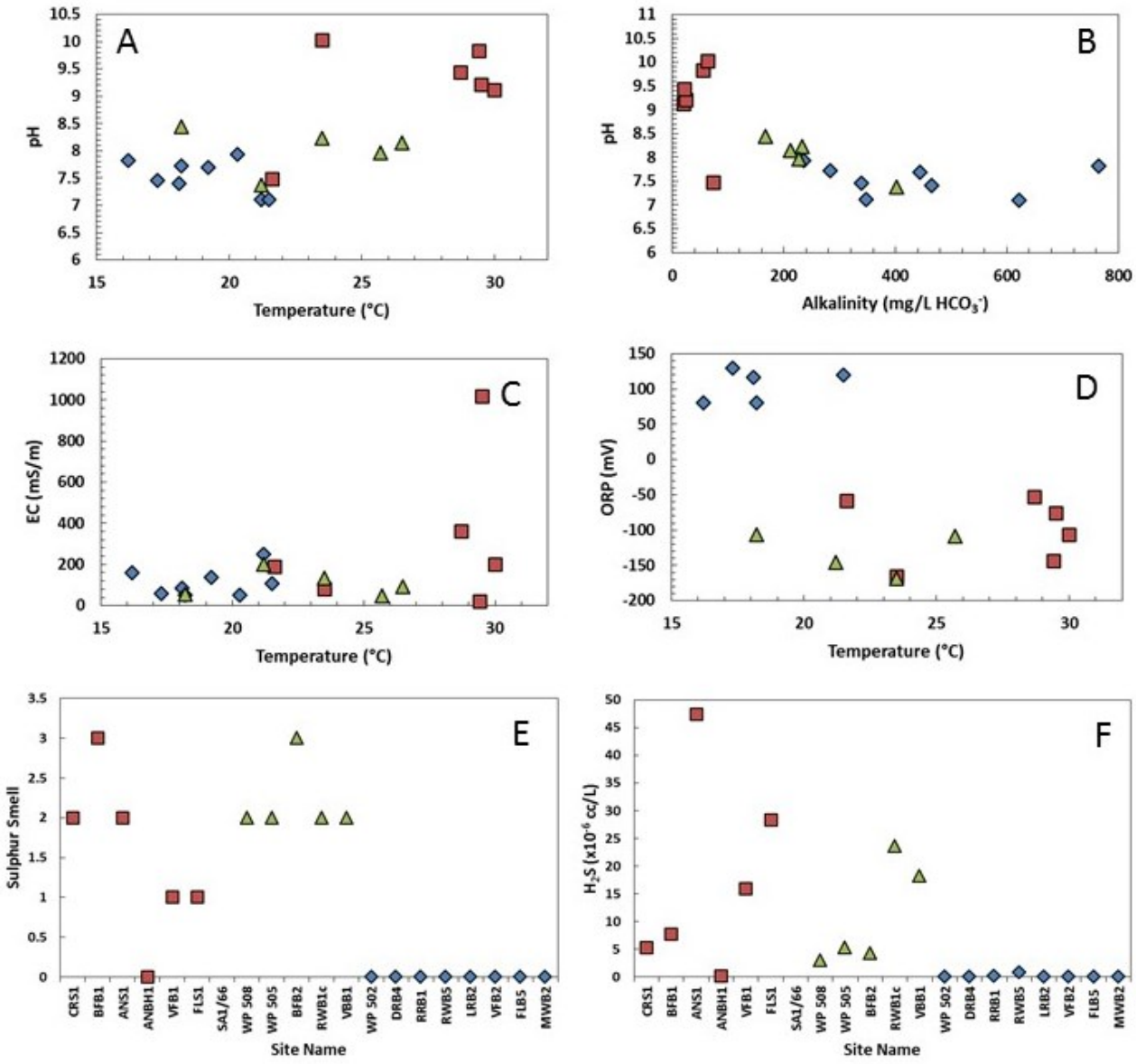

Figure 23: *Relationship between A) pH and temperature; B) pH and alkalinity; C) EC and temperature; D ORP and temperature); E) presence of sulphur smell and site name; F) H_2S and site name of the groundwater samples collected in the Karoo Basin. Red squares = deep sites, blue diamonds = shallow sites, green triangles = mixed sites.*

2.4.2 Major ion chemistry

Sodium concentrations are generally much lower in the shallow groundwater samples when compared to the deep samples (Figure 24A) with values between 23 and 280 mg.L^{-1}. The deep samples contain higher concentrations between 144 and 2363 mg.L^{-1} with Cradock warm spring, CRS1, being an outlier with a significantly lower concentration of 43 mg.L^{-1}. This is also reflected in the Stiff diagram shape of CRS1 shown in Figure 9 in Chapter 1. The mixed group overlaps with the deep and shallow group with values from 81 to 266 mg.L^{-1}. When Na is represented as a percentage of all cations in milli equivalents (100 * Na/ (Ca + K + Mg + Na)), it distinguishes between deep, shallow and mixed samples better than when Na is represented in mg.L^{-1} (Figure 24B). The deep samples contain much higher percentages of

Na^+ between 78 and 96%, whereas the shallow samples have the lowest percentages between 11 and 40% and the mixed samples plot between the deep and shallow samples with intermediate percentages between 47 and 89%. Magnesium and to some extent, Ca^{2+} concentrations show the opposite trend to Na^+ concentrations as seen in Figure 24C and D. Higher Mg^{2+} concentrations between 10 and 73 $mg.L^{-1}$ are measured in the shallow group, whereas only one deep site, ANBH1, contains any measurable Mg^{2+} at 1.3 $mg.L^{-1}$. Only one mixed site, BFB2 in Fort Beaufort, contains significant Mg^{2+} with a concentration of 39.1 $mg.L^{-1}$, whereas the rest of the mixed sites have concentrations lower than 3 $mg.L^{-1}$ (Figure 24C). Calcium concentrations overlap between the three groundwater groups (Figure 24D). In general, the shallow samples have higher concentrations between 26 and 148 $mg.L^{-1}$. The deep samples have concentrations between 3 and 86 $mg.L^{-1}$ and the mixed group have concentrations ranging from 14 to 76 $mg.L^{-1}$. Potassium concentrations are relatively uniform throughout the different groundwater groups with concentrations between 0.3 and 17 $mg.L^{-1}$, although VFB1 and FLB5 are outliers from both the deep and shallow groups respectively (Figure 24E).

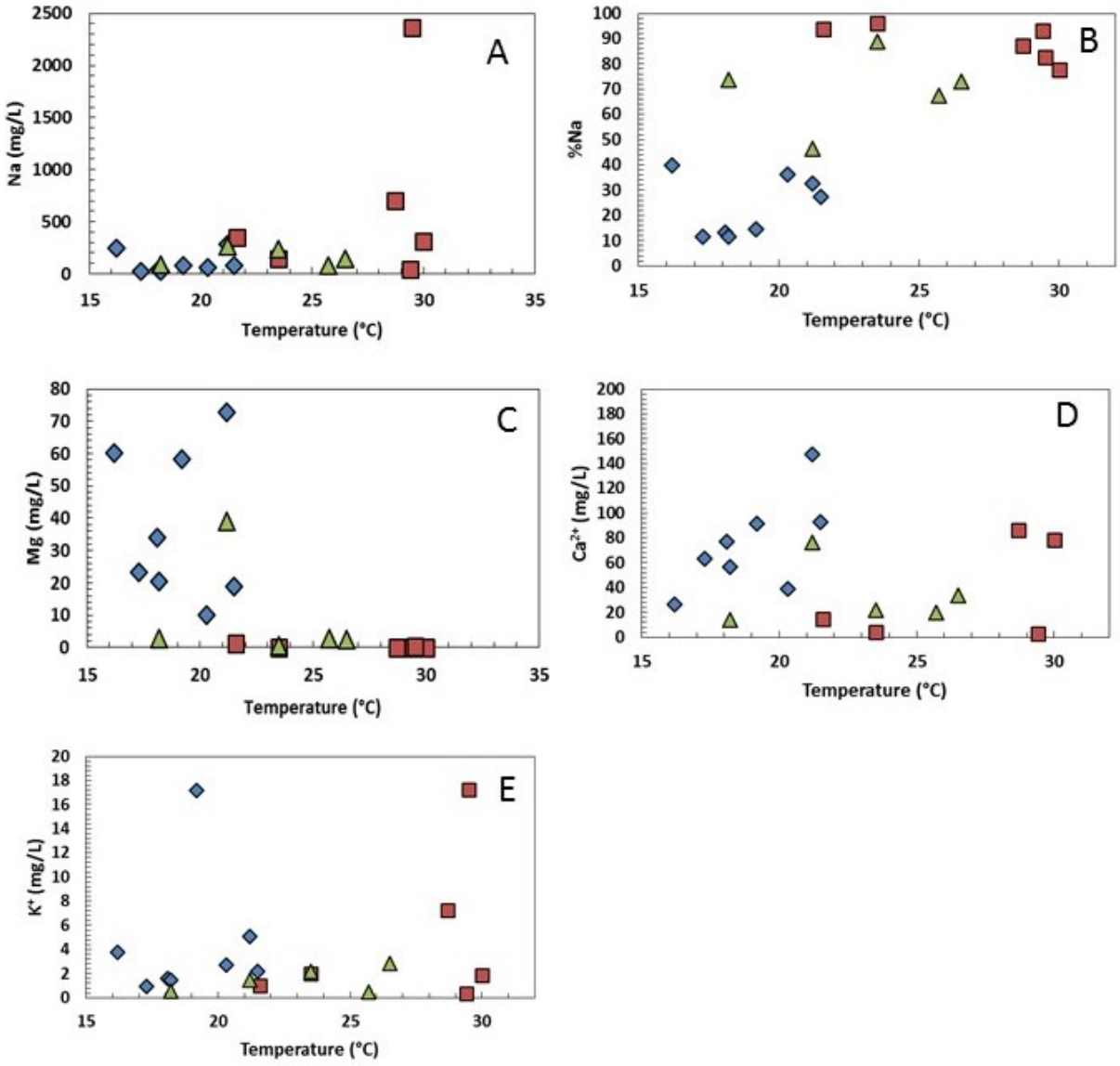

Figure 24: *Relationship between A) Na^+ concentrations; B) %Na; C) Mg^{2+} concentrations; D) Ca^{2+} concentrations, site VFB1 is an outlier containing 432 mg.L^{-1}, which is not shown; E) K^+ concentrations and temperature as a proxy for depth in the groundwater samples from the Karoo Basin. Red squares = deep sites, blue diamonds = shallow sites, green triangles = mixed sites.*

Chloride concentrations are higher in most of the deep groundwater samples than in the shallow samples, with concentrations between 191 and 1034 mg.L^{-1} except for site CRS1 which is an outlier containing only 24 mg.L^{-1} (Figure 25A). This is also reflected by the shape of the Stiff diagram for CRS1 in Figure 9 in Chapter 1. The shallow samples slightly overlap with the deep samples with concentrations between 12 and 463 mg.L^{-1} (Figure 25A). The mixed samples overlap quite significantly with the shallow samples with concentrations between 32 and 452 mg.L^{-1} (Figure 25A). Nitrate concentrations differ significantly between the three groundwater depth groups (Figure 25B). The shallow samples were the only group to contain any significant NO_3^- concentrations ranging from 0.5 to 24 mg.L^{-1}. FLB5, the shallow site in Florisbad contains a much higher concentration than the other shallow sites, at 93.1

mg.L^{-1}. The only deep site to contain any NO_3^- is FLS1, the deep site in Florisbad (Figure 25B). The mixed group also contains negligible NO_3^- concentrations. Figure 25C indicates that the deep groundwaters have higher fluoride levels than the shallow groundwaters. Little to negligible F^- concentrations (less than 1.3 mg.L^{-1}) are present in the shallow groundwater group. Moderate concentrations of between 2.1 and 3.7 mg.L^{-1} are present in the mixed groundwater group, and relatively high concentrations between 3.7-16.1 mg.L^{-1} are present in the deep groundwater group. Sulphate concentrations are not well distinguished between the deep, shallow and mixed groundwater samples (Figure 25D). Lower SO_4^{2-} concentrations are observed in the deep samples, from below the detection limit of 2 to 23 mg.L^{-1}. The concentrations of the shallow samples vary from 14 to 84 mg.L^{-1}, whilst the mixed samples vary from below the detection limit to 219 mg.L^{-1}. There is a slight increasing trend of Br^- concentrations from the shallow to the deep samples (Figure 25E). The deep samples have concentrations between 0.1 and 4 mg.L^{-1}, the mixed samples are between 0.2 and 1.5 mg.L^{-1}, and the shallow samples have concentrations between 0.1 and 2 mg.L^{-1}.

Total alkalinity (mg.L^{-1} HCO_3^-) was measured in the field as well as in the laboratory. Although the lab and field alkalinities results were similar (the lab alkalinity values were consistently higher than field alkalinities), a better charge balance was calculated when using the lab alkalinity. A significant decrease in alkalinity is observed with an increase in depth and temperature (Figure 25F). The deep sites have very low values ranging from 22 to 73 mg.L^{-1} HCO_3^-. The shallow sites have higher values ranging from 236 to 764 mg.L^{-1} HCO_3^-. The mixed group is again intermediate and overlaps slightly with the shallow group with values ranging between 167 and 403 mg.L^{-1} HCO_3^-.

Several molar ratios were assessed along with the absolute ion concentrations. The Na/Ca ratios of the shallow group are the lowest and range from 0.71 to 3.31 with DRB4 (shallow site in Cradock) being an outlier at 16.13 (Figure 26A). The mixed group overlaps with deep group and contains moderate ratios of between 6 and 18. The deep group contains the highest ratio values of between 7 and 62. The opposite trend seen with the Na/Ca ratio is observed with K/Na (Figure 26B) as well as with Mg/Ca (Figure 26C). These molar ratios show a decrease from the shallow samples to the deep samples, with the lowest values observed in the deep samples. The Na/Cl molar ratio also shows a decrease from the shallow samples to the deep samples (Figure 26D). The Cl/Br ratios of all groundwater samples overlap quite considerably and range from 295 to 877 (Figure 26E). The use of the Cl/Br molar ratio is important in Understanding the source of Cl^- (Phillips, 2013), which is discussed further in Chapter 3.

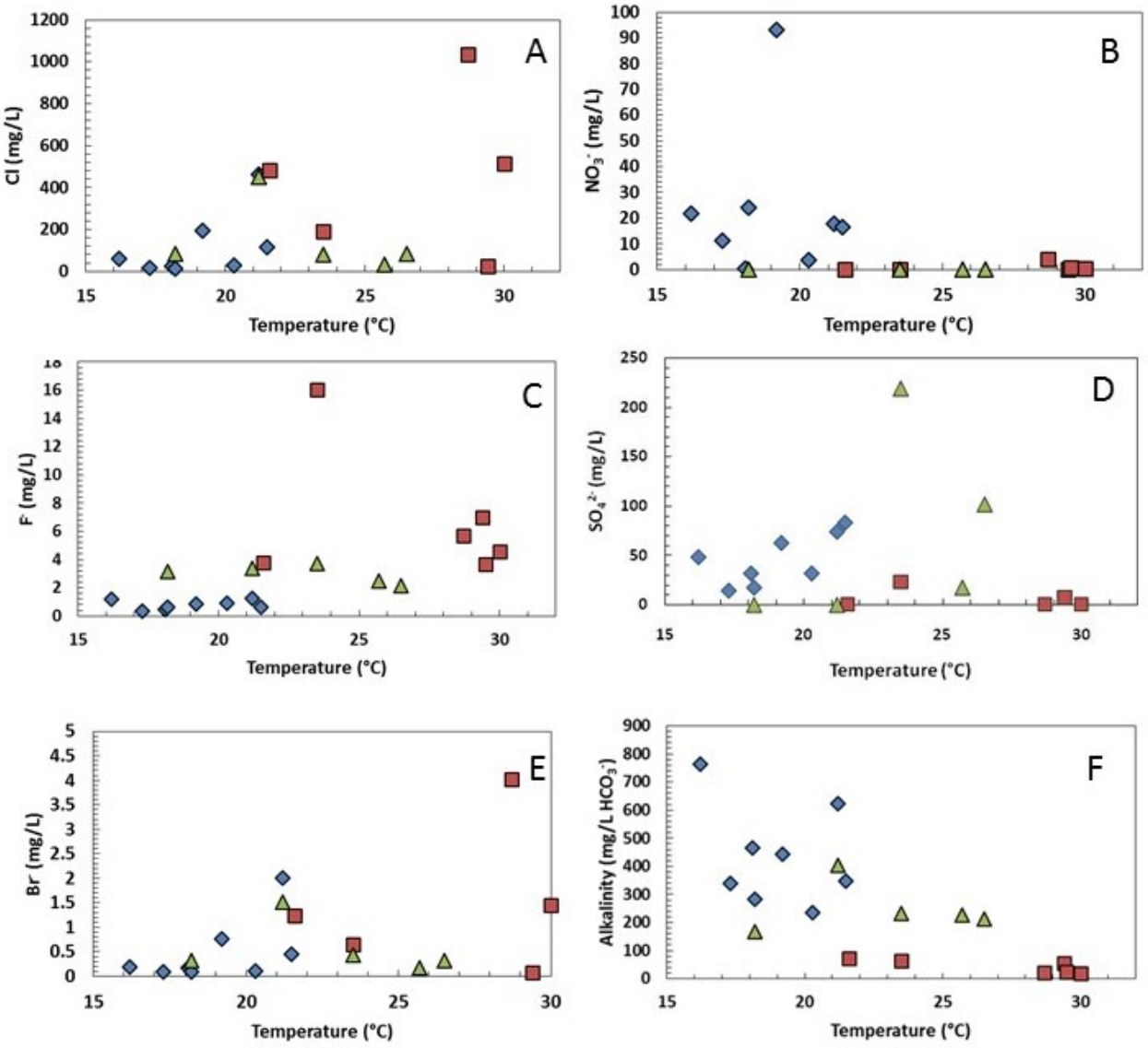

Figure 25: *Relationship between A) Cl^- concentrations, site VFB1 with a concentration of 3869 mg.L^{-1} is not shown here; B) NO_3^- concentrations; C) F^- concentrations; D) SO_4^{2-} concentrations, site VFB1 with a concentration of 956 mg.L^{-1} is not shown here; E) Br^- concentrations, site VFB1 with a concentration of 23.39 mg.L^{-1} is not shown here; F) alkalinity and temperature of the groundwater samples collected in the Karoo Basin. Red squares = deep sites, blue diamonds = shallow sites, green triangles = mixed sites.*

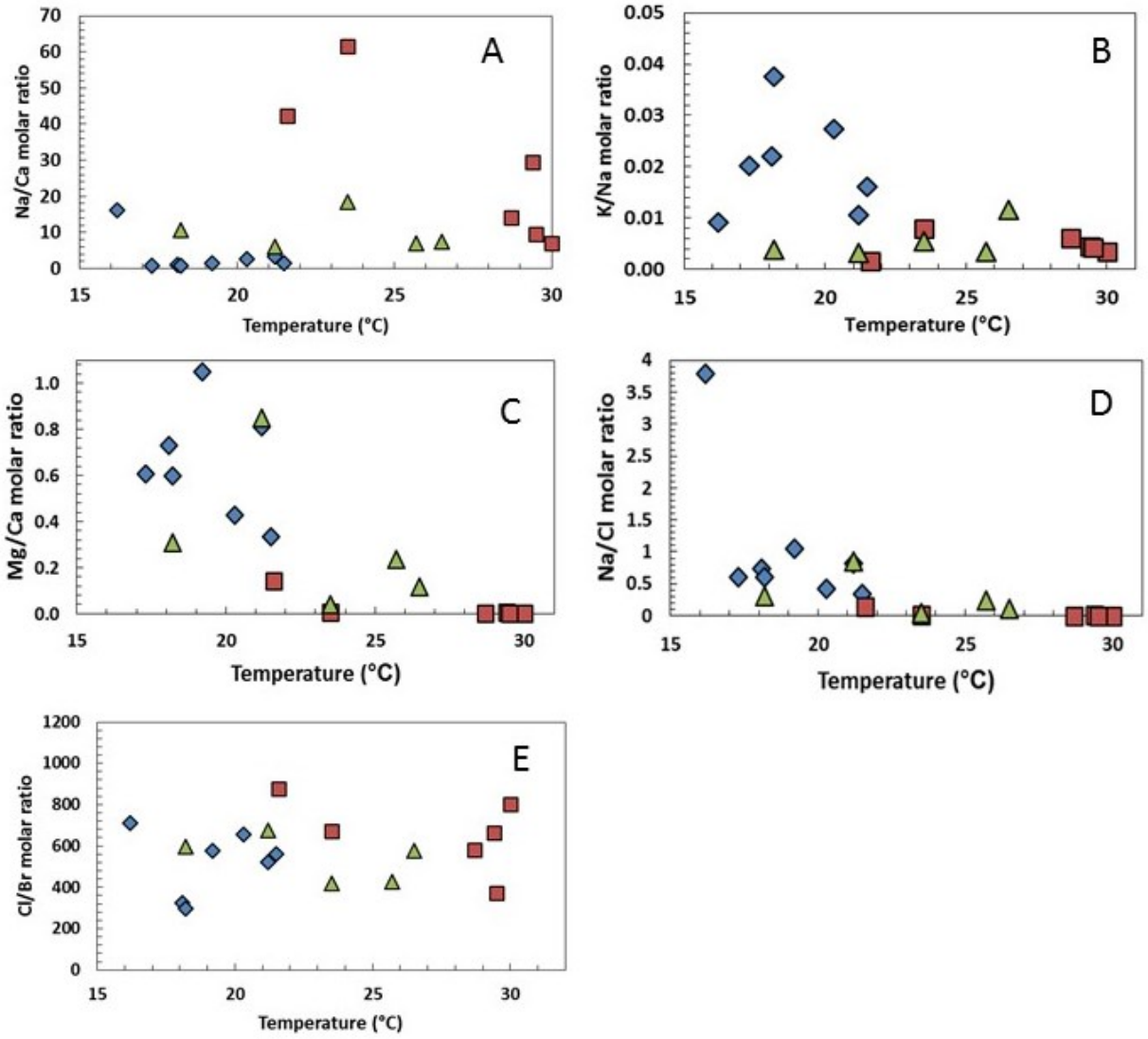

Figure 26: *Relationship of various molar ratios and temperature; A) Na/Ca molar ratio; B) K/Na molar ratio; C) Mg/Ca molar ratio; D) Na/Cl molar ratio; E) Cl/Br molar ratio of the groundwater samples collected in the Karoo Basin. Red squares = deep sites, blue diamonds = shallow sites, green triangles = mixed sites.*

2.4.3 Trace elements

Of the 39 trace elements analysed, majority of the samples were below the detection limits and only four (U, V, Li and B) showed any significant trends between the three groundwater depth groups. Deep and shallow groundwater samples are well differentiated in lithium concentrations with higher concentrations observed in the deep group (Figure 27A). However, there is significant overlap of the mixed samples with the deep and shallow samples. The deep group contains Li concentrations ranging from 167 to 843 µg/L, the shallow group concentrations are between 15 and 265 µg/L and the mixed group concentrations are between 50 and 946 µg/L. Site VFB1 in Trompsburg is an outlier with an anomalously high concentration of 6814 µg/L (not shown in Figure 27A). Vanadium is present in significantly higher concentrations in the shallow group when compared with the mixed and deep groups (Figure 27B). The shallow group has concentrations of between 0.6 and 93 µg/L, while the

mixed and deep groups contain negligible vanadium concentrations (<0.6 µg/L). Like vanadium, uranium is present in significantly higher concentrations in the shallow group when compared with the mixed and deep group (Figure 27C). Uranium concentrations for the shallow group range between 2.5 and 41 µg/L, while the deep and mixed groups contain less than 0.36 µg/L, except for site BFB2 (a mixed site in Fort Beaufort), which contains 1.3 µg/L. Like lithium, boron concentrations are present in higher concentrations in the deep samples, and show relatively good differentiation between the deep, shallow and mixed sites (Figure 27D). The deep group has a wide spread in boron concentration from 473 to 3065 µg/L. The shallow group contains the lowest B concentrations of between 42 – 753 µg/L, while the mixed group plots between the deep and shallow groups with some overlap between 333 and 761 µg/L.

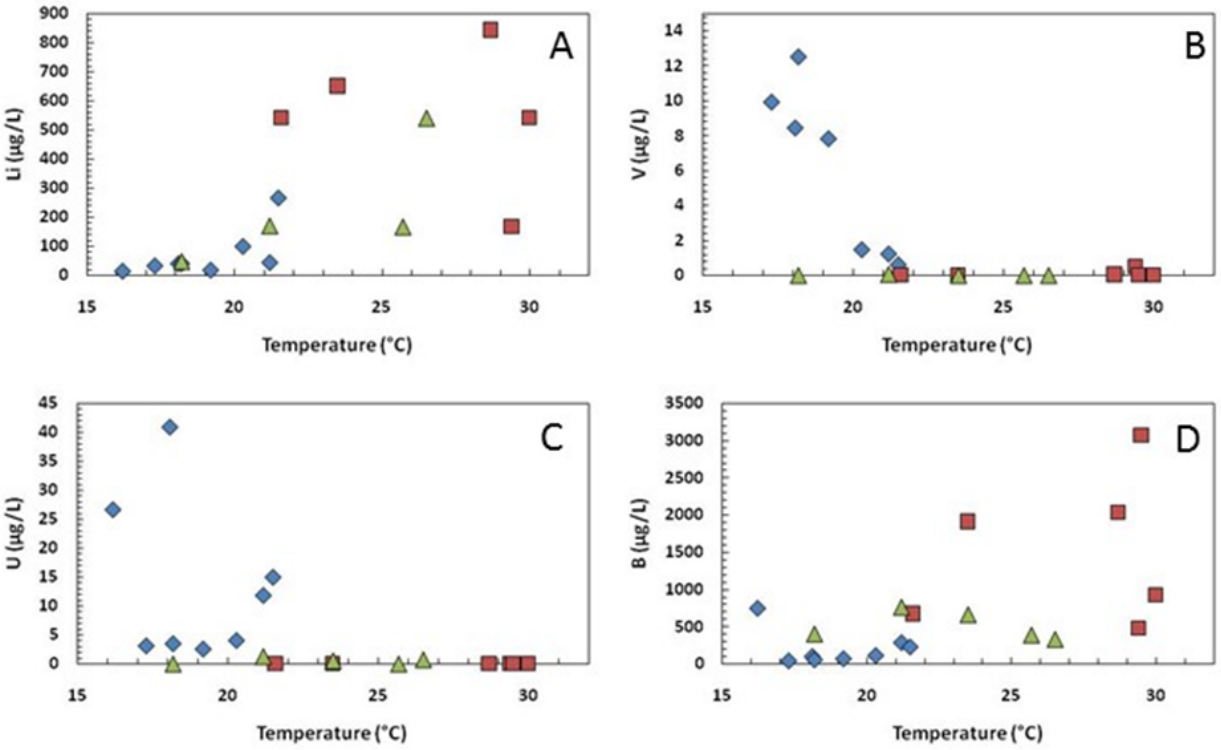

Figure 27: *Relationship between A) Li concentrations, site VFB1 containing Li a concentration of 6814 µg/L is not shown; B) V concentrations, site DRB4 containing the highest V concentration of 93 µg/L is not shown in this figure; C) U concentrations; D) B concentrations, and temperature for the groundwater samples collected in the Karoo Basin. Red squares = deep sites, blue diamonds = shallow sites, green triangles = mixed sites.*

2.4.4 Stable isotopes (O, H, C and B)

The standard $\delta^{2}H$ versus $\delta^{18}O$ plot showing results from the groundwater samples collected throughout the Karoo Basin in reference to the Global Meteoric Water Line (GMWL) (Craig, 1961) as well as the Local Meteoric Water Line (LMWL) for southern Africa where $\delta D = 6.1\ \delta^{18}O + 5‰$ (IAEA, 1981) is displayed in Figure 28. The results of this study correlate well with the LMWL (Figure 28A). A weak evaporation and condensation trend is observed by the

samples in comparison to the GMWL. Comparison of the δ^2H and $\delta^{18}O$ values shows the deep groundwater is depleted in the heavy isotopes with respect to the shallow group. The deep group has $\delta^{18}O$ ratios ranging from -6.7 to -7.7‰ and δ^2H values ranging from -36 to -39‰. The shallow group plots higher up the GMWL, with a considerably wider range in δ^2H and $\delta^{18}O$ values. The shallow group has $\delta^{18}O$ values ranging from -5.2 to 0.4‰ and a wide range of δ^2H values between -28 and 3‰. The shallow site from Leeu Gamka, WP 502, is the only site with a positive δ^2H and $\delta^{18}O$ value. The mixed group records a relatively narrow range of $\delta^{18}O$ values between -4.7 and -5.7‰ and δ^2H values between -32 and -34‰ which is distinct from the deep group but overlaps slightly with the shallow group.

$\delta^{13}C_{DIC}$ values of the groundwater samples are shown in Figures 28B, C and D. Overall the $\delta^{13}C_{DIC}$ values are generally high, with one of the deep samples (BFB1) recording a positive value of 4.7‰. $\delta^{13}C_{DIC}$ values for the deep boreholes are much more variable and range from -26‰ to 4.7‰. The $\delta^{13}C_{DIC}$ values for the shallow and mixed groups overlap considerably and are more homogenous ranging from -4.6 to -13.6‰ and -11.3 to -14.8‰ respectively.

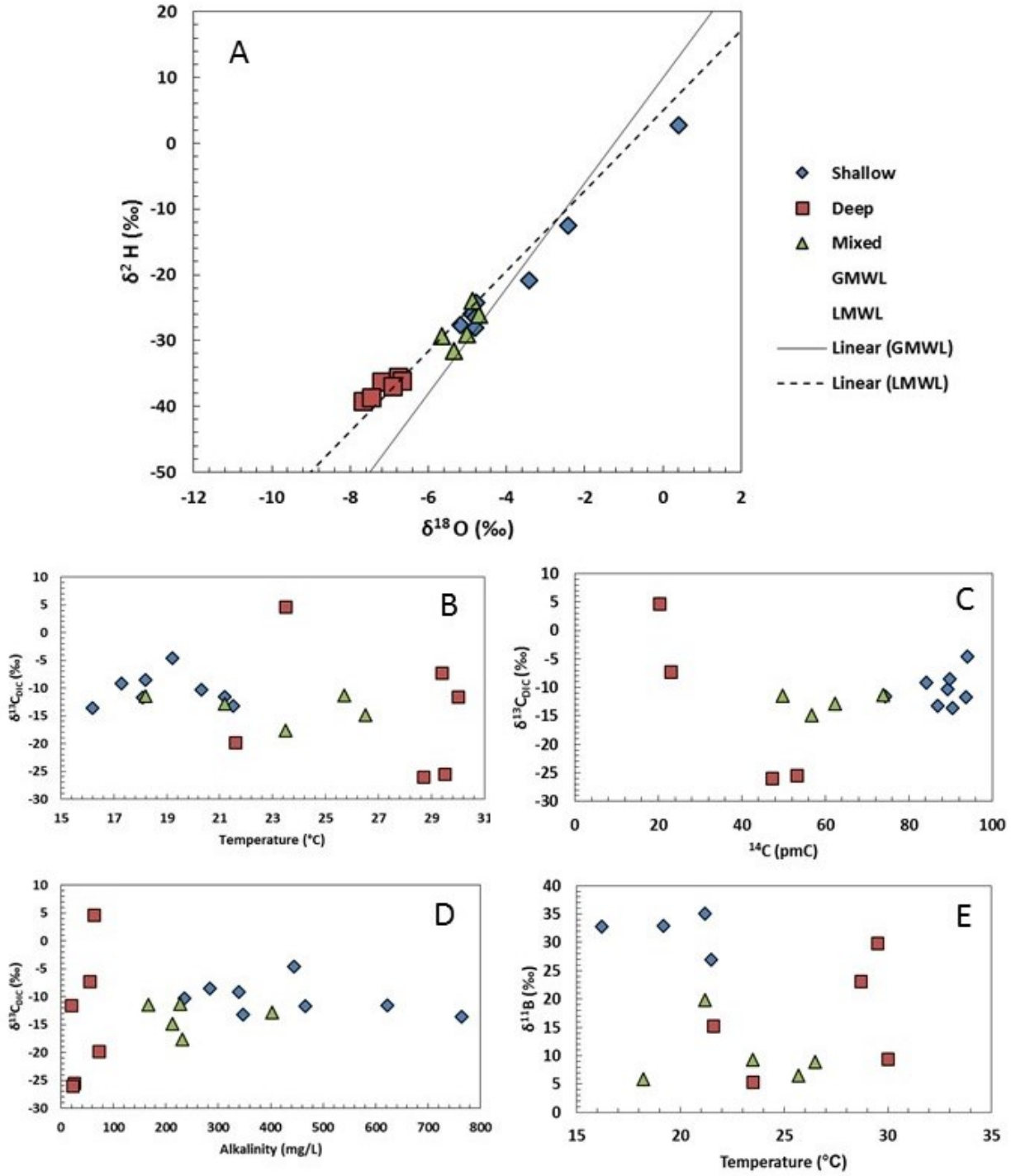

Figure 28: *Relationship between A) $\delta^{18}O$ and $\delta^{2}H$ with the GMWL and LMWL; B) $\delta^{13}C_{DIC}$ and temperature; C) $\delta^{13}C_{DIC}$ and ^{14}C as an indicator of depth; D) $\delta^{13}C_{DIC}$ and alkalinity; E) $\delta^{11}B$ isotopic ratio and temperature of the groundwater samples collected throughout the Karoo Basin. Red squares = deep sites, blue diamonds = shallow sites, green triangles = mixed sites.*

The groundwater samples were also analysed for $\delta^{11}B$ isotopic ratios (Figure 29), although only four of the shallow samples could be analysed because of the low to very low B concentrations in the shallow group. There is a general trend of increasing boron content with an increase in $\delta^{11}B$ ratios observed in the mixed and deep groundwater samples (Figure 29). The shallow sites have relatively high $\delta^{11}B$ ratios between 27 and 35‰ coupled with low B

concentrations between 43 and 753 µg/L (Figure 29), whereas both of the deep and mixed samples have a wide range of $\delta^{11}B$ values between 5 and 30‰, coupled with higher B concentrations between 473 and 3065 µg/L. The mixed group plots between the deep and shallow groups (Figure 29).

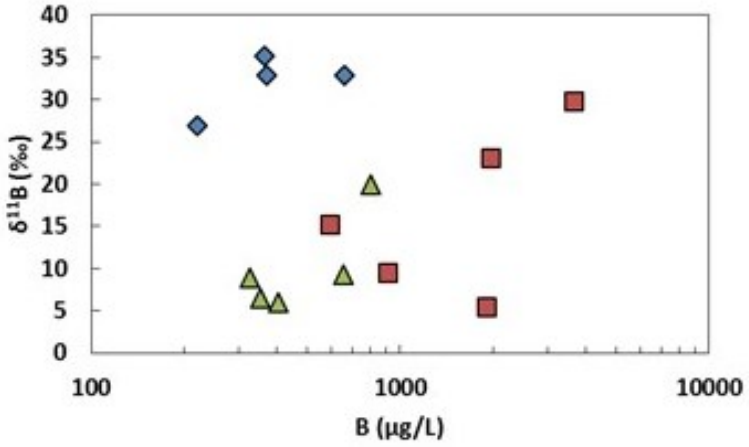

Figure 29: *Relationship between $\delta^{11}B$ and B concentrations for the groundwater samples from the Karoo Basin. Red squares = deep sites, blue diamonds = shallow sites, green triangles = mixed sites.*

2.4.5 Radiogenic isotopes (Sr)

$^{87}Sr/^{86}Sr$ ratios for the deep, mixed and shallow groundwaters are relatively uniform and vary between 0.70887 and 0.71840. Two of the deep groundwater samples have highly radiogenic $^{87}Sr/^{86}Sr$ ratios of 0.77719 and 0.75392 (Figure 30 A). These samples are the two northern-most sites in the study area, FLS1 and VFB1 in Florisbad and Trompsburg respectively, where the base of the Karoo Basin shallows. At least one of these boreholes, VFB1, is known to intersect basement rocks consisting of mafic igneous rocks. Sr concentrations in the deep and shallow groups are correlated with Cl concentrations but the Sr/Cl molar ratio is markedly different between the groups with higher values observed in the shallow group (average values of 0.001 for the deep groundwater compared to 0.01 for the shallow groundwater) (Figure 30 B).

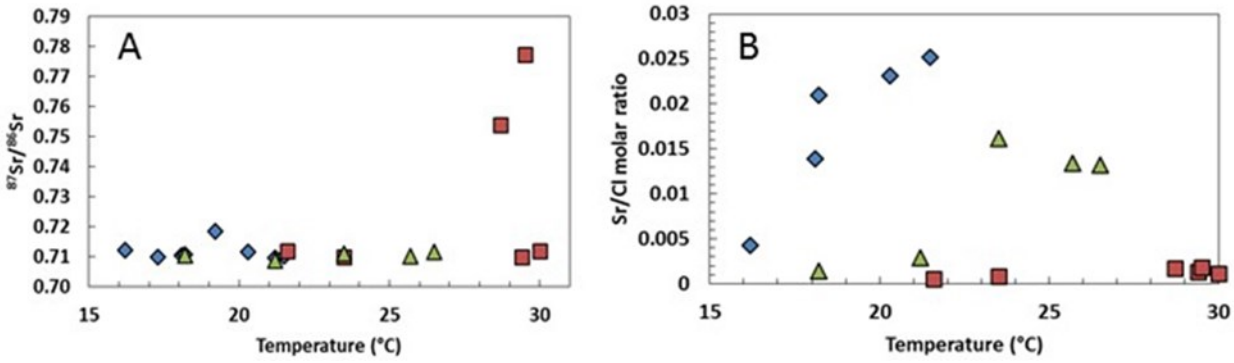

Figure 30: *Relationship between A) $^{87}Sr/^{86}Sr$ ratio; B) Sr/Cl molar ratio versus the temperature of the samples collected in the Karoo Basin. Red squares = deep sites, blue diamonds = shallow sites, green triangles = mixed sites.*

2.5 Discussion

Chapter 1 classified the groundwater samples collected throughout the Karoo Basin into three groups: deep, shallow and mixed. This was based on temperature and major ion chemistry in the form of Stiff Diagrams. This classification was then validated using radiocarbon activities of the samples. The remaining parameters, such as field measurements, trace element chemistry as well as stable isotopes and radiogenic isotopes, were presented in this chapter. Differences observed between the deep, shallow and mixed groundwaters are likely controlled by geochemical processes and/or length of contact time with the host lithologies. A general overview of the main characteristics of and differences between the deep, shallow and mixed groundwaters, in addition to potential explanations for these differences are discussed in the sections below.

2.5.1 Characterisation of Karoo groundwater

A piper diagram was constructed using the major anions and cations of all of the samples collected in this study in order to identify the dominant groundwater type for each group (Figure 31). The dominant cation and anion of the deep groundwater samples are Na and Cl respectively, making this group NaCl-type water. The dominant anion of the shallow group is HCO_3^- and the dominant cations are mixed, making the shallow groundwater mixed-HCO_3^--type water. The dominant cation of the mixed group is Na and the dominant anions are HCO_3^- and Cl^-, making this a Na-HCO_3^--Cl-type water. Stiff diagrams were also used to differentiate between deep, shallow and mixed groundwaters in this project. A summary of the Stiff diagram shape of each site was discussed in Chapter 1. In summary, the deep sites had 'Y' shaped Stiff diagrams and the shallow sites had hexagonal shaped Stiff diagrams. The mixed samples had ambiguously shaped Stiff diagrams that could be categorized with neither the deep nor shallow sites.

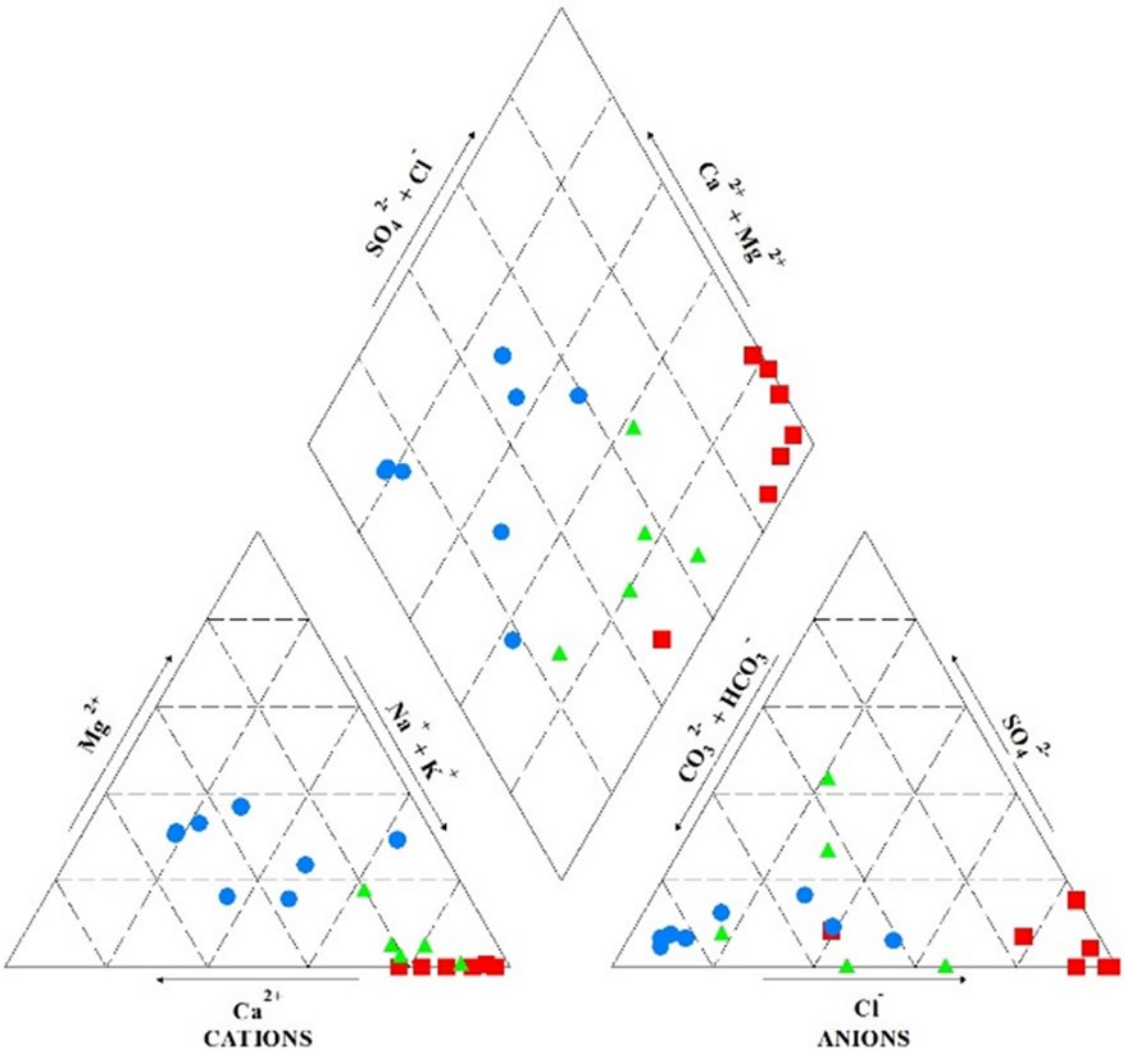

Figure 31: *Piper diagram of the Karoo Basin groundwater samples showing the three groundwater depth groups and their respective groundwater types/facies depending on where they plot on the piper diagram. Red squares = deep sites, blue circles = shallow sites, green triangles = mixed sites.*

2.5.1.1 Shallow groundwater

The shallow groundwater samples collected throughout the Karoo Basin as part of this project can be described by the following characteristics. The groundwater is a mixed-HCO_3^-- type water that is typically cooler than 25°C. pH values lower than 8, positive ORP values and negligible H_2S concentrations were observed in the field. In general, the shallow groundwater is experiencing aerobic conditions in an oxidising environment. A trend of higher concentrations of Mg^{2+}, Ca^{2+}, NO_3^-, SO_4^{2-} and alkalinity in $mg.L^{-1}$ HCO_3^- in comparison to the deep groundwater is observed, whereas lower concentrations of Na^+, K^+, Cl^-, F^- and Br^- are observed. Higher V and U concentrations are observed in comparison to the deep groundwater, whereas lower Li and B concentrations are present. Higher $\delta^{18}O$ and $\delta^{2}H$ ratios are characteristic in comparison to the deep and mixed samples. The Sr isotopic ratios of the

shallow groundwater samples are relatively homogenous with respect to the deep and mixed groups.

2.5.1.2 Deep groundwater

In general, the deep groundwater can be classified as a NaCl type water. Field indicators of deep groundwater include pH levels above 9, negative ORP values, significant concentrations of H_2S indicated by a sulphur/rotten egg smell and temperatures above 25°C. As previously mentioned in Chapter 1, groundwater with a temperature below 25°C can also be classified as deep, such as with site ANBH1 in Aliwal North. Na^+, Ca^{2+} and K^+ are observed in higher concentrations in the deep groundwater, while Mg^{2+} is the only cation that is more depleted in the deep groundwater samples with respect to the shallow groundwater samples. Cl^- and F^- are observed in higher concentrations in the deep groundwater, while NO_3^- and SO_4^{2-} are more depleted in the deep groundwater with respect to the shallow groundwater samples. The deep site in Cradock, CRS1, is an outlier in that it contains both low Cl and Na concentrations in comparison to the other deep sites. Figure 9 in Chapter 1 shows that the deep sites produced 'Y' shaped Stiff diagrams. In contrast to the shallow groundwater samples, the deep groundwater samples were characterised by low uranium and vanadium concentrations and high boron and lithium concentrations. Lower $\delta^{18}O$ and $\delta^{2}H$ values than those in shallow groundwater are observed. As mentioned above, the Sr isotopic ratios produced relatively uniform results for all the groundwater samples, with the exception of two deep samples, namely VFB1 and FLS1. In summary, the deep groundwater is experiencing anaerobic conditions in a reducing environment with respect to the shallow groundwater.

2.5.1.3 Mixed groundwater

Overall, the mixed groundwater samples can be identified as a combination between a $NaHCO_3$ and a NaCl type water. In general, the mixed groundwater has field parameters, major ion and trace element concentrations as well as stable isotopic values in between those of the deep and shallow groundwaters. Figure 8 in Chapter 1 shows that ambiguously shaped Stiff diagrams were produced for the mixed groundwater samples, which could not be classified with either the deep or shallow samples. This suggests that the mixed groundwaters have been influenced by deeper groundwaters yet they also some have some characteristics more indicative of shallow groundwater, and probably represent mixtures between the two groundwater systems.

2.5.2 Controls on water chemistry

Groundwater samples collected throughout the Karoo Basin for this project were categorised as deep, shallow or mixed in Chapter 1, and their specific characterisations were identified in

previous sections of Chapter 2. The following sections aim to identify geochemical processes occurring in the Karoo Basin which could potentially explain the differences observed between deep, shallow and mixed groundwater. The three processes identified as important are: (1) redox reactions; (2) precipitation-dissolution reactions and (3) water-rock interactions, although these are not likely to operate independently of each other.

2.5.2.1 Role of redox reactions

Anoxic conditions and reducing environments are expected in deeper groundwater aquifers where there is little to no contact with the atmosphere. Some evidence of reducing conditions is seen in the results of this study. For example, negative ORP values are observed in the deep samples, whereas positive ORP values are observed in the shallow samples (Figure 33A and B). This suggests that the deep groundwater is in a reducing environment with respect to the shallow groundwater in this study, which is in an oxidizing environment. The mixed groundwater also have negative values, however, these are more positive than the deep samples, suggesting that the mixed samples have been influenced by deeper groundwater at some point in time. Furthermore, U and V concentrations, and potentially other metals, may be low in the deep groundwater as a result of anoxic conditions. Uranium concentrations were further investigated as a result of the presence of the Uranium Province in the Karoo Basin (Figure 32).

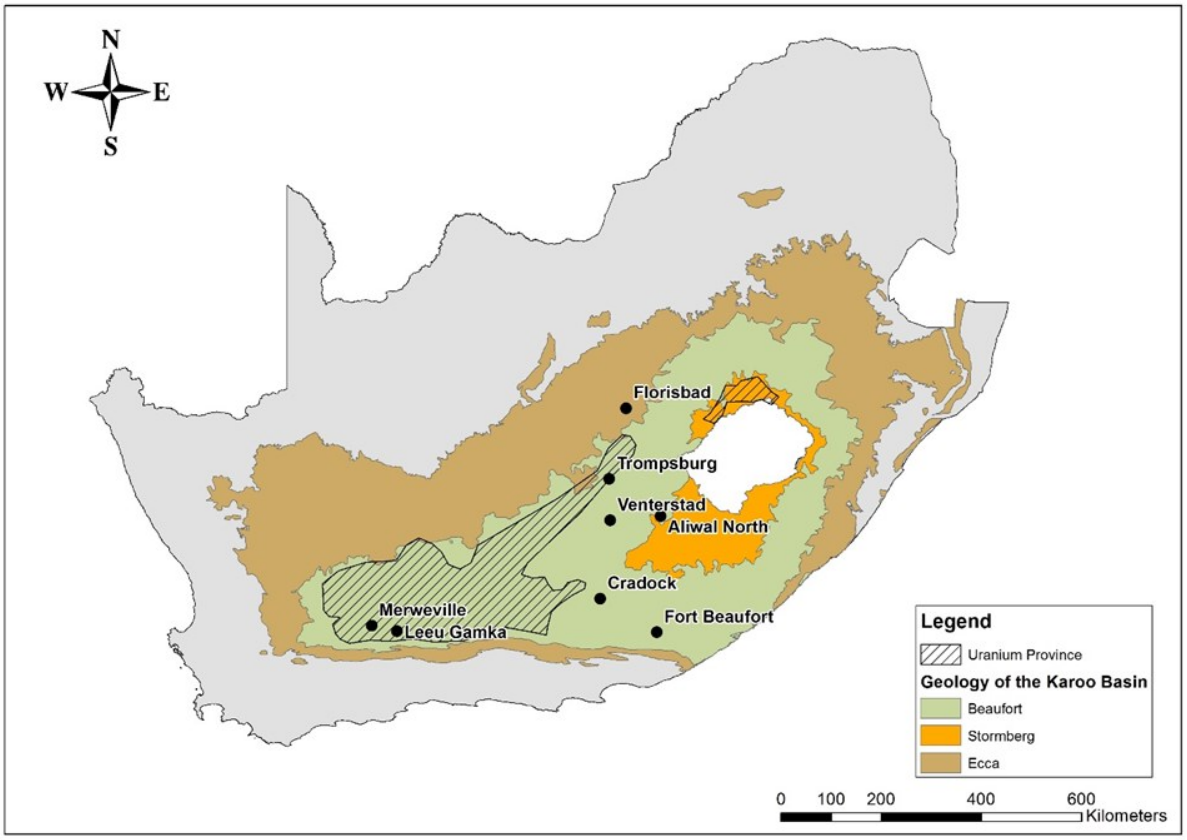

Figure 32: *Map of the Karoo Basin in South Africa, including the Uranium Province of the Adelaide Subgroup in the Beaufort Group (Cole, et al., 1991). The Beaufort, Stormberg and Ecca Groups are shown. The shapefiles were provided by the Council for Geoscience of South Africa.*

Significant U concentrations in the shallow groundwater samples (Figure 33A and C) correlates well with the presence of the uranium province in the Karoo (Figure 32), more specifically in the Adelaide Subgroup of the Beaufort Group. The Adelaide Subgroup is not very deep stratigraphically and is thought to occur above the depths at which the deeper groundwater samples are sourced. This could potentially explain why there are no significant U concentrations in the deep or mixed groundwater samples. This is one potential explanation for the presence of U in the shallow groundwater. Another explanation is that the U is mobilized by NO_3^- in the shallow groundwater (Figure 33C). In the Karoo uranium province, U is likely to be present as U^{4+} in minerals. Nitrate has been shown to abiotically oxidize U^{4+} minerals to U^{6+} making it available to form soluble uranium carbonate complexes. This is particularly so in alkaline groundwater, where U is normally present in the form of U carbonate or U hydroxide anions (Ryan, 2014). Although the deep groundwater is alkaline, carbonate concentrations are abnormally low and this probably acts to prevent the formation of soluble U species (Nolan & Weber 2015; Senko et al., 2002). Moreover, the absence of nitrate in the deep groundwater (along with very low iron concentrations) prevents the formation of soluble U species in the first place (Nolan & Weber, 2015). Schwerdtfeger (2015) suggests that organic carbon (OC) can act as a buffer against the mobilization of U in deeper groundwater systems. It is for this

reason that OC and dissolved organic carbon (DOC) should be measured in future monitoring schemes.

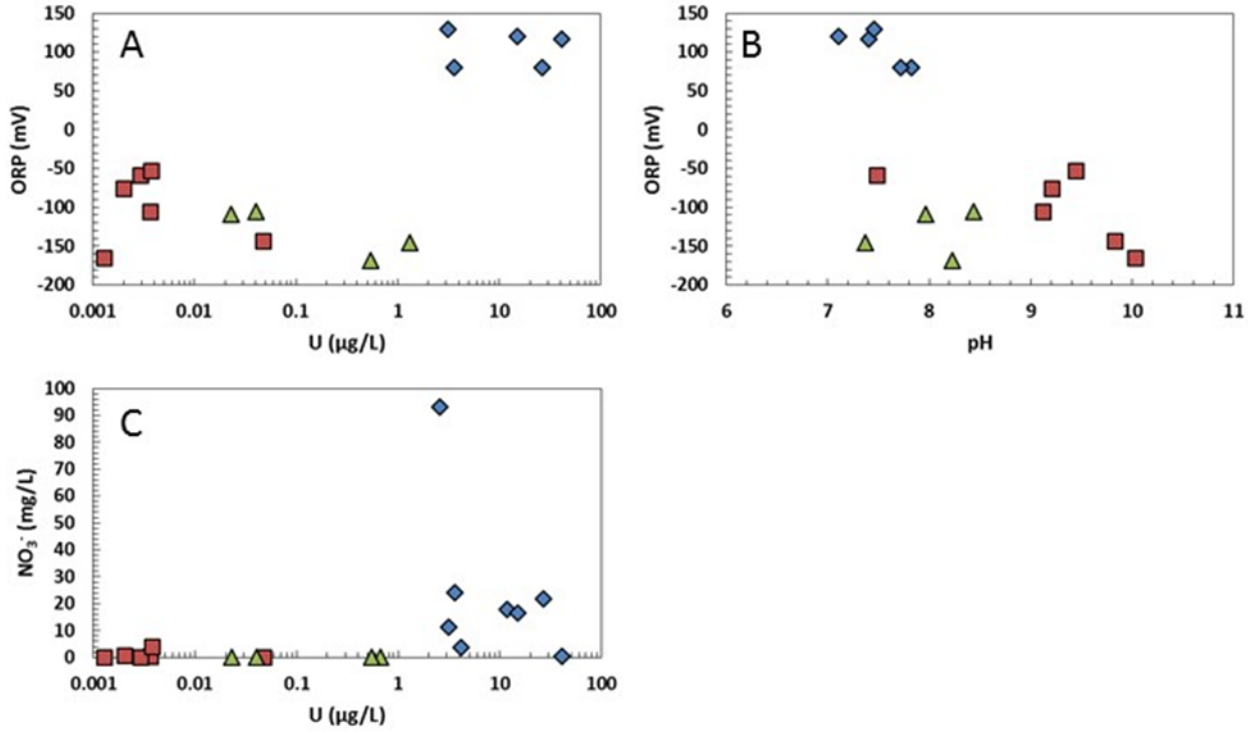

Figure 33: *Relation between A) ORP and U concentrations; B) ORP and pH; C) NO_3^- and U concentrations of the samples collected in the Karoo Basin. Red squares = deep sites, blue diamonds = shallow sites, green triangles = mixed sites.*

As previously discussed, elevated NO_3^- concentrations exist in the shallow groundwater samples. This is not unexpected as NO_3^- contamination of groundwater is a common finding in agricultural areas (Tredoux & Talma, 2006; Heaton, et al., 1983). This is a result of the use of fertilizers in which ammonium (NH_4^+) is oxidized to NO_3^- through the process of nitrification (Kim, et al., 2003). The oxidation process of NH_4^+ is consistent with the oxidizing conditions occurring in the shallow groundwater of the Karoo Basin. The reaction equation for nitrification is as follows:

$$2NH_4^+ + 3O_2 \rightarrow 2NO_2^- + 2\,H_2O + 4H^+$$

$$2NO_2^- + O_2 \rightarrow 2NO_3^-$$

$$NH_3 + O_2 \rightarrow NO_2^- + 3H^+ + 2e^-$$

$$NO_2^- + H_2O \rightarrow NO_3^- + 2H^+ + 2e^-$$

The deep groundwater samples contain little to negligible NO_3 as a result of denitrification. This is the reduction process through which NO_3^- is reduced to N_2 gas (Knowles, 1982; Tredoux & Talma, 2006). The reduction of NO_3^- is consistent with the reducing conditions

occurring in the deeper groundwater samples. The reaction equation for denitrification is as follows:

$$NO_3^- \rightarrow NO_2^- \rightarrow NO + N_2O \rightarrow N_2\ (g)$$

$$2NO_3^- + 10e^- + 12H^+ \rightarrow N_2 + 6H_2O$$

2.5.2.2 Role of precipitation-dissolution reactions

Several molar ratios as well as absolute major ion values show evidence of various precipitation and/or dissolution processes for different minerals (Negrel & Petelet-Giraud, 2005; Edmunds & Smedley, 2000).

Lower Mg^{2+} and Ca^{2+} concentrations, including the Mg/Ca molar ratio, are recorded in the deep groundwater in comparison to the mixed and shallow samples. This is possibly due to cation exchange within the aquifer matrix. Another possible solution to the decrease of Mg is that both Mg^{2+} and CO_3^- are lost due to the formation of $MgCO_3$. The same trend was also observed by Edmunds & Smedley, (2000) in their research of the Sherwood Sandstone Aquifer in the East Midlands, UK. It was concluded that the Mg/Ca molar ratio decreases with an increase in depth due to the dissolution of gypsum which in turn forces the precipitation of calcite ($CaCO_3$) (Edmunds & Smedley, 2000). This is consistent with the low alkalinity (HCO_3^- alkalinity) observed in the deep groundwater as a result of the precipitation of $CaCO_3$. This is also consistent with the pattern of increasing pH with an increase in depth and temperature observed throughout this project.

Sodium concentrations are significantly higher in the deep groundwaters which could be the result of dissolution of Na rich plagioclase feldspar present in the host lithologies (Edmunds & Smedley, 2000; Shabalala, et al., 2015). The K/Na ratio decrease from the shallow to deep samples is consistent with the reaction of illite with kaolinite which was also observed by Edmunds and Smedley (2000). The reaction is as follows:

$$2KAl_3Si_3O_{10}(OH)_2 + 2K^+ + 3H_2O \rightarrow 3Al_2Si_2O_5(OH)_4 + 2K^+$$

Elevated F^- has previously been observed in deep groundwater throughout the Karoo Basin (Kent, 1949; Bond, 1946). It is thought to be the result of longterm dissolution of fluorite and concomitant partial removal of calcium, as mentioned above.

$$CaF_2 + 2H_2O \rightarrow Ca(OH)_2 + 2F^- + 2H^+$$

Patterns in B concentrations are interesting due to the potential importance of $\delta^{11}B$ isotope ratios for tracing contamination of fracking fluids. Studies regarding the use of the $\delta^{11}B$ isotope as a tracer of fracking fluids have been conducted in the United States (Warner, et al., 2014). Boron is derived from various minerals and is known to be present in significant quantities in

thermal water where it is speculated to develop due to slow dissolution rates, enhanced by higher temperatures (Vengosh, et al., 1994). This is consistent with the B results of this study, where higher concentrations of B were observed in the deep groundwater samples compared to the shallow and mixed groups.

2.5.2.3 Role of water-rock interaction

Lithium is frequently found in association with sodium and its isotopes have been suggested as tracers for fracking fluids (Warner, et al., 2014). Edmunds and Smedley (2000) also observed an increase in Li concentrations with an increase in depth. It was concluded that this is due to the presence of Li in clay minerals, which are released in to the groundwater over extended periods of time. As previously mentioned, high Na^+ concentrations are observed in the deep groundwaters. One potential explanation of this trend is the dissolution of Na rich plagioclase feldspar, mentioned above. Another reason could be the result of longer contact time of the deep groundwaters and the host lithologies which consist of sodium rich plagioclase feldspars (Shabalala, et al., 2015). Another source of Na^+ could be fossil salts locked up in marine sediments. This supports the B data described below.

Boron isotope ratios of the groundwater sampled in this project display a wide variation in values. These values reflect the range of $\delta^{11}B$ found in nature; from +40 ‰ in the marine environment, and values of approximately 30‰ reflect boron from sediments, such as clay, deposited in a marine environment. More negative values are observed in continental sediments (Vengosh, et al., 1994). Another source of isotope fractionation is preferential absorption of ^{10}B during interaction with clays which tends to increase $\delta^{11}B$ during increased contact with clays underground (Warner, et al., 2014). The values of the samples from the Karoo Basin did not exceed 35‰. The shallow groundwater samples, as well as one deep sample, VFB1, have $\delta^{11}B$ values of approximately 30‰, reflecting clay sediments deposited in a marine environment. This is consistent with the host lithologies and the depositional environment of the Karoo Basin. Seawater remnants are expected to have $\delta^{11}B$ of >39‰, hence the lower $\delta^{11}B$ values in the groundwater in this study more likely reflects mobilization of exchangeable boron from marine clay minerals (Vengosh et al., 1994). Two of the deep sample sites (VFB1 and FLS1) are from the most northern part of the study area where the basin begins to thin. The groundwater samples from these two sites are therefore suspected to come from basement rocks underlying the Karoo Basin. These two sites have the lowest $\delta^{11}B$ values for the deep group and these values may reflect a contribution from crustal rocks.

2.5.3 Palaeorecharge signature

Lower, more depleted $\delta^{18}O$ and $\delta^{2}H$ values are observed in the deep samples with respect to the shallow samples. The higher, more enriched $\delta^{18}O$ and $\delta^{2}H$ values observed in the shallow group suggest these groundwaters are recently recharged. This is expected from shallow groundwater samples collected from boreholes of less than 100m deep. Furthermore, a slight evaporation trend is observed in the shallow samples is characteristic of shallow groundwater near the surface as the aquifers are more susceptible to evaporation, especially in arid to semi-arid areas such as the Karoo Basin. However, the deeper samples with more depleted $\delta^{18}O$ and $\delta^{2}H$ values show trends consistent with paleoclimate recharge of about 6000 years ago during the Holocene Epoch. This is a well-known phenomenon regarding stable isotopes of O and H and has also been documented in the South African context (Kulongoski, et al., 2004; Heaton, et al., 1986; Holmgren, et al., 2003; Kulongoski, et al., 2004; Stute & Talma, 1997).

The $^{87}Sr/^{86}Sr$ ratio of the Permian seawater was approximately 0.7077 when the Karoo Basin was deposited at 283 Ma (McArthur, et al., 2001). The $^{87}Sr/^{86}Sr$ ratios measured in the groundwater samples collected for this project, which range from 0.70887 to 0.77719, are higher, in two instances significantly, than the seawater. This has also been observed in a study conducted in the Karoo Basin by Herbert & Compton (2007). Therefore the $^{87}Sr/^{86}Sr$ ratios observed in the Karoo Basin could be influenced from another source, such as the basement granitic rocks, which contain higher isotopic ratios. While this confirms that the water from the deep Trompsburg borehole VFB1 originates, at least partly, from the basement gneisses where water was struck, it also suggests that the groundwater sourced from the deep site at Florisbad, FLS1, may have a very deep flow path and be in contact with basement rocks. This also gives reason to why sample sites VFB1 and FLS1 are often outliers in trends observed throughout the data.

2.5.4 Impact of methanogenesis

The wide range of $\delta^{13}C_{DIC}$ values between -26 to 4.7‰ for all of the groundwater analysed in this project implies that majority of the DIC is derived from carbonates (Edmunds & Smedley, 2000). However, the Karoo Basin is dominated by silicate rocks and not carbonates. $\delta^{13}C_{DIC}$ values of between -20 and -17‰ are derived from the weathering of silicate minerals which are widespread throughout the basin. Interestingly only two samples (WP 505 which is a mixed sample from Leeu Gamka, and ANBH1 which is a deep sample with a lower temperature in Aliwal North) have isotopic values within this range. Therefore the DIC must be derived from another source. The majority of the shallow and mixed samples have relatively uniform $\delta^{13}C$ ratios which are consistent with those indicative of C4 plants by which the Karoo Basin is

dominated. However, two of the deep sites, VFB1 and FLS1, have more negative $\delta^{13}C$ values which are more consistent with C3 plants. It is possible that a change in vegetation occurred over time and that these samples reflect $\delta^{13}C$ ratios indicative of the Karoo Basin being previously dominated by C3 plants. Moreover, the remaining deep samples, CRS1 and BFB1, have less negative and even positive $\delta^{13}C$ ratios, in the case of site BFB1. These higher $\delta^{13}C$ values suggest another process is the cause, which could potentially be methanogenesis caused by the direct reduction of CO_2. It is thought that direct reduction of the CO_2 is responsible, as opposed to the other method of methanogenesis, acetate fermentation, which results in a significant increase in $\delta^{13}C_{DIC}$ values (meaning that all values would be more positive). However, this increase would also result in a significant increase in the ^{14}C content of the samples, suggesting that the deeper groundwaters are in fact relatively young with some component of mixing. This idea was excluded because of the low ^{14}C content in percent modern Carbon (pmC) of the deeper groundwater samples, which indicates longer residence times. This is further supported by the low tritium activities as well as the low chlorine 36 and high helium content measured in the deep samples. These isotopes and estimated residence times are discussed further in Chapter 3.

Methanogenesis also explains the unexpected trend of increasing pH with a decrease in alkalinity in deeper groundwaters, whereby carbon is consumed by microbial activities resulting in a decrease in the alkalinity and an increase in the pH. Methanogenesis is a more likely reason because this hypothesis also supports the relatively high values of the $\delta^{13}C_{DIC}$ measured in the samples. This further suggests that the deeper groundwater samples are in fact occurring in an anoxic, reducing environment which is supported by the negative ORP values as well as high H_2S concentrations observed in the deep groundwater samples. H_2S, when present in natural, unpolluted situations is an indicator for anoxic or reducing conditions generally associated with deeper flow.

Results from a study conducted by Cartwright (2010) focussed on a silicate-dominated basin in Australia, concluded that enriched $\delta^{13}C$ values ranging from -18 to 2‰ were the result of methanogenesis via direct reduction of CO_2 in the groundwater. Figure 34 displays three trends (represented by the black arrows) observed by Cartwright (2010) as well as Coetsiers & Walraevens (2009), which are in good agreement with the data collected in this project. Figure 34A displays a trend of increasing alkalinity with an increase in $\delta^{13}C$ from the deep, to the shallow samples and correlates with the methanogenesis trend shown by the black arrow (Cartwright, 2010). Figure 34B shows Ca^{2+} as a function of $\delta^{13}C$. The data from this study corresponds well to the two trends seen in Coetsiers & Walraevens (2009), namely (1) calcite dissolution and (2) methanogenesis. Figure 34C presents SO_4^{2-} concentrations as a function of $\delta^{13}C$. The deep samples have uniformly low SO_4^{2-} concentrations which are in good agreement with the methanogenesis trend observed in the study by Coetsiers & Walraevens (2009).

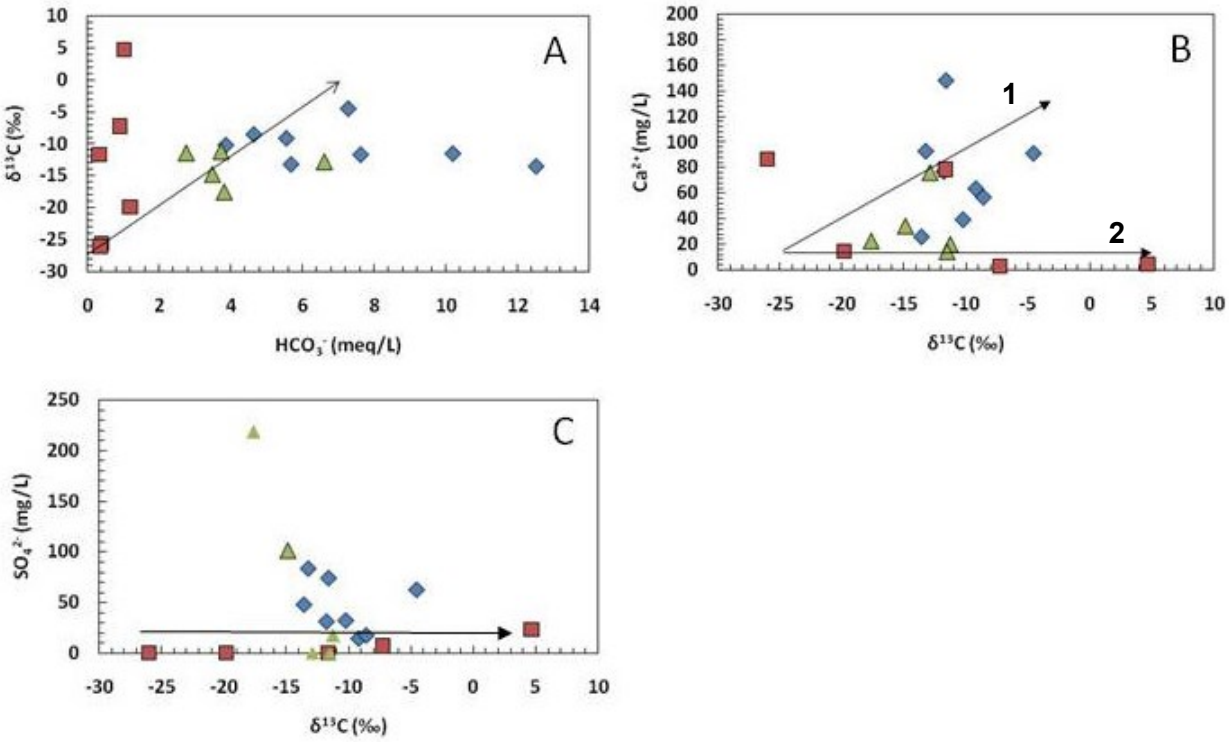

Figure 34: *Relationship between A) $\delta^{13}C$ values and alkalinity in mg.L^{-1} HCO_3^-. The arrow indicates the expected trend for calcite dissolution, cation exchange and methanogenesis (Coetsiers & Walraevens, 2009); B) Ca^{2+} concentrations and $\delta^{13}C$ values. The arrows indicate the expected trend for (1) calcite dissolution and (2) methanogenesis (Coetsiers & Walraevens, 2009); C) SO_4^{2-} concentrations and $\delta^{13}C$ values. The arrow indicates the expected trend for methanogenesis (Coetsiers & Walraevens, 2009; Cartwright, 2010). Red squares = deep sites, blue diamonds = shallow sites, green triangles = mixed sites.*

Figure 35 shows $C_1/(C_2+C_3)$ as a function of $\delta^{13}C_{CH4}$, more commonly known as a Bernard Plot. The results from this study are shown on the reference diagram (Darling, 2013). A microbial oxidation trend is observed, further supporting the hypothesis of methanogenesis affecting in the deep groundwater samples.

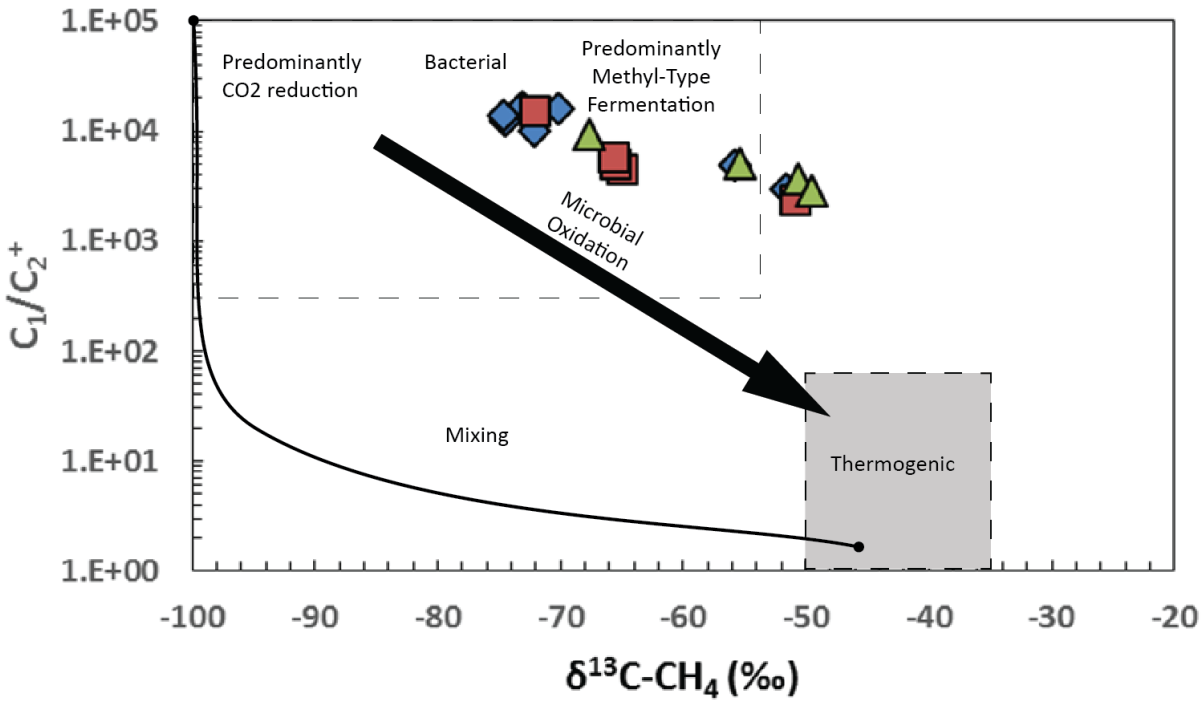

Figure 35: *Bernard plot of the samples collected throughout the Main Karoo Basin. References from the Bernard plot in Darling (2013) are indicated on the diagram.*

2.5.5 Variation in the deep groundwater signature

All six of the deep samples show the same trends when observing some parameters such as pH, alkalinity, NO_3^-, $\delta^{18}O$ and $\delta^{2}H$. However, when looking at the temperature, $^{87}Sr/^{86}Sr$, $\delta^{13}C$ and $\delta^{13}B$ ratios of the deep groundwater samples, some of the sites do not conform to the general trends. This suggests that the deep groundwater samples collected in this study originate from multiple sources which are being affected by different recharge timescales. This is further investigated in Chapter 3 where residence times of the groundwater samples will be calculated using four different isotopic dating methods.

As mentioned in Chapter 1, temperature is a common indicator of deep groundwater. This is based on the assumption that warmer water must come from deeper crustal levels due to the lack of another obvious heat source in the Karoo Basin and hence why thermal springs and boreholes were targeted in this project. However, it would appear that low temperature is not a sufficient condition to classify a source as shallow. Two sites (ANBH1 located in Aliwal North and BFB1 from the Fort Beaufort Sulphur Baths) have temperatures below 25°C while all other

parameters are indicative of deep groundwater. The most likely explanation for this would be the slow migration of the groundwater, which could be extremely variable and site specific, to the surface. As a result of this slower migration process, the temperatures of the groundwaters cool. This further supports the contention that although high temperatures are a clear indicator of deep groundwater, a low temperature does not preclude the possibility that the groundwater has circulated at depth.

2.5.6 Origin of mixed groundwater samples

Five of the groundwater samples collected could not be classified as either deep or shallow based on explanations discussed in Chapter 1. Therefore, these samples were categorised as 'mixed' groundwater. There are three potential origins of the groundwater labelled as mixed: (1) the samples are either deep or shallow samples that have been wrongly identified; (2) the samples represent genuine mixtures of the deep and shallow groundwaters; or (3) they could be a completely different groundwater type originating from a different source altogether. To test which is the more likely explanation, the mixed groundwater samples were evaluated against how many indicators from Groups 1 and 2 in Table 1 they conformed with. It was concluded that the mixed sites conformed to half of the parameters indicative of deep groundwater, implying that the mixed samples are in fact a mixture of the deep and shallow groundwater samples. Although the mixed groundwater samples seem to genuine mixtures of the deep and shallow groundwater sampled in this project, the classification is based on only 5 samples. Therefore, other explanations cannot be excluded. Because of the concerns regarding contamination of shallow groundwater by either deep groundwater of poorer quality or by fracking fluids, understanding the formation of these mixed groundwaters and their significance to deeper flow systems is of paramount importance.

2.6 Conclusions

From the vast number of geochemical parameters measured for the 19 samples collected for this study, it was possible to characterise the deep, shallow and mixed groundwaters based on patterns and reaction processes that emerged from the results. In general, the shallow groundwater samples of the Karoo Basin sampled in this project have cooler temperatures below 25°C, low pH values less than 8, high alkalinity values and the groundwater can be classified as a mixed-HCO_3^--type water. The deep groundwater can be characterised by a higher temperature above 25°C, however, this is not always the case. Higher pH values above 9, low alkalinity values below 80 $mg.L^{-1}$ HCO_3^-, negative ORP values and considerable H_2S concentrations are prevalent. The groundwater can be classified as NaCl-type water. Overall, the mixed samples have characteristics that are intermediate with respect to the deep and

shallows samples. As mentioned in Chapter 1, these sites could not be classified as either deep or shallow on the basis of temperature, Stiff diagram shape and ^{14}C value and were therefore labelled as mixed groundwater. There are thought to be three possible origins for these samples: (1) the samples are either deep or shallow samples that have been wrongly identified; (2) the samples represent genuine mixtures of the deep and shallow groundwaters; or (3) they could be a completely different groundwater type originating from a different source altogether.

The process of nitrification occurs in the shallow groundwaters and is exacerbated by the agricultural practices near to many of the shallow sampling sites, resulting in an increase in NO_3^- concentrations. In contrast, the process of denitrification occurs in the deep groundwater resulting in an absence of NO_3^- concentrations. It is also thought that NO_3^- allows for the mobilization of U, hence why U is only present in the shallow groundwater samples. Evidence of cation exchange is present in the deep groundwater samples when observing low Ca^{2+} and Mg^{2+} concentrations. However, low Mg/Ca molar ratios coupled with low alkalinity in the deep groundwater, could also indicate evidence of calcite precipitation. Increased Na^+ concentrations in the deep groundwater occur as a result of increased contact time with the host lithologies, the reaction of illite with kaolinite or fossilised salts present in marine sediemnts. Elevated F^- in the deep groundwater is the result of dissolution of F^-. Enriched B concentrations in the deep groundwater in comparison to the shallow groundwater are the result of slow dissolution rates occurring in groundwaters with higher temperatures.

The $\delta^{11}B$ values of the shallow samples reflect values typical of boron from sediments, such as clay, deposited in a marine environment which is consistent with the Karoo Basin depositional environment. Depleted $\delta^{18}O$ and $\delta^{2}H$ values in the deep groundwater samples are in agreement with Paleoclimate conditions from at least 6000 years ago. In general, the shallow groundwater is experiencing oxidizing conditions as is evident by the positive ORP values and the lack of H_2S. In contrast, the deep groundwater is experiencing anoxic conditions in a reducing environment as is evident by the negative ORP values, significant presence of H_2S as well as the indications of methanogenesis. Significant variations in the characteristics of some of the deep groundwater samples are observed, suggesting that the deep groundwater sampled in this project originates from multiple sources.

Further investigation and characterisation of the groundwater in the Karoo will allow for a more in depth understanding of the different groundwater systems and how they may potentially be affected through the fracking process.

CHAPTER 3 – Distinguishing groundwater systems using multiple radiometric dating techniques

3.1 Introduction

Groundwater is an important resource and requires proper management and protection, particularly in arid and semi-arid regions. Two of the key questions often asked in groundwater resource management are how old is the resource and how long will it last. These questions are frequently answered using radiometric dating and it implies the length of time that the groundwater has been in the aquifer. The basic principle of radiometric dating is that if the rate of decay of a radioactive parent isotope is known, and the concentration of the daughter isotope can be measured, then the time taken to accumulate the daughter isotope gives an indication of how old a sample is (Bethke & Johnson, 2008). For groundwater systems, radiometric dating works along the assumption that the concentrations of the daughter and parent isotopes are in secular equilibrium with the atmosphere. When the groundwater becomes isolated from the atmosphere, the concentration of the parent isotope decreases and the concentration of the daughter isotope increases and accumulates at which point it can be measured (Torgersen, et al., 2013). This is a simplistic explanation of radiometric dating which has many complexities to it (Torgersen, et al., 2013).

In order to determine the rate of decay of the parent isotope either the half-life ($T_{1/2}$) or the decay constant (λ) of the isotope must be known. In most instances, some of the daughter isotope is already present in the sample, therefore this must be accounted for by subtracting this initial activity (A_0) from the measured activity in the sample (A_t) (Torgersen, et al., 2013). Many assumptions are made as various factors may influence the concentrations of the initial isotope activity (A_0). For example, the initial activity for radiocarbon (^{14}C) is dependent on the rock, soil and plant types of the region. The radiometric clock starts when there is no more replenishment from the atmosphere. However, the isolation point from the atmosphere is not always clear because equilibrium can be maintained with the atmosphere through root respiration. In arid and semi-arid regions, it is a common occurrence for the root systems to be very deep, therefore this point of isolation is even more indistinct (Schenk & Jackson, 2002). Furthermore, different radiometric isotopes have different half-lives and different factors of influence, therefore, the “age” of a sample calculated by each radiometric isotope may be different.

Attaining a residence time from one isotope makes it difficult to evaluate whether it is in fact the true age of the sample. Therefore, there is an advantage in using multiple isotopes as it allows for the improvement of the statistics on the residence time calculations by ideally getting

similar results from multiple isotopes. Various studies have used multiple isotopic tracers in groundwater age dating (Plummer, et al., 2012; Lehmann, et al., 2003; Corcho Alvarado, et al., 2005; Lavastre, et al., 2010). Plummer, et al., (2012) estimated groundwaters ages along two different flow paths in Maryland, USA, using ^{14}C, chlorine-36 (^{36}Cl) and helium-4 (^{4}He). Lehmann, et al., (2003) analysed groundwater in the Great Artesian Basin in Australia for krypton-81, ^{36}Cl and ^{4}He. Corcho Alvarado, et al., (2005) analysed groundwater in the Odense Pilot River Basin, Denmark, for krypton-85, ^{36}Cl, tritiogenic helium ($^{3}H/^{3}He$), SF_6 and CFC-12. Lavastre, et al., (2010) estimated groundwater ages of the eastern Paris Basin, France, using ^{36}Cl, ^{14}C, tritium (^{3}H) as well as noble gases. These studies indicate that using multiple isotopes to estimate groundwater residence times aids in understanding different aquifer systems of the same region which is important for long term groundwater management programmes.

The Karoo Basin in South Africa has been identified as a potential shale gas region with possible economically viable resources within the Whitehill Formation of the Ecca Group. However, it is uncertain how the process of fracking will affect the Karoo Basin from an environmental perspective. This has previously been discussed in detail in Chapter 1. One of the major concerns is the potential contamination of the shallow groundwater aquifers in close proximity to the drill sites. Subsistence and commercial farmers as well as local communities are dependent on groundwater resources for agricultural and domestic purposes. One way in which this could occur is the contamination with deeper groundwater which may be of poor quality, such as in the Marcellus Shale play in Pennsylvania, USA (Vengosh, et al., 2013; Warner, et al., 2012). The Karoo is an already water-stressed region experiencing a semi-arid climate. Therefore any pollution of the scarce groundwater sources would be detrimental not only to the Karoo Basin, but also to the country as a whole because the Karoo is an important agricultural region. It is therefore, important to have a better understanding of the deeper groundwater in the Karoo Basin.

The chemical composition of the groundwater samples collected throughout the Karoo Basin was discussed in Chapter 2. The main objective of this chapter is to compare and contrast residence times of the deeper and shallow groundwater samples using multiple radiogenic isotopes, specifically tritium, tritiogenic helium, radiocarbon and chrloine-36. This will allow for an assessment of how robust the division of the shallow and deep groundwater (determined in Chapter 1) is and further assessment of what the mixed groundwater might represent. Tritium is useful for tracing and dating young, recently recharged groundwaters due to its short half-life of only 12.43 years (Schlosser, et al., 1988). Simultaneous analysis of ^{3}H with its decay product, helium-3 (^{3}He), known as tritiogenic helium ($^{3}H/^{3}He$) allows for significantly more information to be derived (Schlosser, et al., 1988). Tritiogenic helium is also useful for dating

groundwater containing recent recharge and post 1950's water (Eby, 2004; Schlosser, et al., 1988). Radiocarbon has a half-life of 5730 year and can date intermediate aged groundwaters ranging from 1000-30000 years old (Eby, 2004). Chlorine-36, with a half-life of 301000 years, is useful in dating older groundwaters aged up to 1000000 years old (Phillips, 2013; Bentley, et al., 1986). Helium-4 has the longest potential age dating range from 100 to 1000000 years (Plummer, et al., 2012).

Knowledge about the residence times of the deeper, mixed and shallow groundwaters will provide an insight into the connectivity of the deeper and shallower aquifer systems in the Karoo Basin. This could aid in predicting potential upward migration patterns of the deep seated groundwater into the shallow aquifer systems. This information would be beneficial if fracking takes place in the Karoo. Moreover, this information can be used to investigate the timescales and implications of the recharge processes of the deeper aquifer systems throughout the Karoo Basin.

3.2 Sampling and analysis techniques

Sampling was carried out in June-July 2014 for two weeks. Eight locations throughout the Karoo Basin (Figure 13) were selected because of known or suspected deep groundwater flow, and within a few kilometres of these sites, one or two shallow boreholes were selected to represent shallow groundwater in the area. In total, 19 samples were collected which include 8 shallow samples, 5 mixed samples and 6 deep samples. See Chapter 2 for a full description of the sampling sites and locations.

3.2.1 Groundwater sampling

All boreholes were pumped for at least 30 minutes prior to sampling in order to remove any stagnant water and to ensure that "fresh" groundwater was sampled. The electrical conductivity (EC) was monitored whilst pumping took place and the sample was collected once the EC had stabilized. pH and temperature were then measured using an Extech EC500 combined pH, EC and temperature probe. All the probes were calibrated on a daily basis. Field alkalinity was determined using a Hach digital titrator, and titrated to a pH of 4.5 using 1.5M or 0.15M sulphuric acid and Green-Methyl Red and Phenolphthalein indicators. In all samples the total alkalinity was equal to the bicarbonate alkalinity ($mg.L^{-1}$ HCO_3^-). Alkalinity was also measured in the Central Analytical Facility (CAF) laboratory in the Department of Soil Science at Stellenbosch University using a Metrohm 905 Titrano Autotitrator as well as at Duke University, USA. ^{3}H, ^{14}C and ^{36}Cl samples were collected in HDPE acid washed bottles. For radiocarbon samples with alkalinity below 100 $mg.L^{-1}$ HCO_3^-, 1L was collected and filtered into acid washed Nalgene bottles. For ^{14}C analysis, the volume of water to be processed was

determined from the alkalinity such that at least 2 g of C could be collected per sample. For samples with alkalinities above 100 mg.L^{-1} HCO_3^- this involved the collection of either 25L or 50L of groundwater. Directly on collection of the groundwater sample, 250g of $BaCl_2$, 200ml of 400g/L NaOH solution and 10ml of phenolphthalein indicator were added to each sample. This resulted in the precipitation of $BaCO_3$ which was allowed to settle for 2 hours after which the supernatant was allowed to drain away and the resultant $BaCO_3$ slurry was collected in 1L HDPE bottles. ^{36}Cl samples were filtered in the laboratory during processing (discussed in further detail in the section below). Tritium samples were not filtered because the samples were distilled in the laboratory during analysis (discussed in further detail below). Noble gas samples were collected in copper tubes and sealed with end caps to avoid interaction with the atmosphere. All samples were kept at less than 4°C in the field and transferred to fridges in the laboratory.

3.2.2 Analytical techniques

Eleven samples with alkalinities above 100 mg.L^{-1} HCO_3^- were analysed for radiocarbon via Liquid Scintillation Counting (LSC) at iThemba LABS in Johannesburg. Analytical errors were ± 2.5 pmC. Five of the samples with alkalinities below 100 mg.L^{-1} HCO_3^- were analysed for radiocarbon by Accelerator Mass Spectrometer (AMS) at Beta Analytic in Miami, Florida. Analytical errors were ± 0.2 pmC. The samples are relative to NIST standards of RM-8539, 8540, 8541 and 8542. Tritium samples were analysed using a Packard Tri-Carb 2770TR/SL, a low level liquid scintillation analyser at iThemba LABS in Johannesburg, South Africa. Analytical errors were ± 0.3 TU. The samples were distilled and introduced to an electrolytic cell before being placed in the counter. Chlorine-36 samples were acidified and prepared using $AgNO_3$ to produce AgCl precipitate. The resultant precipitate was sealed in PP containers and wrapped in foil to exclude any light. The concentration of the ^{36}Cl isotope was measured via AMS at the Australian National University in Canberra, Australia. Analytical errors of the $^{36}Cl/Cl$ ratio were ± 82 x10^{-15}. Major gas components (e.g., N_2, O_2, Ar, and CH_4) were measured using an SRS quadrupole mass spectrometer (MS) and an SRI gas chromatograph (GC) whereas isotopic noble gas samples were extracted from their copper tubes and measured via a Helix SFT noble gas mass spectrometer at Ohio State University, USA. Duplicate samples were collected and analysed. Standard analytical errors were ± 3% for noble gas concentrations ([^4He], [^{22}Ne] and [^{40}Ar]). Isotopic errors were approximately ±0.01 times the ratio of air (or 1.4 x10^{-8}) for $^3He/^4He$ ratio, <±0.5% and <±1% for $^{20}Ne/^{22}Ne$ and $^{21}Ne/^{22}Ne$, respectively, and <±1% for $^{38}Ar/^{36}Ar$ and $^{40}Ar/^{36}Ar$, respectively (higher than normal because of interferences from C_3 on mass=36).

3.3 Results

Radiocarbon, tritium, chlorine-36 and helium-4 data are presented in the sections below. Tables 6 through 9 present the data discussed in the following sections. Note, not all of the samples were analysed for every isotope presented in this chapter. Table 5 gives a summary of which samples were analysed for the different isotopes. In all of the graphs the deep samples are represented by red squares, the shallow samples by blue diamonds and the mixed samples by green triangles.

Table 5: *Summary of the isotope analyses of the groundwater samples collected throughout the Main Karoo Basin.*

	Town	Sample No.	^{3}H	$^{3}H/^{3}He$	^{14}C	^{4}He	^{36}Cl
			TU	TU	pmC	μcm^3 STP/kg	atoms/L
SHALLOW GROUP	Leeu Gamka	WP 502	X	X	X	X	X
	Cradock	DRB4	X	X	X	X	X
	Fort Beaufort	RRB1	X	X	X	X	X
	Venterstad	RWB5	X	X	X	X	X
	Venterstad	LRB2	X	X	X	X	
	Trompsburg	VFB2	X		X	X	X
	Florisbad	FLB5	X		X	X	X
	Merweville	MWB2	X	X	X	X	X
MIXED GROUP	Leeu Gamka	WP 508	X	X	X	X	X
	Leeu Gamka	WP 505	X	X		X	X
	Fort Beaufort	BFB2	X	X	X	X	X
	Venterstad	RWB1c	X	X	X	X	X
	Venterstad	VBB1	X	X	X	X	X
DEEP GROUP	Cradock	CRS1	X	X	X	X	X
	Fort Beaufort	BFB1	X		X	X	X
	Aliwal North	ANS1	X			X	X
	Aliwal North	ANBH1	X			X	X
	Trompsburg	VFB1	X		X	X	X
	Florisbad	FLS1	X		X	X	X

Notes: *Samples analysed for a specific isotope are marked with an 'X'.*

3.3.1 Tritium and tritiogenic helium

The tritium and tritiogenic helium data is shown as a function of temperature and $\delta^{18}O$, as these parameters were used as proxies for groundwater depth (Figure 36). The deep sites generally have low ^{3}H activities between 0 and 0.5 TU, except for site FLS1 which contains a higher activity 1.6 TU (Figure 36B and C). The ^{3}H activities of the shallow group range between 0.5 and 3.1 TU (Figure 36B and C). The mixed sites have ^{3}H activities that fall in between and overlap with both the deep and shallow groups between 0.1 and 0.9 TU (Figure 36B and C). Tritiogenic helium activities are only present in the shallow and mixed groups as well as in one deep sample (CRS1). Figure 36C and D display the opposite trend observed in Figure 36A and B. However, it is clear that the mixed samples contain higher activities of $^{3}H/^{3}He$ than the shallow samples. The shallow samples contain $^{3}H/^{3}He$ activities between 2.5 and 8.84 $x10^{19}$ TU. The mixed samples contain $^{3}H/^{3}He$ activities ranging from 6.46 $x10^{19}$ to 8.03 $x10^{20}$ TU. The deep sample, CRS1, has a $^{3}H/^{3}He$ activity of 4.4 $x10^{19}$ TU.

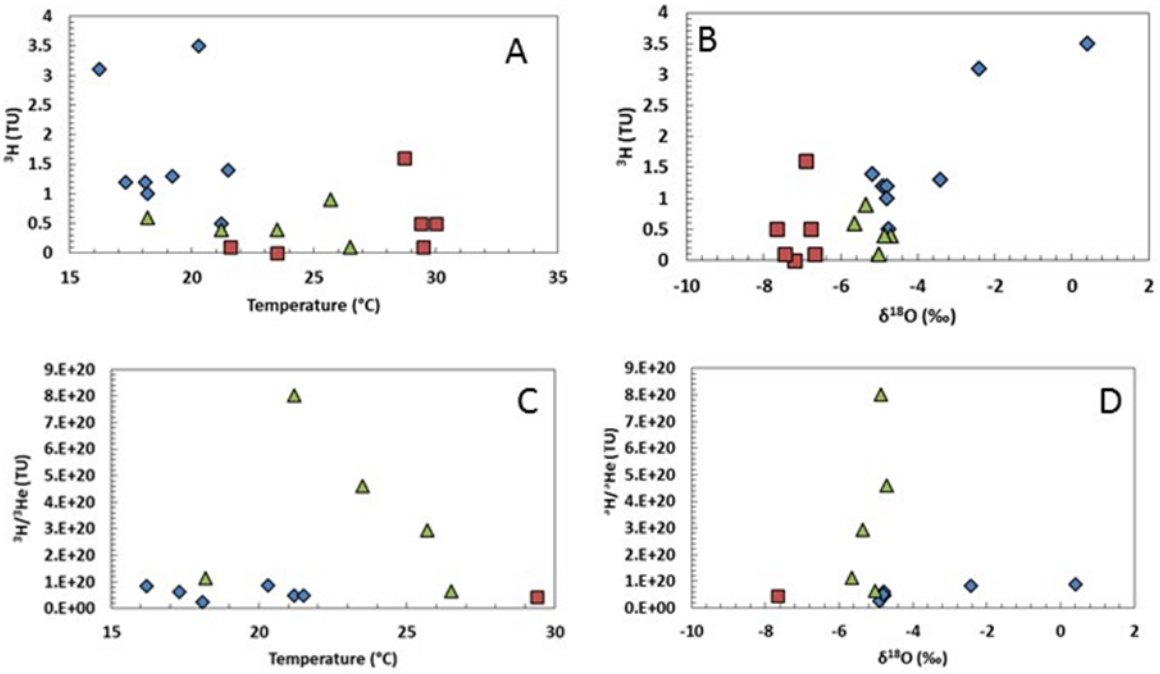

Figure 36: *Relationship between A) ^{3}H and temperature; B) ^{3}H and $\delta^{18}O$ C) $^{3}H/^{3}He$ and temperature; D) $^{3}H/^{3}He$ and $\delta^{18}O$ of the samples collected throughout the Karoo Basin. Red squares = deep sites, blue diamonds = shallow sites, green triangles = mixed sites.*

3.3.2 Radiocarbon

The radiocarbon data is shown as a function of temperature as this parameter is used as a proxy for groundwater depth (Figure 37). Only four of the deep samples (CRS1, BFB1, VFB1 and FLS1) were analysed for radiocarbon as a result of their extremely low alkalinities. WP 508, a mixed site in Leeu Gamka, was analysed for radiocarbon but not site WP 505 as it is

also a mixed site at the same location. The shallow samples contain the highest ^{14}C contents between 74 and 94 pmC (Figure 37). The deep samples contain the lowest ^{14}C contents ranging from 20 to 53 pmC (Figure 37). The mixed samples plot between the deep and shallow samples with intermediate ^{14}C activities between 50 and 74 pmC (Figure 37).

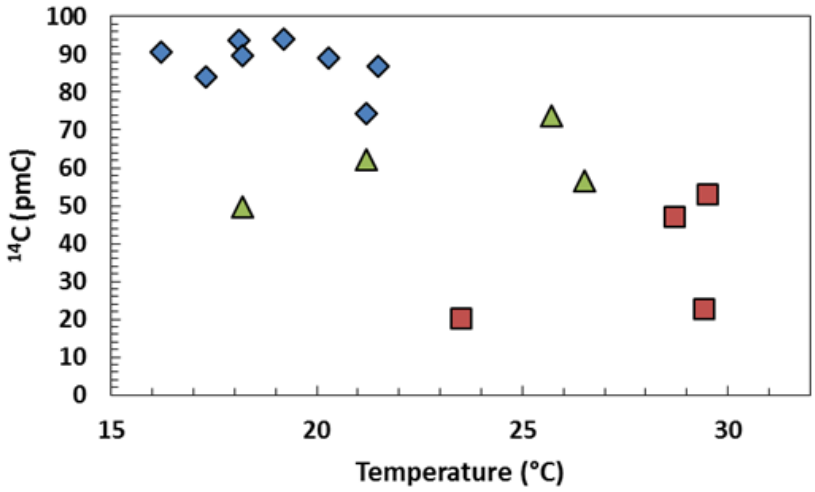

Figure 37: *Relationship between ^{14}C and temperature of the samples collected throughout the Karoo Basin. Red squares = deep sites, blue diamonds = shallow sites, green triangles = mixed sites.*

3.3.3 Helium-4

This data is shown as a function of temperature and ^{14}C as these parameters are used as proxies for groundwater depth (Figure 38). The distribution of ^{4}He for the different depth groups shows that the shallow samples contain lower ^{4}He contents between 87 and 987 μcm^3 STP/kg (Figure 38 A and B). Two of the shallow sites, RRB1 and FLB5, contain anomalously high ^{4}He contents of 10151 and 7513 μcm^3 STP/kg respectively. Whereas the deep samples contain higher ^{4}He contents between 120583 and 483493 μcm^3 STP/kg. Two deep sites, CRS1 and BFB1, contain very little ^{4}He in comparison to the other deep samples of 412 and 71 μcm^3 STP/kg respectively. The mixed sites plot in between the deep and shallow groups slightly overlapping with the deep group with contents from 6753 to 84513 μcm^3 STP/kg. The distribution of the $^{3}He/^{4}He$ ratio follows the opposite pattern to that of ^{4}He with higher ratios observed in the shallow samples and lower ratios in the deeper samples (Figure 38 C and D).

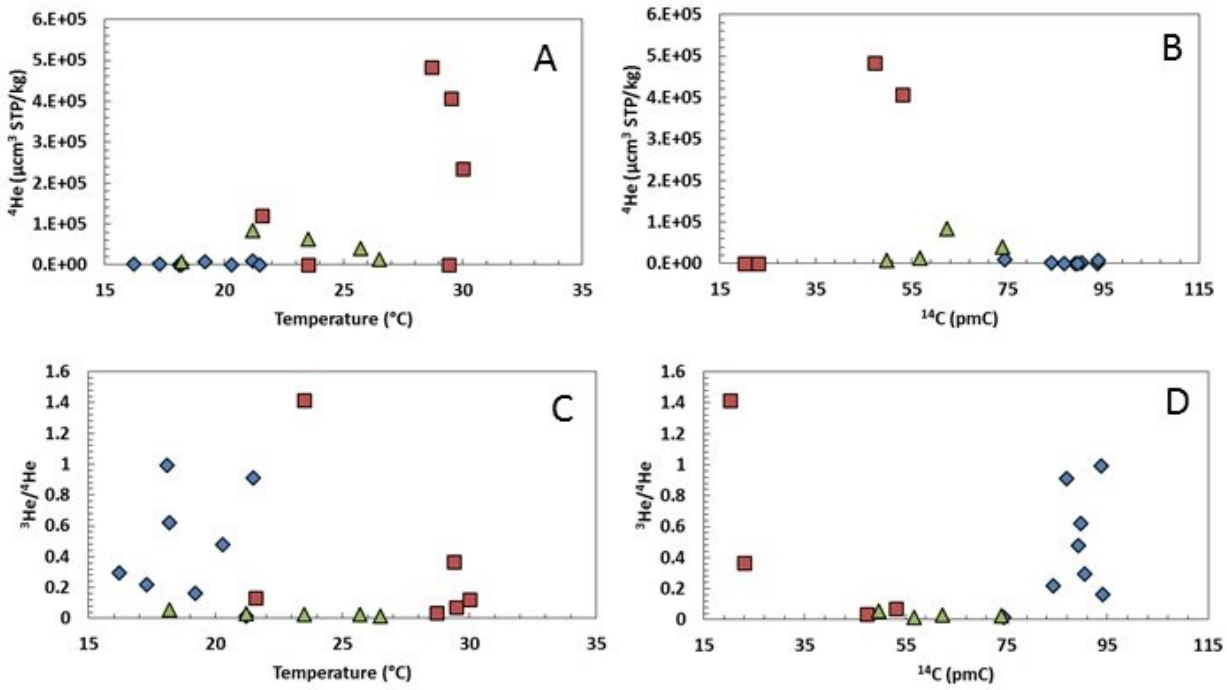

Figure 38: *Relationship between A) ^{4}He and temperature; B) ^{4}He and ^{14}C; C) ^{3}He/ ^{4}He and temperature; D) ^{3}He/ ^{4}He and ^{14}C of the samples collected throughout the Karoo Basin. Red squares = deep sites, blue diamonds = shallow sites, green triangles = mixed sites.*

3.3.4 Chlorine-36

The ^{36}Cl data is shown as a function of temperature and ^{14}C as these parameters are used as proxies for groundwater depth (Figure 39). Chlorine-36 displays a large variation in the data, especially within the deep group (Figure 39). The ^{36}Cl concentration varies from 2 to 78 x 10^{-12} atoms/L in the deep samples, the shallow samples vary between 22 and 65 x 10^{-12} atoms/L, and the mixed samples overlap substantially with the deep and shallow groups varying between 8 and 40 x 10^{-12} atoms/L (Figure 39A and B). However, when ^{36}Cl is expressed as a ratio of ^{36}Cl/Cl, a clear differentiation of the deep group from the other groups emerges (Figure 39C and D). The deep samples have low ^{36}Cl/Cl ratios between 20 and 126 x10^{-15}, and the shallow group with considerably higher and more variable ^{36}Cl/Cl ratios between 500 and 2294 x10^{-15}. The mixed group ^{36}Cl/Cl ratios lie in between the deep and shallow samples with some overlap. The mixed site RRB1 in Fort Beaufort is an outlier in this pattern in that it is a shallow sample but has a very low ^{36}Cl/Cl ratio of 113 x10^{-15} more consistent with the deep group ratios.

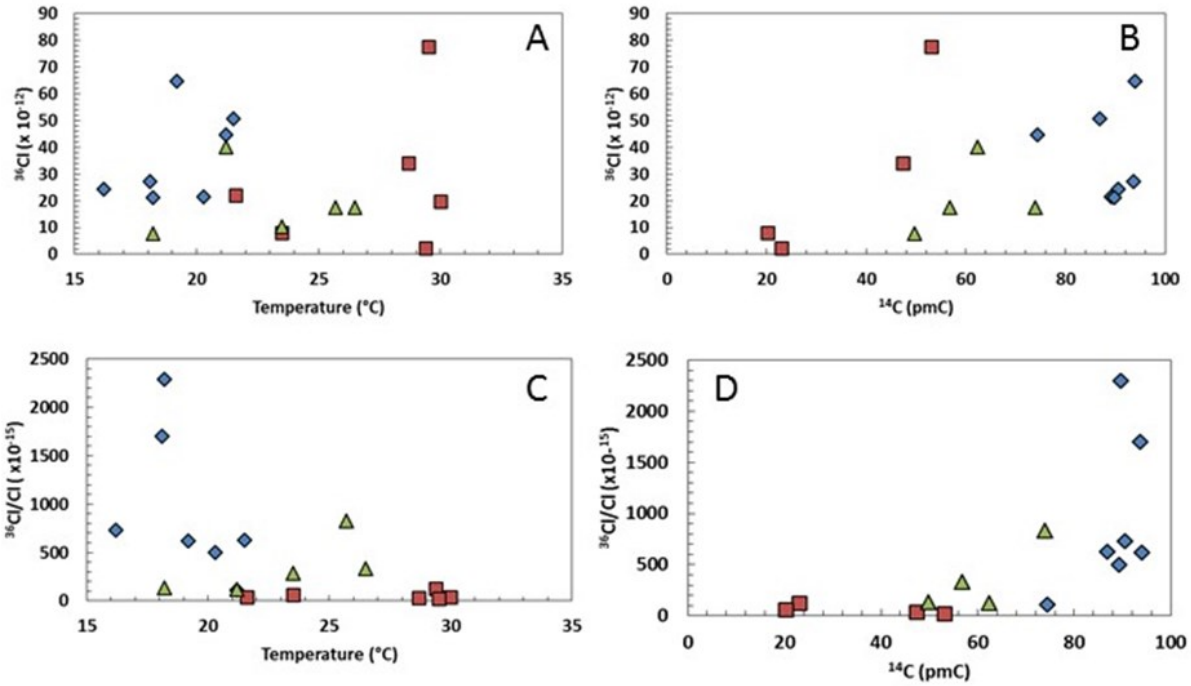

Figure 39: *Relationship between A) ^{36}Cl x 10^{-12}atoms/L and temperature; B) ^{36}Cl x 10^{-12}and ^{14}C; C) ^{36}Cl/Cl x 10^{-15} and temperature; D) ^{36}Cl/Cl x 10^{-15}and ^{14}C of the samples collected throughout the Karoo Basin. Red squares = deep sites, blue diamonds = shallow sites, green triangles = mixed sites.*

3.4 Calculation of residence times

3.4.1 Tritium and tritiogenic helium

The groundwater samples collected in the Karoo Basin were analysed for both tritium and helium. Therefore an attempt was made to calculate residence times using the tritiogenic helium activity of the samples. This was conducted using a programme called iNoble (Matsumoto, 2015). A summary of the data required and the residence times calculated using iNoble are given in Table 6. As shown in Table 5, only 1 of the deep samples, CRS1, contains any measureable ^{3}H/^{3}He and the ^{3}H/^{3}He activity of two shallow sites, namely VFB2 and FLB5, could not be calculated. As previously discussed and shown in Figure 36, the shallow samples generally contain more tritium than the deep and mixed samples, however, the ^{3}H/^{3}He activity is higher in the mixed samples than in the shallow samples (Figure 40A and B). This is also reflected in the residence times calculated using iNoble and shown in Figure 40A and B below. A ^{3}H/^{3}He residence time for the deep site in Florisbad (FLS1), with a relatively high ^{3}H content of 1.6 TU, was not able to be calculated. However, a residence time for the deep site in Cradock, CRS1, with a low tritium content of 0.5 TU was able to be calculated at 816 years. The residence times of the younger, shallow sites are between 791 and 818 years, whereas the mixed sites have slightly older residence times ranging from 800 to 872 years.

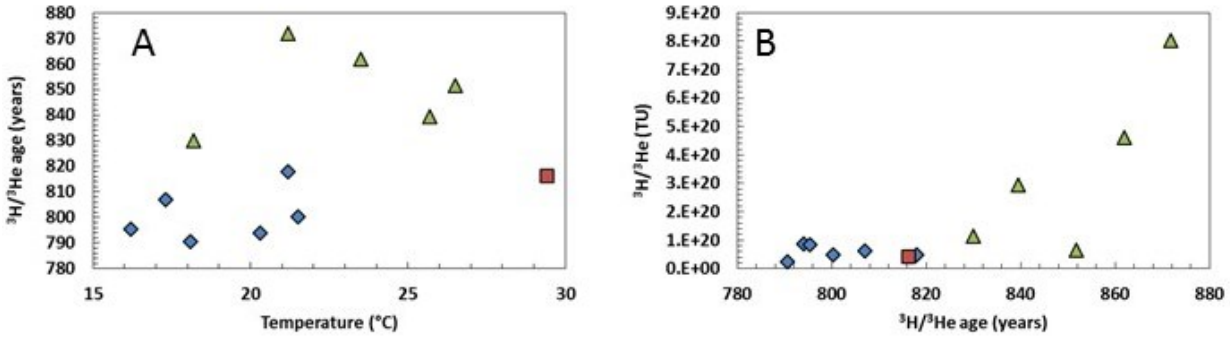

Figure 40: *Relationship between A) calculated $^3H/^3He$ ages and temperature; B) the $^3H/^3He$ concentrations and the calculated $^3H/^3He$ ages of the samples collected throughout the Karoo Basin. Red squares = deep sites, blue diamonds = shallow sites, green triangles = mixed sites.*

Table 6: *Summary of data used in the iNoble programme in order to determine residence times using $^{3}H/^{3}He$.*

	Sample No.	He	Ne	Ar	Kr	Xe	$^{3}He/^{4}He$	Altitude	Temp	Salinity	Tritium		Terrigenic ^{4}He	^{3}He trit	Error	T-^{3}He age	Error	$^{3}He/^{4}He$
		cm^3 STP/g	cm^3 STP/g	cm^3 STP/g	cm^3 STP/g	cm^3 STP/g	uncorected	m	°C	‰	TU	±	±0.03	TU		years		corrected
SHALLOW GROUP	WP 502	638564	268295.6342	1562394.555	105930.4	4286.5	0.344	537	20.3	0.255	3.5	0.3	638563.9	8.84E+19	7.64E+12	794	1.30	0.344
	DRB4	987045	332689.0159	1435725.484	84277.1	3728.1	0.211	729	16.2	0.813	3.1	0.3	987045.2	8.39E+19	9.82E+12	795	1.70	0.211
	RRB1	10153271	167076.2236	1143580.030	74904.5	3262.0	0.012	484	21.2	1.281	0.5	0.2	10153271.2	4.83E+19	1.03E+14	818	12.74	0.012
	RWB5	87051	211131.519	908944.130	54000.4	2322.2	0.713	1308	18.1	0.419	1.2	0.3	87051.2	2.50E+19	8.95E+12	791	5.01	0.713
	LRB2	980184	199724.6655	1182704.091	78110.5	3180.0	0.159	1275	17.3	0.281	1.2	0.3	980184.0	6.27E+19	9.21E+12	807	4.65	0.159
	VFB2	185590	155452.459	1392804.630	87886.0	3598.0	0.441	1368	18.2	0.243	1.0	0.3	185590.0					
	FLB5	7567803	341936.4521	1162474.786	53136.7	2400.3	0.115	1266	19.2	0.691	1.3	0.3	7567802.8					
	MWB2	189000	202130.11	1339364.276	83509.4	3575.2	0.657	774	21.5	0.528	1.4	0.3	189000.0	5.00E+19	8.19E+12	800	4.60	0.657
MIXED GROUP	WP 508	14146362	180609.66	1225260.357	80132.0	3597.8	0.011	549	26.5	0.457	0.1	0.2	14146361.6	6.46E+19	1.42E+14	852	15.35	0.011
	WP 505	62531544	214764.3704	1150890.856	72022.7	3111.5	0.018	526	23.5	0.661	0.4	0.2	62531544.0	4.61E+20	6.57E+14	862	8.58	0.018
	BFB2	84512664	335431.756	955705.013	48836.5	2013.5	0.024	419	21.2	1.017	0.4	0.2	84512664.0	8.03E+20	7.66E+14	872	10.61	0.024
	RWB1c	39636061	290502.42	1123921.302	60927.8	2169.8	0.018	1319	25.7	0.236	0.9	0.3	39636061.2	2.94E+20	3.60E+14	840	6.02	0.018
	VBB1	6752690	321986.88	1147402.542	68890.0	2824.7	0.042	1272	18.2	0.263	0.6	0.2	6752690.0	1.14E+20	6.49E+13	830	8.20	0.042
DEEP GROUP	CRS1	411884	214717.2997	1316391.771	84907.3	3754.3	0.265	894	29.4	0.101	0.5	0.2	411883.6	4.40E+19	5.12E+12	816	7.84	0.265
	BFB1	71229	348395.4926	1028391.423	56129.6	2283.4	1.016	380	23.5	0.403	0.0	0.2	71229.4					
	ANS1	235141200	359240.4	827635.944	41483.6	1907.3	0.088	1356	30	1.022	0.5	0.2	235141200.0					
	ANBH1	120582791	526653.0611	1323392.619	67823.9	2856.5	0.097	1350	21.6	0.962	0.1	0.2	120582791.4					
	VFB1	40631813	121416.09	561437.031	30441.1	1005.4	0.052	1397	29.5	5.743	0.1	0.2	40631813.2					
	FLS1	483492815	475504.04	990531.956	72000.0	2202.9	0.027	1288	28.7	1.902	1.6	0.3	483492814.9					

3.4.2 Radiocarbon

The reality of dating groundwater is always more complex than it seems as multiple processes, other than decay, may alter the ^{14}C content of the groundwater (Plummer, et al., 2012). Therefore, some assumptions were made regarding potential dissolution/loss of ^{14}C. Factors that may influence the ^{14}C are calcite or dolomite dissolution (which typically only contain ^{12}C and ^{13}C and hence dilute ^{14}C concentrations) and exchange with the aquifer matrix. The assumptions made for the samples collected during this project are described in the section below. A summary of the residence times calculated using ^{14}C is given in Table 7. As mentioned previously and seen in Table 5, only four of the six deep samples were analysed for ^{14}C.

The following equation was used to determine the time taken for the ^{14}C activity to decay to the amount measured in the sample:

$$t = \frac{1}{\lambda} \times \ln \frac{A_o}{A_t} \qquad (1)$$

where t = the residence time of the sample in years

λ = is the decay constant for ^{14}C

A_o = the initial ^{14}C activity

A_t = the measured ^{14}C activity of the sample after some time (t)

However, as previously mentioned, corrections regarding the dilution factor of the ^{14}C through dissolution of carbonate rocks were accounted for by using the $\delta^{13}C$ Mixing Model (Clark & Fritz, 1997). $\delta^{13}C$ was used to determine the source of dissolved inorganic carbon in groundwater because CO_2 concentrations in soil and carbonates are easily quantifiable and provide reliable results for estimating the ^{14}C dilution through carbonate dissolution (Clark & Fritz, 1997). The $\delta^{13}C_{Carb}$ values range from 1.4 to 2‰ for the minimum and maximum ages respectively. The Karoo Basin is dominated by C4 plants, therefore, $\delta^{13}C_{Soil}$ values range from -12 to -13‰. The mixing model is based on calculating a 'q' value or dilution factor which is between 0-1, where 1 is no dilution, using the following equation:

$$q = \frac{\delta^{13}C_{DIC} - \delta^{13}C_{Carb}}{\delta^{13}C_{Soil} - \delta^{13}C_{Carb}} \qquad (2)$$

where $\delta^{13}C_{DIC}$ = measured $\delta^{13}C$ in the groundwater samples

$\delta^{13}C_{Carb}$ = $\delta^{13}C$ of the calcite being dissolved

$\delta^{13}C_{Soil}$ = $\delta^{13}C$ estimated as a function of vegetation type

When the q value calculated in Equation 2 is incorporated into Equation 1 it becomes:

$$t = -8033 \times \ln\left(\frac{C^{14}{}_{meas}}{q \times 100}\right) \qquad (3)$$

A final corrected age is then determined by including the time elapsed since the year 1950 as this is the standard reference value which is normalised to a fixed value prior to atmospheric testing of atomic bombs. This is substituted into Equation 3:

$$t = C^{14}{}_{meas} + \frac{2015-1950}{1.03} \qquad (4)$$

A good correlation exists between the ^{14}C content and the residence times calculated for the samples, as well as the temperature of that sample (Figure 41). In general, the deep samples have the longest residence times, the mixed group have intermediate residence times in comparison to the deep and shallow groups, and the shallow samples have the shortest residence times. The ages calculated for the shallow samples range from 144 to 1898 years. However, some of the shallow sites resulted in negative ages (Table 7). Negative ages indicate that these samples are either younger than 65 years old (recharged after 1950) or there was an error in the value used. The deep samples resulted in ages between 8149 and 11417 years. However, one of the deep samples, BFB1, displays a ^{14}C age of 0 (Figure 41). This site is the only sample to have a positive $\delta^{13}C$ value. The mixed group resulted in ages that are between the deep and shallow groups ranging from 1789 to 5819 years.

Figure 41: *Relationship between A) ^{14}C content and the calculated age of the samples; B) ^{14}C ages and the temperature of the samples collected throughout the Karoo Basin. Red squares = deep sites, blue diamonds = shallow sites, green triangles = mixed sites.*

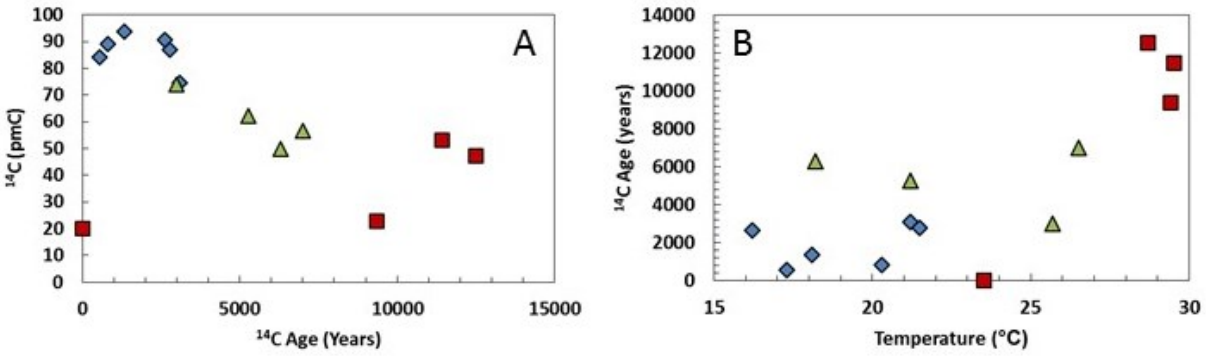

Table 7: *Summary of ^{14}C residence times and calculations.*

	Town	Sample No.	Temp	$\delta^{13}C$	C^{14}		$\delta^{13}C$			Calculated Age [1]			Corrected age [2]		
							-12	-12.5	-13	min	age	max	min	age	max
								‰							
			°C	‰	pmC	±	q value C4 plants				years			years	
SHALLOW GROUP	Leeu Gamka	WP 502	20.3	-10.3	89.2	2.4	0.87	0.84	0.82	-488	-456	-418	-425	-393	-355
	Cradock	DRB4	16.2	-13.6	90.5	2.5	1.12	1.07	1.04	1324	1379	1470	1387	1442	1533
	Fort Beaufort	RRB1	21.2	-11.6	74.4	2.3	0.97	0.93	0.90	1822	1834	1868	1885	1898	1931
	Venterstad	RWB5	18.1	-11.7	93.7	2.5	0.98	0.95	0.92	32	80	150	95	144	213
	Venterstad	LRB2	17.3	-9.2	84.2	2.4	0.79	0.77	0.75	-739	-733	-734	-676	-669	-671
	Trompsburg	VFB2	18.2	-8.6	89.7	2.5	0.74	0.73	0.71	-1702	-1699	-1713	-1639	-1636	-1650
	Florisbad	FLB5	19.2	-4.6	94.0	2.5	0.44	0.44	0.44	-5935	-6017	-6227	-5872	-5953	-6164
	Merweville	MWB2	21.5	-13.3	86.9	2.4	1.09	1.05	1.02	1486	1539	1626	1549	1602	1689
MIXED GROUP	Leeu Gamka	WP 508	26.5	-14.8	56.7	2.1	1.21	1.16	1.12	5771	5756	5790	5835	5819	5853
	Leeu Gamka	WP 505	23.5	-17.6											
	Fort Beaufort	BFB2	21.2	-12.9	62.3	2.2	1.07	1.03	0.99	4036	4023	4045	4099	4086	4108
	Venterstad	RWB1c	25.7	-11.3	73.9	2.3	0.95	0.92	0.89	1717	1726	1752	1780	1789	1816
	Venterstad	VBB1	18.2	-11.5	49.7	0.2	0.96	0.93	0.90	4802	5034	5279	4866	5097	5342
DEEP GROUP	Cradock	CRS1	29.4	-7.2	23.0	0.1	0.64	0.63	0.61	7914	8086	8208	7977	8149	8272
	Fort Beaufort	BFB1	23.5	4.7	20.2	0.1	-0.25	-0.20	-0.18						
	Aliwal North	ANS1	30	-11.6											
	Aliwal North	ANBH1	21.6	-19.8											
	Trompsburg	VFB1	29.5	-25.5	53.1	0.2	2.01	1.91	1.83	9984	10279	10653	10047	10342	10716
	Florisbad	FLS1	28.7	-26.0	47.3	0.2	2.04	1.94	1.87	11062	11354	11726	11125	11417	11789

Notes: (*1) The minimum calculated ages are based on the highest pmC values, the lowest $\delta^{13}C$ value for C4 plants (-13 ‰) and the highest $\delta^{13}C$ value for carbonates (2 ‰). The maximum calculated ages are based on the lowest pmC values, the highest $\delta^{13}C$ value for C4 plants (-12 ‰) and the lowest $\delta^{13}C$ value for carbonmates (1.4 ‰) . (2) The same principle is applied with the corrected ages. These ages have been corrected for the number of years that have passed since 1950.*

3.4.3 Helium-4

Typically only relative ages are estimated using ^{4}He, as opposed to absolute ages. Moreover, the excess Ne that is present results in difficulties in age modelling using ^{4}He as it suggests that the groundwater is older than it actually is (Heaton, 1984). Therefore, some assumptions have been made regarding the samples collected in this project. Elevated methane (CH_4) concentrations coupled with elevated $^{20}Ne/^{36}Ar$ ratios, above 0.121, indicate the presence of exogenous fluid, suggesting that the elevated CH_4 is not the result of decay/build up over time as a result of a longer residence time. This is a common finding in groundwaters situated above shale basins and this has been previously observed in the Karoo Basin (Vogel, et al., 1980; Heaton & Vogel, 1979; Heaton, et al., 1986). A summary of the residence times calculated using ^{4}He is given in Table 8. The following steps were taken in calculating the residence times of the groundwater samples using ^{4}He (Poreda, et al., 1988; Thomas Darrah, personal communication, 16 November, 2015).

Firstly, recharge temperatures were calculated using argon (Ar) concentrations (Table 8). Secondly, estimated neon (Ne) concentrations were calculated by using the recharge temperature calculated in the first step (Table 8). Thirdly, the excess neon concentrations were calculated using the following equation:

$$Ne_{exc} = Ne_{meas} - Ne_{est} \quad (5)$$

where Ne_{exc} = excess neon

Ne_{meas} = measured neon

Ne_{est} = estimated neon (calculated in step 2 above)

The atmospheric ^{4}He is then calculated by using the following equation:

$$He^{4}_{atm} = 1.2 \left(Ne_{exc} \times \frac{He}{Ne}\right) \quad (6)$$

where $^{4}He_{atm}$ = atmospheric helium

Ne_{exc} = excess neon calculated in Equation 5

He/Ne = measured He and Ne concentrations

Finally non atmospheric, or terrigenous ^{4}He is calculated by using the following equation:

$$He^{4}_{Ter} = He^{4}_{tot} - He^{4}_{atm} \quad (7)$$

where $^{4}He_{Ter}$ = terrigenous helium

$^{4}He_{tot}$ = total measured helium

$^4He_{atm}$ = atmospheric helium calculated in Equation 6

Another assumption was then made, that being there is no phase separation of exogenous ^4He based on either the crustal production value (CPV), which is the average crustal release rate, or the measured diffusion constant (MDC) which is the measured release rate. Therefore, two sets of 'ages' have been calculated. The first calculation of residence times is shown by the following equation:

$$t = \frac{He^4_{Ter}}{CPV} \quad (8)$$

where t = residence time of the sample in years

$^4He_{Ter}$ = terrigenous helium calculated in Equation 7

^4He CPV = crustal production value of 0.5 μcm^3/year

The second calculation of residence times is shown by the following equation:

$$t = \frac{He^4_{Ter}}{MDC} \quad (9)$$

where t = residence time of the sample in years

$^4He_{Ter}$ = terrigenous helium calculated in Equation 7

^4He MDC = measured diffusion constant of 0.62 μcm^3/year

Both sets of residence times calculated by Equations 8 and 9 are in relatively good agreement with one another. Average residence times were calculated using the average from Equations 8 and 9 (Figure 42). In general, there is a good trend showing that the deep samples have longer residence times than the shallow samples (Figure 42). The deep sites have the longest residence times between 217468 and 872609 years. The shallow sites have the shortest residence times from 120 to 18324 years. The mixed sites plot in between the deep and shallow sites with residence times ranging from 12104 to 152456 years. However, two of the deep sites, BFB1 and CRS1, have characteristics and residence times similar to that of the shallow sites with low ^4He concentrations as well as young residence times of 18 and 717 years respectively.

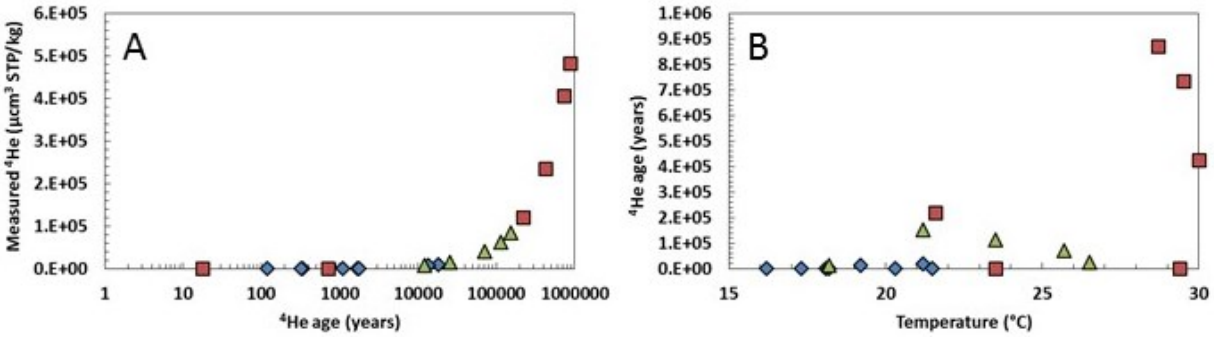

Figure 42: *Relationship between A) measured ^{4}He concentration and the calculated residence times; B) residence times and the temperature of the samples collected throughout the Karoo Basin. Red squares = deep sites, blue diamonds = shallow sites, green triangles = mixed sites.*

Table 8: *Summary of data used for ^{4}He age dating.*

	Town	Sample No.	Temp	Measured Neon	Measured Total Ar	Est. Ar Temp	Estimated Neon	Excess Neon	Measured ^{4}He	^{3}He/^{4}He	Excess Helium from Ne	Terrigenic He	CPV age[1]	MDC age[2]	Average age
			°C	cm^3 STP/kg	cm^3 STP/kg	°C	cm^3 STP/kg	cm^3 STP/kg	µcm^3 STP/kg		µcm^3 STP/kg	µcm^3 STP/kg	0.5 cm^3 STP/g/yr	0.621 cm^3 STP/g/yr	year
SHALLOW GROUP	Leeu Gamka	WP 502	20.3	296.690	0.468	9.2	172.29	124.40	638.56	0.48	34.21	604.35	1209	973	1091
	Cradock	DRB4	16.2	366.905	0.426	8.4	173.71	193.19	987.05	0.29	52.90	934.15	1868	1504	1686
	Fort Beaufort	RRB1	21.2	184.490	0.350	7.2	175.86	8.63	10153.27	0.02	2.35	10150.92	20302	16346	18324
	Venterstad	RWB5	18.1	233.351	0.273	17.0	160.68	72.67	87.05	0.99	20.78	66.27	133	107	120
	Venterstad	LRB2	17.3	220.795	0.352	7.0	176.22	44.57	980.18	0.22	12.11	968.07	1936	1559	1748
	Trompsburg	VFB2	18.2	171.783	0.415	8.3	173.90	-2.12	185.59	0.62	0.00	185.59	371	299	335
	Florisbad	FLB5	19.2	377.992	0.350	7.3	175.12	202.87	7567.80	0.16	55.24	7512.57	15025	12098	13561
	Merweville	MWB2	21.5	223.292	0.399	3.1	183.86	39.43	189.40	0.91	10.49	178.92	358	288	323
MIXED GROUP	Leeu Gamka	WP 508	26.5	199.402	0.391	4.1	181.80	17.60	14146.36	0.02	4.71	14141.65	28283	22772	25528
	Leeu Gamka	WP 505	23.5	236.893	0.352	7.0	176.22	60.67	62531.54	0.03	16.49	62515.06	125030	100668	112849
	Fort Beaufort	BFB2	21.2	371.082	0.312	11.8	167.13	203.96	84512.66	0.03	56.86	84455.80	168912	136000	152456
	Venterstad	RWB1c	25.7	321.344	0.360	11.7	168.29	153.05	39636.06	0.03	42.63	39593.43	79187	63758	71472
	Venterstad	VBB1	18.2	356.218	0.370	5.0	180.01	176.21	6752.69	0.06	47.37	6705.32	13411	10798	12104
DEEP GROUP	Cradock	CRS1	29.4	237.225	0.390	4.1	181.80	55.42	411.88	0.37	14.83	397.06	794	639	717
	Fort Beaufort	BFB1	23.5	384.997	0.306	13.0	166.31	218.69	71.23	1.41	61.31	9.92	20	16	18
	Aliwal North	ANS1	30	398.048	0.288	14.5	159.35	238.70	235141.20	0.12	67.58	235073.62	470147	378540	424344
	Aliwal North	ANBH1	21.6	584.153	0.410	6.2	172.11	412.05	120582.79	0.13	111.85	120470.94	240942	193995	217468
	Trompsburg	VFB1	29.5	134.924	0.544	8.7	173.21	-38.29	406301.81	0.07	0.00	406301.81	812604	654270	733437
	Florisbad	FLS1	28.7	526.340	0.437	5.7	178.65	347.69	483492.81	0.04	93.82	483398.99	966798	778420	872609

Notes: (1) CPV = ^{4}He crustal producton value of 0.5 µcm^3 STP/g/year; (2) MDC = ^{4}He measured diffusion constant of 0.62 µcm3 STP/g/year.

3.4.4 Chlorine-36

The principal application of ^{36}Cl to the dating of old groundwater is by measurement of the decay of atmospheric ^{36}Cl which is produced in the atmosphere by cosmic-ray bombardment of ^{40}Ar (Bentley, et al., 1986). Once in the subsurface, ^{36}Cl is a conservative tracer as the only sink in the aquifer in radioactive decay. However, the main complication in using ^{36}Cl to date old groundwaters is the variation in the chloride concentration in those groundwaters. This can be the result of variable evapotranspiration during recharge or addition of chloride in the aquifer from additional sources (Phillips, 2013; Plummer, et al., 2012).

Three equations were used in an attempt to calculate the residence times of the samples (Guendouz & Michelot, 2006; Purtschert, et al., 2015; Phillips, 2013). However, the equation by Phillips, (2013), described below in Equation 10, produced the most realistic results in comparison to the remaining two equations by Guendouz and Michelot, (2006) and Purtschert, et al., (2015). The residence times calculated using Equation 10 were more realistic than the other equations in that the ages were substantially less negative and even positive in the case of most of the deep samples. Approximately half of the samples did not produce an age when using the equation by Guendouz and Michelot, (2006). The other two equations can be found in Appendix 2. A summary of the residence times calculated using ^{36}Cl is given in Table 9. One of the shallow samples, LRB2, was not analysed for ^{36}Cl.

$$t = \frac{-1}{\lambda_{36}} \times \ln \frac{C_{meas} \times (R_{36\,meas} - R_{36\,se})}{C_{re} \times (R_{36\,re} - R_{36\,se})} \quad (10)$$

where t = the residence time of the sample in years

λ_{36} = decay constant for ^{36}Cl

C_{meas} = measured Cl^- concentration of the sample

$R_{36\,meas}$ = measured $^{36}Cl/Cl$ ratio of the sample

R_{36Se} = secular equilibrium $^{36}Cl/Cl$ ratio

C_{re} = recharge Cl^- concentration

R_{36re} = recharge $^{36}Cl/Cl$ ratio

The recharge Cl concentration value of between 31 and 33 $mg.L^{-1}$ was selected based on average values found in literature as no precipitation samples were collected during this project (Van Wyk, et al., 2011). The initial $^{36}Cl/Cl$ ratio in the recharge also had to be estimated as no values in literature could be found. Figure 39C shows that many of the samples are clustered around a $^{36}Cl/Cl$ value of approximately 500 $x10^{-15}$, therefore a natural value/initial $^{36}Cl/Cl$ ratio from 490 to 500 $x10^{15}$ was selected for the minimum and maximum ages

respectively. The secular equilibrium value should lie between 0 and the lowest $^{36}Cl/Cl$ ratio of the samples (Guendouz & Michelot, 2006), therefore a value of 19 was selected for a minimum age and a value of 20 was selected for a maximum age.

The residence times calculated (Table 9) are not realistic as many of them resulted in incredibly small, negative numbers. However, in most samples, a systematic decrease is observed in the $^{36}Cl/Cl$ ratio with an increase in depth (Figure 43). The only shallow sample to produce a positive age of 30315 years was WP 502 in Leeu Gamka. The deep samples produced ages of between 172915 and 1160204 years, with the exception of site FLS1 which resulted in a negative age of -6974 years. Only one of the mixed samples VBB1 in Venterstad, resulted in a positive age of 180842 years.

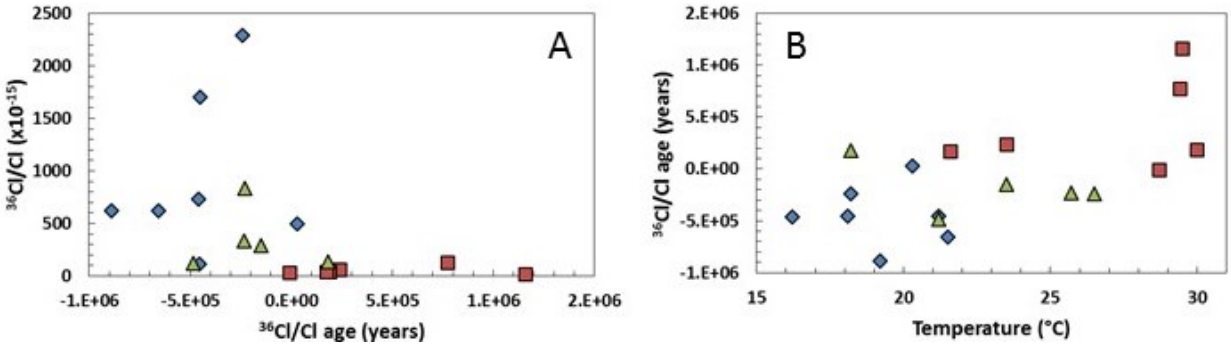

Figure 43: *Relationship between the $^{36}Cl/Cl$ ratios and A) the residence times calculated in years; B) temperature of the samples collected throughout the Karoo Basin. Red squares = deep sites, blue diamonds = shallow sites, green triangles = mixed sites.*

Table 9: *Summary of ^{36}Cl residence times and calculations.*

	Town	Sample No.	Temp	Cl^-	Br^-	Cl/Br	$^{36}Cl \times 10^{-12}$	$^{36}Cl/Cl \times 10^{-15}$		Min [1]	Age	Max [2]
			°C	mg/L	mg/L	molar ratio	atoms/L	±			Years	
SHALLOW GROUP	Leeu Gamka	WP 502	20.3	30	0.10	654	21.5	499.1	18.0	12174	30315	48456
	Cradock	DRB4	16.2	62	0.20	711	24.4	728.5	24.7	-476222	-458228	-440233
	Fort Beaufort	RRB1	21.2	463	2.01	520	44.6	112.7	4.6	-473550	-453533	-433515
	Venterstad	RWB5	18.1	26	0.18	324	27.2	1701.7	54.8	-469737	-451920	-434103
	Venterstad	LRB2	17.3	17	0.09		0.0					
	Trompsburg	VFB2	18.2	12	0.09	295	21.3	2294.0	81.9	-257827	-240043	-222259
	Florisbad	FLB5	19.2	196	0.77	576	64.7	619.3	19.9	-905477	-887427	-869376
	Merweville	MWB2	21.5	114	0.46	563	50.7	624.2	21.4	-676051	-658004	-639957
MIXED GROUP	Leeu Gamka	WP 508	26.5	83	0.33	575	17.6	333.2	11.3	-253478	-235097	-216716
	Leeu Gamka	WP 505	23.5	80	0.43	420	10.2	287.4	10.2	-166935	-148436	-129937
	Fort Beaufort	BFB2	21.2	452	1.51	674	40.1	122.6	4.9	-506155	-486360	-466565
	Venterstad	RWB1c	25.7	32	0.17	425	17.4	830.9	28.0	-249225	-231269	-213313
	Venterstad	VBB1	18.2	85	0.32	595	7.6	137.2	6.8	161308	180842	200376
DEEP GROUP	Cradock	CRS1	29.4	24	0.08	663	2.3	125.7	6.3	754807	774541	794275
	Fort Beaufort	BFB1	23.5	191	0.64	673	7.9	65.4	3.2	216177	238599	261020
	Aliwal North	ANS1	30	515	1.44	803	19.9	38.6	2.2	159502	188535	217569
	Aliwal North	ANBH1	21.6	484	1.24	877	22.2	40.6	2.4	144944	172915	200885
	Trompsburg	VFB1	29.5	3869	23.39	373	77.6	20.1	1.6	547819	1160204	1772588
	Florisbad	FLS1	28.7	1034	4.01	581	34.1	34.5	2.0	-39192	-6974	25243

Notes: (*1) Minimum age was caluclated using the following values: R_{Se} = 19 ($^{36}Cl/Cl \times 10^{-15}$), Cre = 31 (mg/L) and R_{36re} = 490 ($^{36}Cl/Cl \times 10^{-15}$). (2) Maximum age was calculated using the following values: R_{se} = 20 ($^{36}Cl/Cl \times 10^{-15}$), Cre = 33 (mg/L) and R_{36re} = 500 ($^{36}Cl/Cl \times 10^{-15}$).*

3.5 Discussion

Multiple isotopic tracers, namely $^{3}H/^{3}He$, ^{14}C, ^{4}He and $^{36}Cl/Cl$, were used to estimate residence times of the groundwater samples collected for this project. However, these isotopes have different half-lives and are affected by the surrounding environments in different ways as discussed in the above sections. This section focuses on the comparison of the residence times calculated using the different isotopes and assess which isotope was overall most successful at determining probable residence times. The robustness of the division of the groundwater depth groups classified in Chapter 1 will also be investigated evaluated.

3.5.1 Assessment of residence times

In general, there is a good correlation between the three groundwater depth groups and the residence times of the samples showing that the deep samples have longer residence times than the shallow samples and that the mixed samples have residence times between the deep and shallow samples. This suggests that the age of the groundwater increases with an increase in depth and temperature. However, the calculated residence times differ, in some cases substantially, between the different isotopes. Table 10 gives a summary of the residence times calculated using all isotopes. The residence times are shown in combination with an age range, representing the minimum and maximum residence times of each isotope.

Table 10: *Summary of residence times calculated using all isotopes.*

	Town	Sample No.	$^{3}H/^{3}He$		^{14}C			^{4}He			^{36}Cl		
			Age	Error	Age	Range		Age	Range		Age	Range	
			Years		Years	From	To	Years	From	To	Years	From	To
SHALLOW GROUP	Leeu Gamka	WP 502	794	1.3	-393	-425	-355	1091	973	1209	30315	12174	48456
	Cradock	DRB4	795	1.7	1442	1387	1533	1686	1504	1868	-458228	-476222	-440233
	Fort Beaufort	RRB1	818	12.7	1898	1885	1931	18324	16346	20302	-453533	-473550	-433515
	Venterstad	RWB5	791	5.0	144	95	213	120	107	133	-451920	-469737	-434103
	Venterstad	LRB2	807	4.6	-669	-676	-671	1748	1559	1936			
	Trompsburg	VFB2			-1636	-1639	-1650	335	299	371	-240043	-257827	-222259
	Florisbad	FLB5			-5953	-5872	-6164	13561	12098	15025	-887427	-905477	-869376
	Merweville	MWB2	800	4.6	1602	1549	1689	323	288	358	-658004	-676051	-639957
MIXED GROUP	Leeu Gamka	WP 508	852	15.3	5819	5835	5853	25528	22772	28283	-235097	-253478	-216716
	Leeu Gamka	WP 505	862	8.6				112849	100668	125030	-148436	-166935	-129937
	Fort Beaufort	BFB2	872	10.6	4086	4099	4108	152456	136000	168912	-486360	-506155	-466565
	Venterstad	RWB1c	840	6.0	1789	1780	1816	71472	63758	79187	-231269	-249225	-213313
	Venterstad	VBB1	830	8.2	5097	4866	5342	12104	10798	13411	180842	161308	200376
DEEP GROUP	Cradock	CRS1	816	7.8	8149	7977	8272	717	639	794	774541	754807	794275
	Fort Beaufort	BFB1						18	16	20	238599	216177	261020
	Aliwal North	ANS1						424344	378540	470147	188535	159502	217569
	Aliwal North	ANBH1						217468	193995	240942	172915	144944	200885
	Trompsburg	VFB1			10342	10047	10716	733437	654270	812604	1160204	547819	1772588
	Florisbad	FLS1			11417	11125	11789	872609	778420	966798	-6974	-39192	25243

Notes: *Blank spaces indicate that the sample was not analysed for that particular isotope. See Table 5 for further information regarding what samples were analysed for each isotope.*

The $^{3}H/^{3}He$ isotope only produced residence times for the shallow, mixed and one of the deep groundwater samples. These results are consistent with the absence of tritium in the mixed and deeper samples and is expected for recently recharged and shallow groundwater. Relatively uniform and young residence times ranging from 794 to 872 years old are observed between the shallow and mixed samples.

Residence times calculated using ^{14}C produced a clear distinction between the three groundwater depth groups. The longest residence times are found in the deep samples, indicating they are in fact older, and the shortest residence times in the shallow, younger samples. The shallow samples have the shortest residence times of between 114 and 1898 years, the oldest residence times between 8149 and 11417 years for the deep samples and intermediate residence times between 1789 and 5819 years for the mixed samples. The residence times of the samples are consistent with the ^{14}C content in pmC of the samples, with lower content in the deep samples and higher content in the shallow samples. The fact that the mixed samples have residence times between those of the deep and shallow groups further supports the idea discussed in Chapter 2 that the mixed samples are in fact a mixture of the deep and shallow groundwater sampled in the study area. In Chapter 2 it was estimated that the deeper groundwaters are associated with recharge during the Holocene, indicated by lower $\delta^{18}O$ and $\delta^{2}H$ values, approximately 6000 years ago. However, older ages of between 8000 and 11500 years have been calculated in this chapter, indicating these groundwaters are associated with a pre-Holocene recharge event. A few exceptions of the radiocarbon residence times are mentioned in Section 3.4.2 above. For example, four out of the eight shallow samples collected resulted in negative residence times. This is most likely the result of either the influence of mixing with more modern recharged groundwater (younger than 1950) which contains higher ^{14}C content or it suggests that these groundwaters contain ^{14}C derived from nuclear weapons testing (bomb carbon). If the latter is true, these groundwater sources are mixing with younger sources which were recharged post 1950.

The widest range of residence times were produced with ^{4}He which is expected seeing that this isotope has the potential for dating groundwaters aged 100 to 1000000 years old (Plummer, et al., 2012). A definite distinction exists between the residence times of the deep, shallow and mixed groundwaters when using ^{4}He. The longer residence times of the deep groundwaters are consistent with the higher ^{4}He concentrations which accumulate gradually over longer periods of time, or as a result of mixing with deeper, older fluids. In some cases, the deep samples resulted in extremely long residence times, much longer than those calculated using ^{14}C. In contrast, the shallow samples have lower ^{4}He concentrations and shorter residence times as a result of being more recently recharged groundwater. Some of the samples produced similar residence times to those calculated using ^{14}C. As result of the

elevated ^{4}He and CH_4 it was assumed there is no phase separation of exogenous ^{4}He. Furthermore, assuming the ^{4}He is derived from a terrigenic origin, two options were available during the calculations of the residence times regarding the source of the helium. Therefore two ages were calculated, one based on each option. The first age was calculated using the ^{4}He crustal production value of 0.5 μcm^3 STP/g/year and the second age was calculated using the ^{4}He measured diffusion constant of 0.62 μcm^3 STP/g/year (Equations 8 and 9 respectively). As mentioned previously, two of the deep samples, BFB1 and CRS1, resulted in very short residence times in comparison to the remaining deep samples. This could be the result of mixing processes with younger groundwater sources in the area. A possible explanation for the elevated methane is that it originated from a deeper source and migrated upwards, potentially giving an explanation as to why some of the shallow sites have high ^{4}He concentrations.

Several equations were used in an attempt to date the groundwater samples using ^{36}Cl. The residence times calculated using $^{36}Cl/Cl$ consistently gave extremely negative ages for most of the shallow and mixed samples as well as for one deep sample, FLS1. The remaining deep samples resulted in extremely high, positive residence times, substantially higher than the residence times calculated using ^{14}C. Although realistic ages were not able to be calculated, the systematic decrease in the ratio values with an increase in depth and temperature suggests that the deeper samples are in fact older than the shallow samples, albeit not on the timescales associated with the half-life of ^{36}Cl. The two shallow samples (RWB5 and VFB2) with the highest ratios of 1700 and 2294 $x10^{-15}$ respectively, are likely to reflect the nuclear bomb effect, therefore the recharge of these groundwaters is post 1950. These two samples also have two of the highest ^{14}C in pmC content. Future research should include ^{36}Cl analysis of precipitation, particularly of continental interior precipitation as opposed to coastal precipitation which contains stable chloride.

Overall, the residence times calculated using ^{14}C gave the most realistic ages across the board for the deep, shallow and mixed samples. This is indicated by the considerably younger residence times of the shallow samples in comparison to the older, deep samples, and that the mixed samples plot in between these two groups. Probable residence times were not calculated using the remaining three isotopic tracers, which is indicated by negative ages and/or extremely old ages. The activities of each isotope are shown as a function of the ages calculated using ^{14}C (Figure 44) in order to assess how well the isotopic activities correlate with the ^{14}C ages. Figure 44A presents the $^{3}H/^{3}He$ data as a function of the ^{14}C residence times. With the exception of two mixed samples, the $^{3}H/^{3}He$ activities are relatively uniform. An increase in residence time is observed from the shallow, to the mixed and finally to the deep samples, however, a systematic decrease in $^{3}H/^{3}He$ activity with an increase in age trend

with the ^{14}C ages is not observed. This suggests that the ages calculated using $^{3}H/^{3}He$ are not accurate in demonstrating an increase in age with depth. Figure 44B presents the ^{4}He concentrations and the ^{14}C residence times. A trend of increasing residence time and ^{4}He concentration is observed, with the exception of one deep sample which has a low ^{4}He concentration more consistent with the shallow groundwater concentrations. Therefore, the ages calculated using ^{4}He generally demonstrate an increase in age with an increase depth making ^{4}He a useful isotopic tracer for determining residence times in the Karoo. A strong correlation exists between the $^{36}Cl/Cl$ ratio and the ^{14}C content of the groundwater samples (Figure 39D). When the $^{36}Cl/Cl$ ratios are plotted against the residence times calculated using ^{14}C a good trend is also observed (Figure 44C) suggesting an increase in age with an increase in depth. Following ^{14}C, $^{36}Cl/Cl$ ratios were the most successful at distinguishing between deep, shallow and mixed groundwater.

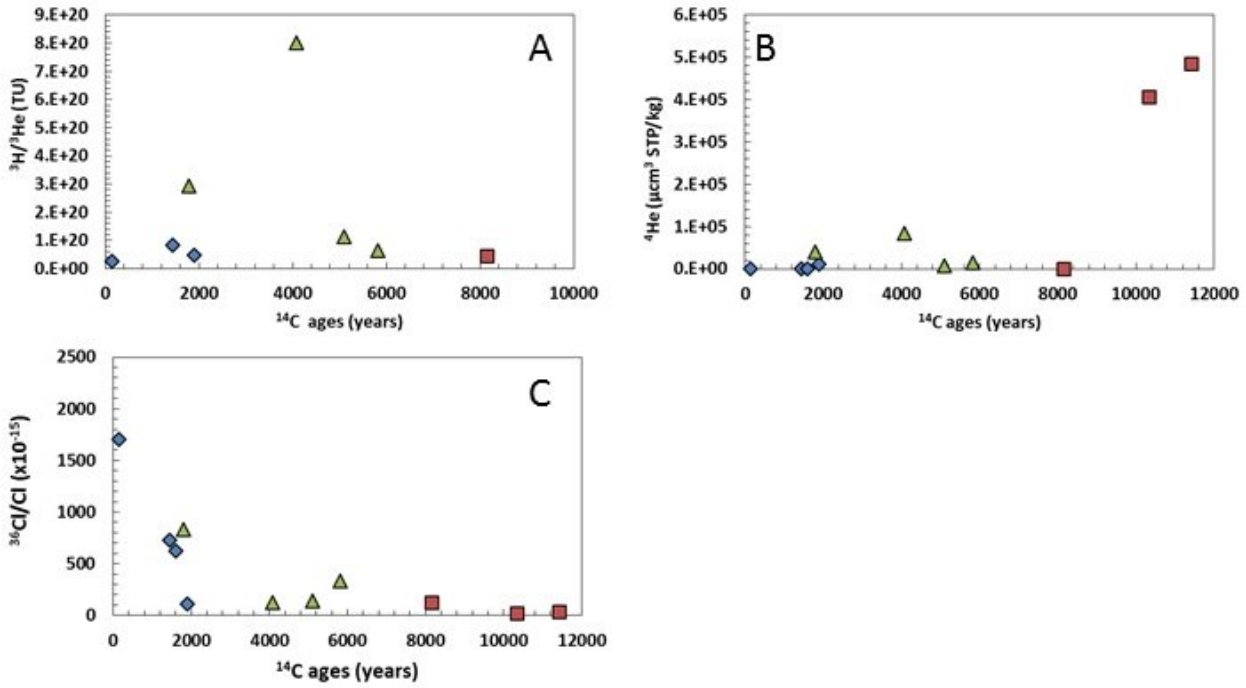

Figure 44: *Relationship between A) $^{3}H/^{3}He$; B) ^{4}He; C) $^{36}Cl/Cl$ ratio and the residence times calculated using ^{14}C of the samples collected throughout the Karoo Basin. Red squares = deep sites, blue diamonds = shallow sites, green triangles = mixed sites.*

As discussed in Chapter 2, there are substantial differences between some of the deep groundwater samples. When observing the residence times calculated using ^{14}C, there is approximately 3000 years difference between the youngest deep sample and the oldest deep sample (Table 10). This could potentially be through error. Although a more likely explanation is that the deep samples originate from multiple sources and are thus recharged on different timescales. This supports the idea discussed in Chapter 2.

3.5.2 Origin of chloride

The Cl/Br molar ratio is an important geochemical tool that when used in conjunction with ^{36}Cl data, can aid in determining the origin of Cl^- in groundwater (Phillips, 2013). The Cl/Br ratio of most meteoric waters situated over the continents is lower than that of seawater, which is 290 (Phillips, 2013). This is because during the formation of marine aerosols Br^- is preferentially fractionated into the smaller particles which survive longer in the atmosphere and are thus more readily transported toward the continental interiors (Davis, et al., 2004). Therefore, lower Cl/Br ratios between 50 and 150 are characteristic of continental interiors, including Cl^- sourced from recharge (Phillips, 2013). In contrast, solutions originating from dissolution of marine evaporites or from connate fluids tend to have higher ratios between 300 and 1000 (Whittemore, 1995). These characteristics are convenient for the differentiation of Cl^- sources, since recharge water will generally possess a low Cl/Br and subsurface sources of Cl will have high Cl/Br (Phillips, 2013). All of the groundwater samples collected throughout the Karoo Basin for this project have Cl/Br ratios of between 295 and 877, and therefore imply that the origin of the Cl^- is from the subsurface (Figure 45A). Figure 45B indicates theoretical relationships between ^{36}Cl concentration and Cl/Br molar ratios (Phillips, 2013). Cases A and C represent the trend observed where changes in Cl^- are not subsurface-related but rather from decay. Case B shows dilution by 'dead' Cl^- without any aging, whereas Case D shows the evolution due to addition of Cl^- from other sources (Phillips, 2013). The groundwater samples collected in the Karoo Basin follow a similar pattern to that of Case D. This suggests that that the Cl^- is not a result of decay, but from an additional source. This idea is further supported by Figure 45C which displays a mixing trend between the samples as opposed to a decay trend when comparing the $^{36}Cl/Cl$ ratio to the inverse of Cl^-. Therefore, variations in ^{36}Cl concentrations and Cl^- are an indication of rock water interactions over extended periods of time which suggests longer residence times for the deep samples.

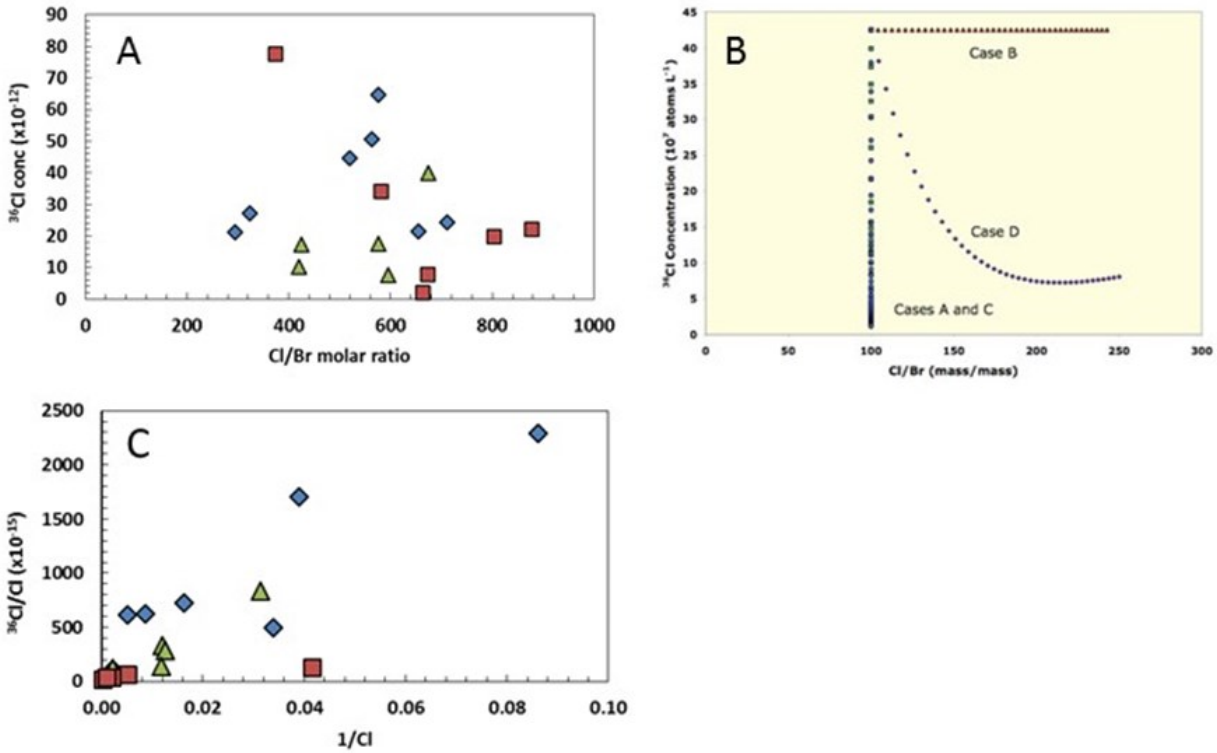

Figure 45: *A) Relationship between ^{36}Cl concentration ($x10^{-12}$) and the Cl/Br molar ratio of the samples collected throughout the Karoo Basin; B) The evolution of the ^{36}Cl concentration and the Cl/Br ratio. Cases A and C represent where changes in Cl^- are not subsurface-related but rather from decay. Case B shows dilution by 'dead' Cl^- without any aging, whereas Case D shows the evolution due to addition of Cl^- from other sources (Phillips, 2013); C) Relationship between $^{36}Cl/Cl$ ratio and the inverse of Cl^- of the samples collected throughout the Karoo Basin. Red squares = deep sites, blue diamonds = shallow sites, green triangles = mixed sites.*

3.5.3 Comparison with existing residence times

Various studies on the residence times of groundwater in the Karoo Basin have been conducted since the 1940's (Kent, 1949; Heaton & Vogel, 1979; Mazor & Verhagen, 1983; Vogel, et al., 1980; Vogel, et al., 1980; Talma & Esterhuyse, 2015). These studies include groundwater analyses for major ion chemistry, as well as ^{3}H, ^{14}C and noble gases. The ^{3}H and ^{14}C data is generally consistent with the findings of this project in that the thermal springs contained relatively low ^{3}H and ^{14}C concentrations. Historical noble gas analyses are available from two of the same locations sampled in this project, namely Venterstad and Beaufort West. Talma and Esterhuyse, (2015) used CH_4 data from a project conducted by Heaton and Vogel, (1979) in order to determine a conceptual model representing the mixing of goundwater in the area. This diagram was reproduced using the data from this project and very similar and consistent results were observed (Figure 46A and B). Similar results from this project and the project conducted by Heaton and Vogel in 1979 indicates that consistent and reputable data was collected.

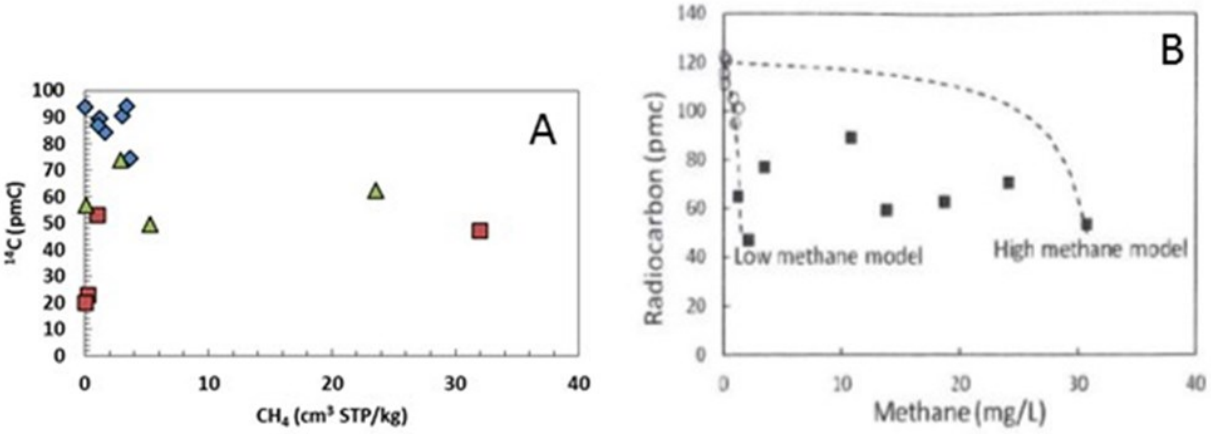

Figure 46: *A) Relationship between ^{14}C and CH_4 of the samples collected throughout the Karoo Basin. Red squares = deep sites, blue diamonds = shallow sites, green triangles = mixed sites; B) Relationship between ^{14}C and CH_4 of the samples collected and analysed in the study conducted by Heaton & Vogel (1979).*

3.5.4 Implications for recharge

Knowledge of residence times for groundwater in the Karoo Basin is important for understanding the deeper groundwater systems and is an important part of building a baseline and developing a monitoring programme for future fracking activities. In general, the residence times of the deeper groundwater samples indicate that the groundwater sources are non-renewable on human timescales. Climate change predictions include reduced precipitation and increased aridity in southern Africa (Hulme, et al., 2001). The likely result of this is an increased demand for groundwater resources in the Karoo Basin. Moreover, should the deeper groundwater become contaminated as a result of fracking processes, it will be detrimental for the water stressed region. This is further emphasizing the importance of effective groundwater management in terms of usage as well as potential contamination and pollution from fracking activities. As mentioned in Section 3.5.1, recharge could account for variable ages through differential recharge.

3.5.5 Recommendations for further study

The analysis of δ^2H_{CH4} as well as additional sampling at greater depths to further investigate the origin of methane is recommended in future projects. This information will also allow for the comparison of isotopic signatures of groundwaters found at greater depths than the ones sampled at for this project. It is important to record natural methane emissions and their isotopic signatures before fracking activities commence in order to distinguish between natural and fracking induced methane (Humez, et al., 2015). Repeated sampling and groundwater "dating" of the same sampling sites is recommended in order to assess the recharge processes and timescales of the deeper groundwater. It is expected that the samples will become progressively younger as they mix with recharge. It is also included that future analyses also include other isotopic tracers, such as CFCs and SF6. These analyses have

previously been conducted in the Karoo Basin by Talma & Weaver, (2003). It is advised that precipiation samples are collected, throughout the entire basin due to the notably different precipitation patterns across the basin. A general overview, as well as ^{36}Cl analysis of the precipitation, will allow for further investigation of the recharge systems of the deeper groundwater aquifers in the basin.

3.6 Conclusions

Longer residence times are observed in the deep samples in comparison with the shallow samples. This is indicated by the low $^{3}H/^{3}He$, ^{14}C, ^{36}Cl and high ^{4}He activities observed in the deep samples. Some of the results found in this study are consistent with other results obtained from the same region. Overall, radiocarbon produced the most realistic residence times for the deep, shallow and mixed samples with the youngest groundwaters being from the shallow group and the oldest in the deep group. Some of the shallow samples resulted in negative residence times whereby indicating the post bomb effect. Therefore, they consist of modern and recently recharged groundwater. The tritiogenic helium residence times produced very uniform and the youngest ages for the shallow and mixed groundwater samples. The ^{4}He isotope produced the widest range of residence times amongst the deep, shallow and mixed groundwater samples. However, elevated methane and therefore excess neon results in difficulty of dating the groundwater using ^{4}He. The origin of methane is from a deeper source than what was sampled, therefore it migrated to a shallower depth of at least the depth at which the deep samples in this project are situated. The vast differences in residence times between the deep samples suggest that these groundwaters originate from various sources and are recharged on different timescales. A larger dataset including additional deep samples is required for further investigations on the sources of the deep groundwaters. As a result of the success in determining the residence times using radiocarbon, the groundwater samples in this study are too young to produce realistic ages using ^{36}Cl. However, a good correlation is observed between the $^{36}Cl/Cl$ ratio and the ^{14}C residence times. Further investigation of the ^{36}Cl concentration and Cl/Br molar ratio indicates that the Cl^- present in the groundwater samples is not from decay, but from an additional source. As a result of the longer residence times of the deeper groundwater sampled in this project, it was determined that the deeper groundwater sources are not renewable on human timescales. This could potentially be a problem in the future if these aquifers are large enough and suitable for extraction for human requirements. This highlights the need for proper management and understanding of the deeper groundwater sources, especially in light of potential fracking activities in the region.

CHAPTER 4 - General conclusions and recommendations for future work

4.1 General conclusions

Overall, the aim of this project was to differentiate between deep and shallow groundwater in the Karoo Basin using the hydrochemical characteristics of the groundwater samples. In total, 19 groundwater samples were collected from springs and boreholes throughout the basin. The samples were originally classified as either deep or shallow based on temperature or historical information. However, it became evident that five of the samples could be neither be classified as deep nor shallow. Therefore, after a second assessment based on major ion chemistry in the form of Stiff diagram shape, the samples were classified into three depth groups; deep, mixed and shallow. This final classification was validated by the radiocarbon content of the samples.

In general, the shallow samples can be identified by temperatures below 25°C, low pH values less than 8, high alkalinity values and the groundwater can be classified as a mixed-HCO_3^--type water. In contrast, the deep groundwater can be identified by temperatures above 25°C, however, this is not always the case, pH values above 9, alkalinity values below 80 $mg.L^{-1}$ HCO_3^-, negative ORP values and considerable H_2S concentrations. The groundwater can be classified as NaCl-type water. Overall, the mixed samples have characteristics that are intermediate with respect to the deep and shallows samples and can be classified as a combination between a $NaHCO_3$ and a NaCl-type water. The results of the mixed samples consistently fall between the deep and shallow groups. As discussed in Chapter 2, it is thought that the mixed groundwater samples consist of different proportions of shallow and deep groundwater, although other explanations including completely different groundwater sources cannot be excluded. The identification of a mixed groundwater group provides evidence that mixing occurs between the deep and shallow groundwater systems, implying that connectivity between the deep and shallow groundwater systems exists. Therefore, this could allow for the upward migration of potentially poor quality deeper groundwater. Because of the concerns regarding contamination of shallow groundwater from either poor quality deep groundwater or fracking fluids, understanding the formation of these mixed groundwaters and their significance to deeper flow systems is of paramount importance.

Multiple redox conditions, precipitation-dissolution and water-rock reactions control the hydrochemistry of the groundwater, and are responsible for the differences observed between the deep and shallow groundwaters. Nitrification occurs in the shallow groundwater and is intensified by agricultural activities occurring near the sampling sites, resulting in elevated n nitrate concentrations. In contrast, the process of denitrification occurs in the deep groundwater resulting in an absence of nitrate concentrations. Evidence of cation exchange

is present in the deep groundwater samples indicated by low Ca and Mg concentrations. However, low Mg/Ca molar ratios coupled with low alkalinity in the deep groundwater could also show evidence of calcite precipitation. It is thought that deep groundwater has more interaction with the host lithologies and aquifer matrix as a result of increased residence time. This is evident by elevated sodium concentrations observed in the deep groundwater samples in comparison to the shallow groundwater. The slow dissolution rate in warmer groundwater also allows for elevated fluorine and boron concentrations. The $\delta^{11}B$ values of the shallow samples reflect boron from sediments, such as clay, deposited in a marine environment. This is consistent with the depositional environment of the Karoo Basin. In general, the shallow groundwater is experiencing oxidizing conditions as is evident by positive ORP values and the lack of H_2S. In contrast, the deep groundwater is experiencing anoxic conditions in a reducing environment as is evident by negative ORP values, significant presence of H_2S as well as the indications of methanogenesis. Evidence of palaeorecharge in the Holocene epoch is indicated by lower $\delta^{18}O$ and $\delta^{2}H$ values observed in the deep groundwater samples. However, further analysis of the deep groundwater residence times indicates a pre-Holocene recharge event. Although the deep samples all have similar results for parameters such as pH, alkalinity, NO_3^-, $\delta^{18}O$ and $\delta^{2}H$, the results of other parameters such as, temperature, $^{87}Sr/^{86}Sr$, $\delta^{13}C$ and $\delta^{13}B$ ratios differed. This indicates that the deep groundwater samples originate from multiple sources.

Knowledge of the residence times of the groundwater in the Karoo Basin is important in understanding the deeper groundwater systems as a whole, as well as the recharge systems associated with the deeper and shallow groundwater systems. Longer residence times were recorded in the deeper samples in comparison with the shallow samples. This is consistent with lower tritiogenic helium, radiocarbon, chrloine-36 and higher helium-4 activities observed in the deep samples in comparison to the shallow samples, as well as with historical residence times of the groundwater in the same region. The youngest residence times were calculated using tritiogenic helium, and the oldest residence times were calculated using helium-4. In general, the most probable residence times were calculated using radiocarbon on the basis that the deep samples gave the oldest ages, the shallow samples gave the youngest ages and the mixed samples gave intermediate ages. The only negative ages were produced by four of the shallow samples implying that these groundwaters represent modern and recent recharge, post 1950. Residence time calculations of the deep samples resulted in ages that indicate the deep groundwater sources are non-renewable on human timescales. These groundwater sources will be of utmost importance as the semi-arid Karoo Basin becomes dryer with climate change. This further accentuates the requirement of successful groundwater managing schemes.

Variation in residence times of the deep samples indicates that the groundwaters originate from multiple sources. For example, there is approximately a 3000 year age difference between the deep samples when evaluating the residence times calculated using radiocarbon. This supports the hypothesis mentioned above with regards to varying results of other geochemical parameters, implying that several deep groundwater sources exist scattered throughout the basin.

Given the fact that a mixed groundwater group was identified from a small sample group of only 19 samples, it is probable that the deeper and shallow groundwater systems are linked. This potential connectivity between deep and shallow aquifers could have a damaging effect on the shallow groundwater systems as a result of fracking activity pollutants. Therefore, it is important to have a monitoring programme in place so that should contamination issues arise as a result of fracking it will be possible to identify the source of pollution. Furthermore, a broad spectrum of parameters, such as described in Chapter 1 in the form of a baseline, should be continuously measured before, during and after fracking occurs. However, with proper management of the deep wells as well as effective waste disposal and transparency regarding the chemicals included in the fracking fluid, the process of fracking could be effective and beneficial and avoid negative environmental impacts.

4.2 Recommendations for future work

Further investigation and characterisation of the groundwater in the Karoo will allow for a more in depth understanding of the different groundwater systems and how they may potentially be affected through the fracking process. Future work should include a more statistical approach as well as the use of PHREEQC modelling with regards to the controls on groundwater chemistry. Sampling of groundwater at greater depths is required to compare and contrast the findings of the deeper groundwater in this study. This will also allow further investigation of the origin of methane present in the basin. Repeated sampling and age dating of the same sites is recommended in order to assess the recharge processes and timescales of the deeper groundwater. It is expected that the samples will become progressively younger as they mix with recharge. Future analyses should also include other isotopic tracers, such as CFCs and SF6. Precipiation should be collected throughout the entire basin as a result of the notably different precipitation patterns across the basin. A general overview, as well as ^{36}Cl analysis of the precipitation, will allow for further investigation of the recharge systems of the deeper groundwater aquifers in the basin.

REFERENCES

Adams, S., Titus, R., Pieterson, K., Tredoux, G., & Harris, C. (2001). Hydrochemical characteristics of aquifers near Sutherland in the Western Karoo, South Africa. Journal of Hydrology, 241, 91-103.

Adgate, J. L., Goldstein, B. D., & McKenzie, L. M. (2014). Potential public health hazards, exposures and health effects from unconventional natural gas development. Environmental Science and Technology, 48, 8307-8320.

Aggarwal, P. K., Gat, J. R., & Frohlich, K. F. (2005). Isotopes in the water cycle: Past, present and future of a developing science (1 ed.). Springer Netherlands.

Anhaeusser, C. R. (2006). Ultramafic and mafic intrusions of the Kaapvaal Craton. In M. R. Johnson, C. R. Anhaeusser, & R. J. Thomas, The Geology of South Africa (pp. 95-134). Pretoria: Council for Geoscience.

Bentley, H. W., Phillips, F. M., & Davis, S. N. (1986). Chlorine-36 in the terrestrial environment. In P. Fritz, & J. C. Fontes, Handbook of Environmental Isotope Geochemistry (pp. 427-480). Amsterdam: Elsevier.

Bethke, C. M., & Johnson, T. M. (2008). Groundwater age and groundwater age dating. Annual Reviews of Earth and Planetary Sciences, 36, 121-152.

Boggs, S. (2009). Petrology of Sedimentary Rocks (2 ed.). New York: Cambridge University Press.

Bond, G. W. (1946). A geochemical survey of the underground water supplies of the Union of South Africa. Geological Survey Memoir, 41, 216.

Boyer, C., Clark, B., Jochen, V., Lewis, R., & Miller, C. (2011). Shale Gas: A global resource. Oilfield Review, 23(3), 28-39.

Cadle, A. B., Caincross, B., Christie, A. D., & Roberts, D. L. (1993). The Karoo Basin of South Africa: type basin for the coal-bearing deposits of southern Africa. International Journal of Coal Geology, 23, 117-157.

Cartwright, I. (2010). Using groundwater geochemistry and environmental isotopes to assess the correction of 14C ages in a silicate-dominated aquifer system. Journal of Hydrology, 382, 147-187.

Catuneanu, O., Wopfner, H., Eriksson, P. G., Carincross , B., Rubidge, B. S., Smith, R. M., & Hancox, P. J. (2005). The Karoo Basins of south-central Africa. Journal of African Earth Sciences, 43, 211-253.

Cheung, K., Klassen, P., Mayer, B., Goodarzi, F., & Aravena, R. (2010). Major ion and isotope geochemistry of fluids and gases from coalbed methane and shallow groundwater wells in Alberta, Canada. Applied Geochemistry, 25, 1307-1329.

Clark, I., & Fritz, P. (1997). Environmental Isotopes in Hydrogeology. New York: Lewis Publishers.

Coetsiers, M., & Walraevens, K. (2009). A new correction model for 14C ages in aquifers with complex geochemistry - Application to the Neogene Aquifer, Belgium. Applied Geochemistry, 24, 768-776.

Cole, D. I., Labuschagne, L. S., Sohnge, S. E., & Schneider, G. I. (1991). Aeroradiometric survey for uranium and ground follow-up in the Karoo Basin. Geological Survey Memoirs, 76, 172.

Corcho Alvarado, J., Purtschert, R., Hinsby, K., Troldborg, L., Hofer, M., Kipfer, R., et al. (2005). 36Cl in modern groundwater dated by a multi-tracer approach (3H/3He, SF6,

CFC-12, 85Kr): a case study in quaternary sand aquifers in the Odense Pilot River Basin, Denmark. Applied Geochemistry, 20, 599-609.

Craig, H. (1961). Isotopic variation in meteoric waters. Science, 133, 1702-1703.

Darling, B. K. (2013). Beyond the Headlines: Origins of Natural Gas Discharging From Shallow Groundwater. Retrieved from Journal of Petroleum Technology: http://www.spe.org/jpt/article/9692-beyond-the-headlines-origins-of-natural-gas-discharging-from-shallow-groundwater/

Davis, S. N., Fabryka-Martin, J. T., & Wolfsberg, L. E. (2004). Variations of bromide in potable groundwater in the United States. Groundwater, 42 (6), 902-909.

Dept of Mineral Resources. (2012). Report on investigation of hydraulic fracturing in the Karoo Basin of South Africa. Pretoria: Department of Mineral Resources.

Eby, G. N. (2004). Principles of Environmental Geochemistry (1st ed.). Belmont, California: Brooks/Cole, Cengage Learning.

Edmunds, W. M., & Smedley, P. L. (2000). Residence time indicators in groundwater: the East Midlands Triassic sandstone aquifer. Applied Geochemistry, 737-752.

EIA/ARI. (2013). Shale gas and shale oil resource assessment methodology. Advanced Resources International.

Elliot, T., Andrews, J. N., & Edmunds, W. M. (1999). Hydrochemical trends, palaeorecharge and groundwater ages in the fissured Chalk aquifer of the London and Berkshire Basins, UK. Applied Geochemistry, 14, 333-363.

Ellsworth, W. L. (2013). Injection-induced earthquakes. Science, 341(6142).

Engelder, T., Cathles, L. M., & Taras Bryndzia, L. (2014). The fate of residual treatment water in shale gas. Journal of Unconventional Oil and Gas Resources, 7, 33-48.

Flewelling, S. A., Tymchak, M. P., & Warpinski, N. (2013). Hydraulic fracture height limits and fault interactions in tight oil and gas formations. Geophysical Research Letters, 40, 3602-3606.

Fox, R. (2012). US Water Alliance. Retrieved October 13, 2015, from http://uswateralliance.org/2012/02/07/webinar-hydraulic-fracturing-facts-frictions-and-trends/

FracFocus. (2015). FracFocus. Retrieved November 13, 2015, from www.fracfocus.org

Geel, C., Schulz, H., Booth, P., De Wit, M., & Horsfield, B. (2013). Shale gas characteristics of Permian black shales in South Africa: results from recent drilling in the Ecca Group (Eastern Cape). Energy Procedia, 40, 256-265.

Grobler, N. J., & Loock, J. C. (1988). The Florisbad mineral spring: Its characteristics and genesis. Navorsinge van die Nationale Museaum Bloemfontein, 5(17), 474-485.

Guendouz, A., & Michelot, J. (2006). Chlorine-36 dating of deep groundwater from northern Sahara. Journal of hydrology, 328, 572-580.

Haluszczak, L. O., Rose, A. W., & Kump, L. R. (2013). Geochemical evaluation of flowback brine from Marcellus gas wells in Pennsylvania, USA. Applied Geochemistry, 28, 55-61.

Heaton, T. H. (1984). Rates and sources of 4He accumulation in groundwater. Hydrological Sciences Journal, 29, 29-47.

Heaton, T. H., Talma, A. S., & Vogel, J. C. (1983). Origin and history of nitrate in confined groundwater in the western Kalahari. Journal of Hydrology, 62, 243-262.

Heaton, T. H., Talma, A. S., & Vogel, J. C. (1986). Dissolved gas paleotemperatures and 0-18 variations derived from groundwater near Uitenhage, South Africa. Quaternary Research, 25(1), 79-88.

Heaton, T. H., & Vogel, J. C. (1979). Gas concentrations and ages of groundwaters in Beaufort Group sediments, South Africa. Water SA, 5(4), 160-170.

Herbert, C. T., & Compton, J. S. (2007). Depositional environments of the lower Permian Dwyka diamictite and Prince Albert shale inferred from the geochemistry of early diagenetic concretions, southwest Karoo Basin, South Africa. Sedimentary Geology, 263-277.

Holmgren, K., Lee-Thorp, J. A., Cooper, G., Lundblad, K., Partridge, T. C., Scott, L., . . . Tyson, P. D. (2003). Persistent millennial-scale climatic variability over the past 25 000 years in Southern Africa. Quaternary Science Reviews, 22, 2311-2326.

Howarth, R. W., Ingraffea, A., & Engelder, T. (2011). Should fracking stop? Nature, 477, 271-275.

Hulme, M., Doherty, R., Ngara, T., New, M., & Lister, D. (2001). African climate change: 1900-2100. Climate Research, 17, 145-168.

Humez, P., Mayer, B., Ing, J., Nightingale, M., Becker, V., Kingston, A., . . . Taylor, S. (2015). Occurrence and origin of methane in groundwater in Alberta (Canada): Gas geochemical and isotopic approaches. Science of the Total Environment, 1268(541), 1253.

IAEA. (1981). Statistical treatment of environmental isotope data in precipitation. Vienna: International Atomic Agency.

IEA. (2014). World Energy Outlook. Paris: International Energy Agency.

Jackson, R. B., Vengosh, A., William Carey, J., Davies, R. J., Darrah, T. H., O'Sullivan, F., & Petron, G. (2014). The environmental costs and benefits of fracking. Annual Reviews Environmental Resources, 39, 327-362.

Jackson, R. E., Gorody, A. W., Mayer, B., Roy, J. W., Ryan, M. C., & Van Stempvoort, D. R. (2013). Groundwater protection and unconventional gas extraction: The critical need for field-based hydrological research. Groundwater, 51(4), 488-510.

Johnson, M. R., Van Vuuren, C. J., Hegenberger, W. F., Key, R., & Shoko, U. (1996). Stratigraphy of the Karoo Supergroup in southern Africa: an overview. Journal of African Earth Sciences, 23(1), 3-15.

Johnson, M. R., van Vuuren, C. J., Visser, J. N., Cole, D. I., de V Wickens, H., Christie, A. D., . . . Brandl, G. (2006). Sedimentary rocks of the Karoo Supergroup. In M. R. Johnson, C. R. Anhaeusser, & R. J. Thomas (Eds.), Geology of South Africa (pp. 461-499). Johannesburg and Pretoria: Geological Society of South Africa and Council for Geoscience.

Kent, L. E. (1949). The thermal waters of the Union of South Africa and South West Africa. Transactions of the Geological Society of South Africa, 52, 241-249.

Kent, L. E., Groeneveld, D., & Temperley, B. N. (1966). Thermal springs and groundwater of the Badfontein Valley, Eastern Transvaal. Annals of the Geological Survey, 5(1), 129-151.

Kim, J. H., Kim, R. H., Lee, J., & Chang, H. W. (2003). Hydrogeochemical characterization of major factors affecting the quality of shallow groundwater in the coastal area at Kimje in South Korea. Environmental Geology, 44, 478-489.

Knowles, R. (1982). Denitrification. Microbiological Reviews, 46(1), 43-70.

Kulongoski, J. T., HIlton, D. R., & Selalo, E. T. (2004). Climate variability in the Botswana Kalahari from the late Pleistocene to the present day. Geophysical Research Letters, 31(10), 1-5.

La Moreaux, P. E., & Tanner, J. T. (2001). Springs and bottled waters of the world. Ancient history, source, occurrence, quality and use. Hydrogeology, 315.

Lavastre, V., La Salle, C., Michelot, J. L., Giannesini, S., Benedetti, L., Lancelot, J., et al. (2010). Establishing constraints on groundwater ages with 36Cl, 14C, 3H, and noble gases: A case study in the eastern Paris basin, France. Applied Geochemistry, 25, 123-142.

Lehmann, B. E., Love, A., Purtschert, R., Collon, P., Loosli, H. H., Kutschera, W., et al. (2003). A comparison of groundwater dating with 81Kr, 36Cl and 4He of four wells in the Great Artesian Basin, Australia. Earth and Planetary Science Letters, 211, 237-250.

Le Maltre, D., Colvina, C., & Maherrya, A. (2009). Water resources in the Klein Karoo: the challenge of sustainable development in a water-scarce area. South African Journal of Science, 105, 39-48.

Loock, J. C., & Grobler, N. J. (1988). The regional geology of Florisbad. Navorsinge van die Nasionale Museum Bloemfontein, 489-497.

Lynch, S. D. (2003). Development of a raster database of annual, monthly and daily rainfall for Southern Africa. School of Bioresources Engineering and Environmental Hydrology. Pietermaritzburg: University of KwaZulu Natal.

Matsumoto, T., 2015. A VBA-Excel program for noble gas data analysis for groundwater dating and recharge temperature. Vienna, IAEA.

Mayer, B., Humez, P., Becker, V., Nightingale, M., Ing, J., Kingston, A., . .. Kloppmann, W. (2015). Prospects and limitations of chemical and isotopic groundwater monitoring to assess the potential environmental impacts of unconventional oil and gas development. Orleans: Procedia Earth and Planetary Science.

Mazor, E., & Verhagen, B. T. (1983). Dissolved ions, stable and radioactive isotopes and noble gases in thermal waters of South Africa. Journal of Hydrology, 63, 315-329.

McArthur, J. M., Howarth, R. J., & Bailey, T. R. (2001). Strontium Isotope Stratigraphy: LOWESS Version 3: Best Fit to the Marine Sr-Isotope Curve for 0-509 Ma and Accompanying Look-up Table for Deriving Numerical Age. Journal of Geology, 109(2), 155-171.

McCreadie, N. (2015). Karoo Space. Retrieved September 5, 2015, from http://karoospace.co.za/fracking-vs-farming-karoo/

Merriman, R., Highley, D. & Cameron, D., 2003. Definition and characteristics of very-fine grained sedimentary rocks: clay, mudstone, shale and slate: British Geological Survey, Commissioned Report CR/03/281N.

Midgley, D. C., Pitman, W. V., & Middleton, B. J. (1994). Surface water resources of South Africa. Pretoria: Water Research Commission Report No 298/3.2/94.

Milton, S. J., & Dean, W. (1999). Biogeographic patterns and the driving variables. In W. Dean, & S. J. Milton, The Karoo: Ecological patterns and processes (pp. 1-8). Cambridge: Cambridge University Press.

Molofsky, L. J., Connor, J. A., Farhat, S. K., Wylie, A. S., & Wagner, T. (2011). Methane in Pennsylvania water wells unrelated to Marcellus fracturing. Oil and Gas Journal, 54-67.

Mook, W. G. (2006). Introduction to Isotope Hydrology. London: Taylor & Francis Group.

Murray, R., Swana, K., Miller, J., Talma, A. S., Tredoux, G., Vengosh, A., & Darrah, T. H. (2015). The use of chemistry, isotopes and gases as indicators of deeper circulating groundwater in the Karoo Basin. Water Research Commission No 2254/1/15.

Negrel, P. & Petelet-Giraud, E., 2005. Strontium isotopes as tracers of groundwater-induced floods: the Somme case study (France). Journal of Hydrology, Volume 305, pp. 99-119.

Nicot, J. P., & Scanlon, B. (2012). Water use for shale-gas production in Texas, US. Environmental Science and Technology, 3580-3586.

Nolan, J. & Weber, K., 2015. Natural uranium contamination in major U.S aquifers linked to nitrate. Environmental Science and Technology Letters, Volume 2, pp. 215-220.

Nunn, J. A. (2012). Burial and thermal history of the Haynesville Shale: Implications for overpressure, gas generation and natural hydrofracture. Gulf Coast Association of Geological Societies, 1, 81-96.

Oesterlen, P. M. (1991). A further report on the geology of the Dande west area (western Cabora Bassa Basin, Mid-Zambezi Valley). Annales Zimbabwean Geological Society, 15, 1-5.

Olivier, J., Jonker, C. Z., & Yibas, B. (2012). Characteristics of South African thermal springs: Benefits and risks. Cape Town: South African Geographic Society Centre.

Olivier, J., Van Niekerk, H. J., & Van der Walt, I. J. (2008). Physical characteristics of thermal springs in the Waterberg area in Limpopo Province, South Africa. Water SA, 34, 163-174.

Osborn, S. G., Vengosh, A., Warner, N. R., & Jackson, R. B. (2011). Methane contamination of drinking water accompanying gas-well drilling and hydraulic fracturing. Proceedings of the National Academy of Sciences, 108(20), 8172-8176.

Pacsi, A. P., Kimura, Y., McGaughey, G., McDonald-Buller, E. C., & Allen, D. T. (2015). Regional Ozone Impacts of Increased Natural Gas Use in the Texas Power Sector and Development in the Eagle Ford Shale. Environmental Science and Technology, 49, 3966-3973.

Paktinat, J., O'Neil, W., Aften, C., & Hurd, M. (2011). Critical evaluation of high brine tolerant additives used in shale slickwater fracs. Society of Petroleum Engineers, 1-19.

Phillips, F. M. (2013). Chlorine 36 Dating of Old Groundwater. In Isotope Methods for Dating Old Groundwater (pp. 125-152). Vienna: IAEA.

Plummer, L. N., Eggleston, J. R., Andreasen, D. C., Raffensperger, J. P., Hunt, A. G., & Casile, G. C. (2012). Old groundwater in parts of the upper Patapsco aquifer, Atlantic Coastal Plain, Maryland, USA: evidence from radiocarbon, chlorine-36 and helium-4. Hydrogeology Journal , 20, 1269-1294.

Poreda, R., Cerling, T. & Salomon, D., 1988. Tritium and helium isotopes as hydrologic tracers in a shallow unconfined aquifer. Journal of Hydrology, Volume 103, pp. 1-9.

Purtschert, R., Lu, Z., Jiang, W., Mueller, P., Yang, G., Shand, P., et al. (2015). Groundwater flow velocities and recharge conditions in the Great Artesian Basin (GAB) determined by noble gas isotopes and 36Cl/Cl measurements. Geochemica et cosmochemica acta. Prague.

Rindl, M. M. (1916). Medicinal springs of South Africa. South African Journal of Science, 13, 528-552.

Rosewarne, P. N., Woodford, A. C., Visser, D., Esterhuyse, C., O'Brien, R., Goes, M., . . . Van Tonder, G. (2013). Karoo Groundwater Atlas Vol. 2. Cape Town: SRK Consulting Report No. 439159.

Roswell, D. M., & De Swart, D. E. (1976). Diagenesis in Cape and Karoo sediments, South Africa, and its bearing on their hydrocarbon potential. Transactions of the Geological Society of South Africa, 79(1), 81-145.

Ryan, P., 2014. Environmental and low temperature geochemistry. 1 ed. s.l.:Wiley Blackwell.

Ryan, J. G., & Langmuir, C. H. (1993). The systematics of boron abundances in young volcanic rocks. Geochemica et Cosmochimica Acta, 57, 1489-1498.

Senko, J., Istok, J., Suflita, J. & Krumholz, L., 2002. In-situ evidence for uranium immobilization and remobilization. Environmental Science and Technology, 36(7), pp. 1491-1496.

Schenk, H. J., & Jackson, R. B. (2002). Rooting depths, lateral root spreads and below-ground/above-ground allometries of plants in water-limited ecosystems. Journal of Ecology, 90 (3), 480-494.

Schlosser, P., Stute, M., Dorr, H., Sonntag, C., & Munnich, K. O. (1988). Tritium/3He dating of shallow groundwater. Earth and Planetary Science Letters, 89, 353-362.

Schwerdtfeger, B. (2015). Origin of high uranium concentrations in the groundwater of North-East Germany. Rome: International Association of Hydrogeologists.

Shabalala, A., Nyabeze, P. K., Mankayi, Z., & Olivier, J. (2015). An analysis of the groundwater chemistry of thermal springs in the Soutpansberg Basin in South Africa: Recent data. South African Journal of Geology, 83-90.

Sharma, S., Mulder, M., Sack, A., Schroeder, K., & Hammack, R. (2014). Isotope approach to assess hydrologic connections during Marcellus Shale drilling. Groundwater, 52(3), 424-433.

Stringfellow, W. T., Domen, J. K., & Camarillo, M. K. (2014). Physical, chemical and biological characteristics of compounds used in hydraulic fracturing. Journal of Hazardous Materials, 275, 37-54.

Stute, M., & Talma, A. S. (1997). Glacial temperatures and moisture transport regimes reconstructed from noble gases and d18O, Stampriet Aquifer, Namibia. Vienna: IAEA.

Talma, A. S., & Esterhuyse, C. (2015). Natural methane in the Karoo: Its occurrence and isotope clues to its origin. South African Journal of Geology, 118, 45-54.

Talma, A. S., & Weaver, J. M. (2003). Evaluation of groundwater flow patterns in fractured rock aquifers using CFCs and isotopes. Pretoria: Water Research Commission No. 1009/1/03.

Talma, A. S., & Van Wyk, E. (2013). Rainfall and groundwater isotopes atlas. In: The use of Isotope Hydrology to characterize and assess Water Resources in southern Africa. Pretoria: Water Research Commission No TT570/13.

Theodori, G. L., Luloff, A. E., Willits, F. K., & Burnett, D. B. (2014). Hydraulic fracturing and the management, disposal and reuse of frac flowback waters: Views from the public in the Marcellus Shale. Energy Research and Social Science, 2, 66-74.

Torgerson, T., Purschert, R., Phillips, F. M., Plummer, L. N., Sanford, W. E., & Suckow, A. (2013). Defining Groundwater Age. In Isotope Methods for Dating Old Groundwater (pp. 17-32). Vienna: IAEA.

Tredoux, G., & Talma, A. S. (2006). Nitrate pollution of groundwater in southern Africa. In Y. Xu, & B. Usher (Eds.), Groundwater pollution in Africa (pp. 15-36). Leiden: Taylor & Francis/Balkema.

USGS, 2015. USGS FAQs. [Online] Available at: www.usgs.gov/faq/categories/9828/3775 [Accessed 16 November 2015].

Van Wyk, E., van Tonder, G. J., & Vermeulen, D. (2011). Characteristics of local groundwater recharge cycles in South African semi-arid hard rock terrains - rainwater input. Water SA, 37(2), 147-154.

Veevers, J. J., Cole, D. I., & Cowan, E. J. (1994). Southern Africa: Karoo Basin and Cape Fold Belt. Memoir Geological Society of America, 184(1), 223-279.

Vengosh, A., Heumann, K. G., Juraske, S., & Kasher, R. (1994). Boron isotope application for tracing sources of contamination in groundwater. Environmental Science and Technology, 28, 1968-1974.

Vengosh, A., Jackson, R. B., Warner, N., Darrah, T. H., & Kondash, A. (2014). A critical review of the risks to water resources from unconventional shale gas development and hydraulic fracturing in the United States. Environmental Science and Technology, A-O.

Vengosh, A., Warner, N., Jackson, R., & Darrah, T. (2013). The effects of shale gas exploration and hydraulic fracturing on the quality of water resources in the United States. Procedia Earth and Planetary Science, 863-866.

Vermeulen, D. (2013). Implications of shale gas development on groundwater resources in the Karoo Basin, a research and academic perspective. Bloemfontein: AgriSA Mining Conference.

Vidic, R., Brantley, S., Vandenbossche, J., Yoxtheimer, D., & Abad, J. (2013). Impact of shale gas development on regional water quality. Science, 340(6134).

Vogel, J. C., Talma, A. S., & Heaton, T. E. (1980). The isotopic, chemical and dissolved gas concentrations in groundwater near Beaufort West. Pretoria: CSIR Report No. 392.

Vogel, J. C., Talma, A. S., & Heaton, T. H. (1980). The isotopic, chemical and dissolved gas concentrations in groundwater near Venterstad, Cape Province. Pretoria: CSIR Research Report 391.

Warner, N. R., Darrah, T. H., Jackson, R. B., Millot, R., Kloppmann, W., & Vengosh, A. (2014). New tracers identify hydraulic fracturing fluids and accidental releases from oil and gas operations. Environmental Science and Technology, A-I.

Warner, N. R., Jackson, R. B., Darrah, T. H., Osborn, S. G., Down, A., Zhao, K., . . . Vengosh, A. (2012). Geochemical evidence for possible natural migration of Marcellus Formation brine to shallow aquifers in Pennsylvania. Proceedings of the Natural Academy of Sciences, 109(30), 11961-11966.

Weber, J. G. (2014). A decade of natural gas development: The makings of a resource curse? Resource and Energy Economics, 37, 168-183.

Whittemore, D. O. (1995). Geochemical differentiation of oil and gas brine from other saltwater sources contaminating water resources: Case studies from Kansas and Oklahoma. Environmental Geosciences, 15-31.

Woodford, A. C., & Chevallier, L. (2002). Hydrogeology of the Karoo Basin: Current knowledge and future needs. Pretoria: Water Research Commission no TT179/02.

Zhao, X., & Yang, Y. (2015). The current situation of shale gas in Sichuan, China. Renewable and Sustainable Energy Reviews, 50, 653-664.

Appendix 1: *Summary table of the parameters analysed but not referred to in this thesis.*

	Town	Sample No.	CH_4	$C_2H_6^+$	N_2	O_2	Total CO_2	$\delta^{13}C\text{-}CO_2$	$\delta^{13}C$	Radon		^{226}Ra	^{228}Ra	$^{228}Ra/^{226}Ra$
			1						2					
			cm^3 STP/kg	μcm^3 STP/kg	cm^3 STP/kg	cm^3 STP/kg	cm^3 STP/kg	‰	‰	Bq/L	error	Bq/L	Bq/L	
SHALLOW GROUP	Leeu Gamka	WP 502	1.14	0.09	15.93	0.001	18.5	-16.37	-11.1	13.6	2.1	0.0	0.0	6.9
	Cradock	DRB4	3.07	0.19	16.46	0.049	34.8	-19.28	-15.4	34.7	3.5			
	Fort Beaufort	RRB1	3.67	0.75	13.49	0.017	37.5	-10.35	-11.2	38.6	3.5			
	Venterstad	RWB5	0.01	bdl	15.38	0.085	17.4	-15.25	-12.3	39.1	3.6			
	Venterstad	LRB2	1.61	0.10	13.79	0.003	19.1	-17.45	-9.6	43.5	4.0			
	Trompsburg	VFB2	1.21	0.12	15.58	0.000	17.0	-18.02	-9.4	48.6	4.0	0.0	0.0	5.1
	Florisbad	FLB5	3.40	1.14	13.71	0.052	23.7	-16.36	-4.7	152.3	8.0			
	Merweville	MWB2	1.05	0.07	14.75	0.069	24.6	-19.84	-13.5	163.5	7.0	0.0	0.0	2.4
MIXED GROUP	Leeu Gamka	WP 508	0.07	0.01	14.24	0.003	16.8	-11.38	-15.1	1.1	0.8			
	Leeu Gamka	WP 505	0.27	0.03	11.64	0.023	19.3	-10.62	-17.6	1.2	0.7			
	Fort Beaufort	BFB2	23.53	4.56	13.79	0.074	12.1	-11.92	-13.3	5.7	1.4			
	Venterstad	RWB1c	2.91	0.79	14.27	0.047	15.6	-12.20	-4.7	20.7	2.6			
	Venterstad	VBB1	5.31	1.85	14.88	0.001	1.1	-10.34	-9.0	17.5	2.4	0.0	0.0	0.9
DEEP GROUP	Cradock	CRS1	0.22	0.01	14.39	0.011	1.2	-13.46	-3.1	2.1	1.0			
	Fort Beaufort	BFB1	0.01	bdl	16.34	0.094	0.1	-13.24	16.4	3.4	1.2	0.0	0.0	2.6
	Aliwal North	ANS1	35.29	7.72	11.03	0.005	0.3	-12.77	-11.6	1.3	0.8	0.0	0.0	1.6
	Aliwal North	ANBH1	39.07	7.59	17.11	0.012	0.6	-17.61	-19.8	57.6	4.4			
	Trompsburg	VFB1	1.00	0.17	24.76	0.010	0.3	-12.72	-19.1	2.5	1.0			
	Florisbad	FLS1	31.95	13.22	13.54	0.040	0.5	-13.12	-32.3	9.1	1.8			

Notes: *These parameters were analysed at (1) Ohio State University; (2) Duke University. bdl = below detection limit.*

APPENDIX 2

Three different equations were used when calculating residence times using ^{36}Cl (Guendouz & Michelot, 2006; Purtschert, et al., 2015; Phillips, 2013). As discussed in Chapter 3, the most realistic ages were calculated by using the equation by Phillips, (2013). The remaining two equations that were not used are given below:

Purtschert, et al., 2015

$$t = \frac{-1}{\lambda} \times \frac{C_i \times (Re_1 - Re_2) + Cm\,(Rm - Re_2)}{Ci\,(Ri - Re_1)}$$

where t = the residence time of the sample in years

λ = the decay constant for ^{36}Cl

Ci = initial Cl^- concentration

Re_1 = first secular equilibrium

Re_2 = second secular equilibrium

Cm = measured Cl^- concentration of the sample

Rm = measured $^{36}Cl/Cl$ of the sample

Ri = initial $^{36}Cl/Cl$ ratio

Guendouz & Michelot, 2006

$$RC = RiCi\,e^{-\lambda t} + ReCi\left(1 - e^{-\lambda t}\right) + Re\,(C - Ci)$$

where R = measured $^{36}Cl/Cl$ ratio of the sample

C = measured Cl^- concentration of the sample

Ri = initial $^{36}Cl/Cl$ ratio

Ci = initial Cl^- concentration

λ = decay constant for ^{36}Cl

t = the residence time of the sample in years

Re = $^{36}Cl/Cl$ ratio at secular equilibrium